Understanding the Loss of Capture During Mechanical Pacing

by

Behzad Taeb

Submitted in partial fulfilment of the requirements
for the degree of Master of Science

at

Dalhousie University
Halifax, Nova Scotia
November 27, 2017

Table of Contents

List of figures

Abstract

Pacemakers are a corner-stone of modern heart rhythm management. However, restrictions related to access (both in the emergency setting and globally, in less-developed nations), implantation/explanation complications, spatial control of stimulation, and energy delivery/consumption motivate exploration of alternative pacing modes. Mechanical stimulation, by external percussion, high intensity focused ultrasound, or implanted microparticles can cause excitation, however pacing capture with repetitive stimulation is unsustainable. Various causes for a loss of pacing capture relating to changes in mechano-electric transduction have been hypothesized, including changes in tissue mechanics and rundown of stretch-activated currents. Our goal is to understand why mechanical pacing fails, in order to define the conditions under which it may be a safe and sustainable clinical intervention.

We performed ventricular mechanical pacing experiments in isolated rabbit hearts. Results demonstrated that the sustainability of mechanical pacing depends on the degree of tissue indentation and that capture is reversibly lost in a stimulation frequency-dependent manner. Increased tissue stiffness (by microtubule stabiliser paclitaxel) decreases the indentation threshold for excitation, but does not affect pacing sustainability. Elimination of active tension development (by excitation-contraction uncoupler blebbistatin) also has no effect on sustainability. Similarly, while reduced background heart rate (by ivabradine) allowed capture of a greater number of beats at lower pacing rates, it did not affect sustainability. Optical mapping showed no change in ventricular activation time, repolarisation, or action potential duration patterns with mechanical pacing but did reveal an increasing delay between mechanical stimulation and excitation with each paced beat, which suggests that a continuous reduction in depolarising current may account for the loss of pacing capture.

Overall, we hope these results will guide future investigations to enable the prediction of when mechanical pacing will fail, providing improved justification for or against its clinical use.

List of Abbreviations Used

AP	Action Potential	LVP	Left Ventricular Pressure
APD	Action Potential Duration	MEC	Mechano-Electric Coupling
ATP	Adenosine Tri-Phospahte	MMC	Machano-mechanic Coupling
AUC	Area Under the Curve	M-PACE	Mechanical Pacing Run
AVN	Atrio-ventricular Node	MSP	Maximum Systolic Pressure
cAMP	Cyclic Adenosine Mono-Phosphate	NADPH	Nicotinamide adenine dinucleotide phosphate
di-4-PQ	di-4-ANBDQPQ	NO	Nitric Oxide
DMSO	Di-Methyl Sulfoxide	PKA	Protein Kinase A
DP	Developed Pressure	PP	Perfusion Pressure
dP/dt_{max}	Maximum rate of Pressure Generation	SAC	Stretch-Activated Channels
ECG	Electrocardiogram	SAC_K	potassium-Selective Stretch-Activated Channels
EDP	End-Diastolic Pressure	SAC_{NS}	Cationic Non-Specific Stretch-Activated Channels
EtOH	Ethanol	SAN	Sino-Atrial Node
GsMTx-4	*Grammostola spatulata* MechanoToxin-4	TRAAK	TWIK-related arachidonic acid-activated K^+ channels
HCN	Hyperpolarization-activated cyclic nucleotide gated	TREK	TWIK-related K^+ channels
ICD	implantable cardioverter-defibrillators	VAC	Volume-Activated Channels
I_f	Funny Current	VE_M	Mechanically-Induced Ventricular Excitation
KH	Krebs-Henseleit	X-ROS	stretch-induced reactive oxygen species
LV	Left Ventricle		

Acknowledgments

First and foremost, I would like to thank Dr. Alex Quinn for the opportunities and the guidance he gave me. Through his continuous support, patience, motivation and immense knowledge, he taught me countless valuable lessons, not only in the academic field, but also in all aspects of life. His unwavering enthusiasm for research kept me constantly engaged with my project. None of this work would have been possible without his open door and numerous hours of discussion with him. I am forever grateful for accepting me to be a part of your research team.

I would also like to thank my past and present lab partners. I thank Peter Baumeister for always motivating me to achieve more and teaching me about the Langendorff apparatus, Eilidh MacDonald for being there during the times of uncertainty, Dr. Matthew Stoyek for his insightful comments and after-hours discussions, Sarah Rafferty for her kindness and helping me with the experiments, Breanne Cameron for her encouraging and passionate nature, and lastly, Martin Mackasey for the much needed distractions. I am thankful for amazing friendships with all of you.

It goes without saying that my appreciation extends to my committee Dr. Robert Rose, Dr. Frank Smith and my chair, Dr. Valerie Chappe for their insightful advice with guidance and my development as a scientist. Also, my appreciation to Dr. Ratika Parkash for providing her clinical expertise as a reader and examiner.

It was an honour to be a part of the Department of Physiology and Biophysics, and I thank the staff, especially Jennifer Graves and Alice Smith, and the graduate students.

Finally, I would like to thank my loving family and friends, especially Esco Moe, Gucci Mane, KD and Triple R, for their prodigious support and love. Thank you all!

Chapter 1: Introduction

1.1 Electrical Pacing of the Heart

The treatment for bradycardia and heart block have been rapidly improving ever since the development of implantable cardiac pacemakers more than half a century ago.[1] It has been reported that about a million new pacemakers and implantable cardioverter-defibrillators (ICDs) are implanted every year worldwide and around 10% of patients face complications with the procedure and/or the device.[2,3] For instance, the first recipient of the first fully implantable pacemaker underwent 23 device implantations throughout his life time.[1] In the beginning, issues with the technical electrical circuitry were not the main problem with these devices, but rather the lack of a reliable power source. The development of lithium-iodine batteries through extensive research ameliorated this limitation and allowed the vast manufacturing and use of pacemaker devices.[4] In addition to the bulk part of the device, the pacing lead has been improved significantly. Older generations of leads were susceptible to dislodgment, insulation failure and caused infections.[1]

Overall, pacemaker technology has advanced considerably and can improve patients' lives significantly, yet the need for technically demanding invasive surgeries to implant and locate the optimal location to place the lead(s) remains a drawback of these devices.

Taking the problems with implantable pacemakers, including implantation/explanation complications, spatial control of stimulation, energy delivery/consumption, and their unavailability for emergency settings into consideration, the concept of leadless pacemakers has become an attractive possible alternative.

Mechanical stimulation, which is a generally well-tolerated, non-invasive means for electrically exciting the heart, has been suggested for this purpose.

Before delving further into mechanical pacing, a basic understanding of the electrical and the mechanical function of the heart is useful. In the following sections, I will briefly summarize the events that lead to excitation and contraction of the heart, and the feedback of the heart's mechanical activity onto its electrical function.

1.2 Cardiac Excitation

It is well known that electrical signals drive contractions of the heart. Based on this, we can divide the cardiac cells into two groups: pacemaker/conducting or working cells. The pacemaker and conducting cells of the heart include the cells of the sinoatrial node (SAN), atrioventricular node (AVN), bundle of His, bundle branches, and Purkinje fibres. SAN pacemaker cells are the main drivers of heart rate. They do not have a resting membrane potential like working myocytes, rather they have a pacemaker potential, known as diastolic depolarization. As the name suggests, this potential causes the spontaneous activation of the pacemaker cells.[5] The main contributors to diastolic depolarization are the funny current and the calcium clock.

1.2.1 Funny Current

The funny current has been shown to contribute to the initial phase of diastolic depolarization. Funny current (I_f) is an inward current of sodium and potassium that is activated by hyperpolarization of the membrane.[5,6] Hyperpolarization-activated cyclic nucleotide gated (HCN) channels are the membrane proteins that allow the passage of this

current. HCN functions in an interesting way in that at more negative membrane potentials more current passes through the channel.[5] This inward current depolarizes the membrane and contributes to diastolic depolarization.

1.2.2 Calcium Clock

Different types and isoforms of calcium channels are expressed in pacemaker cells. They include L- and T-type calcium channels. Ca_v 1.3 isoform of L-type Calcium channels play an important role in depolarizing the membrane via the calcium clock.[7,8] Spontaneous calcium release from these channels cause a slight increase in the calcium concentration of the cytosol. Also, spontaneous calcium release from the ryanodine receptors contributes to the increase in cytosolic calcium concentration. Some of these calcium ions are extruded from the cell by the sodium-calcium exchanger, which exchanges one calcium for three sodium, thus depolarizing the membrane and contributing to diastolic depolarization. In addition, influx of calcium during late depolarization, through Cav 1.3, directly depolarizes the membrane.[9]

The electrical signal initiated in the SAN then propagates through the atria, leading to the contraction of atrial working myocytes, and reaches the AVN. The AVN is also capable of driving heart rhythm, however this only becomes relevant in the absence of SAN function. In the presence of a functioning SAN, AVN serves as a delay point between atrial and ventricular excitation and contraction.[10]

The depolarizing electrical signal is then conducted through the bundle of His, bundle branches and finally the Purkinje fibre network. Purkinje fibres spread the signal

throughout the ventricular tissue. As the depolarizing signal reaches ventricular working myocytes it generates contraction.

1.3 Excitation-Contraction Coupling

The working myocytes are not capable of initiating contraction without a prior depolarizing signal, thus it is the function of Purkinje fibres to transmit the electrical signal to the ventricle cells. The depolarizing signal depolarizes the membrane potential of the sarcolemma of each ventricular myocyte to the threshold of fast sodium channels, which open causing cellular excitation. The depolarization of the sarcolemma is then propagated to transverse (t) - tubules where L-type calcium channels are concentrated. Opening of L-type calcium channels allows influx of calcium ions into the cytosol.[11,12] This increase in intracellular calcium concentration induces release of more calcium through ryanodine receptors on the sarcoplasmic reticulum membrane (which are in close proximity of L-type calcium channels on t-tubules) by a process known as 'calcium-induced calcium release'.[13,14] Calcium ions in the cytosol then bind to troponin C proteins.[15,16] This binding causes dissociation of troponin I from the actin filament.[17] This dissociation is translated to a change in the position of tropomyosin as it is connected to troponin I via troponin T.[16] As tropomyosin is moved, the myosin binding site of the actin becomes free to bind to the myosin heads. Myosin heads then go through a conformational change via ATP hydrolysis and that causes the pulling on the actin filament which causes sarcomere shortening, i.e. contraction.[18,19]

1.4 Mechano-Electric Coupling

The heart is a mechano-sensitive organ, meaning that mechanical alterations can affect its electrical activity. To better understand how mechanical and electrical activity of the heart are intertwined and regulate each other, Kohl *et al*.[20] came up with a useful analogy, which I will use to explain this phenomenon. The heart can be thought of as an electric motor. In many motors, an electrical signal from a power source rotates magnets in the motor that leads to generation of shaft movement and torque. This is analogous to how normal heart contraction occurs; an electrical signal causes depolarization and then contraction of myocytes. Sticking with the motor analogy, in dynamo mode ("reverse mode"), motors can translate the movement of the shaft to an electrical signal. In the heart, changes in the mechanical state of the tissue can cause changes in the electrical function.

To summarize, on one hand an electrical signal provokes a mechanical event, while on the other hand a mechanical signal causes changes in the electrical activity.[20] Together, this comprises the mechano-electric coupling (MEC) phenomenon, an intrinsic feedback loop in the heart that regulates its electrical activity.[21,22] In addition to MEC, mechanical changes can also affect mechanical activity, via another feedback loop termed mechano-mechanic coupling (MMC)[23]. MEC and MMC work in conjunction to keep cardiac output (which is determined by heart rate and stroke volume) at an optimal level. MEC generally regulates the heart rhythm (a classic example is the Bainbridge response, where the heart rate increases in response to increased venous return causing stretch of the right atrium and SAN[24]), while MMC regulates stroke volume (a classic example is the Frank-Starling mechanism, where the force of contraction increases in response to myocyte stretch[25]).[22]

Knowing that mechanical stimulation can affect the electrical function of the heart, it can be utilised to cause mechanically-induced excitation, which leads to contraction.[26–28] If mechanical stimuli are repeatedly applied to the heart, they can theoretically be used to pace the heart. In fact, that is the mechanism behind activation of the heart by chest thumping. Cases of mechanical pacing of the heart for up to 2 hours and 45 minutes have been reported[28,29], suggesting that mechanical stimulation may be used as a well-tolerated and non-invasive means of pacing.

1.5 Mechanical Pacing

One of the first documented cases of mechanical pacing was by Paul Zoll in 1952. It was shown that as long as the ventricles remain excitable, mechanical pacing can be utilized to resuscitate patients with any cause-ventricular asystole or bradycardia.[30] Later in 1976, he designed a safer and more tolerable external mechanical pacing device, which he termed the "cardiac thumper", and demonstrated repeated mechanically-induced heartbeats could be evoked in dogs with normal sinus rhythm and in severe atrioventricular block. The device was also used in patients with disrupted electrical activation of ventricles such as atrial fibrillation, post ventricular fibrillation asystole, and atrioventricular block. The "cardiac thumper" was deemed safe, as there were no cases of mechanically-stimulated tachycardia or fibrillation, and the pain was reported tolerable in most patients, even with energies up to 10 times the threshold intensity. Mechanical pacing utilization is mostly neglected, due to the fear that it might cause ventricular tachycardia or fibrillation.[31] This fear relates to the clear role of MEC in arrhythmogenesis. It has been shown that mechanical stimulation, especially during the vulnerable window (a temporal window

during action potential repolarization in which unidirectional block can be induced by premature excitation in a specific spatial location), may lead to tachycardia or fibrillation.[32,33] For instance, in patients, an increase in ventricular load during valvuloplasty can induce tachycardia[34] and insertion of central venous and pulmonary artery catheters can cause tachycardia when the catheters make contact with ventricular tissue. A more extreme example of mechanical stimulation leading to lethal arrhythmia and fibrillation is *Commotio cordis* (subcontusional mechanical stimulation of the heart that results in ventricular fibrillation).[32]

Based on the evidence provided above, the fear of mechanically stimulated-tachycardia may be justified. Yet mechanical precordial chest thumping has also been demonstrated to terminate ventricular tachycardia.[35] So, the cause can also be the treatment. Although seemingly dangerous, the risk of mechanically-induced ventricular tachycardia is far less than the chance of a patient staying alive until surgical pacemaker implantation.[31] Therefore, it is important to consider mechanical pacing as a means to keep a patient alive in emergency settings. Recently, the potential for mechanical pacing of the heart has been exploited in the form of extracorporeal high intensity focused ultrasound[36] and magnetic bead pulsing.[37]

Extracorporeal high intensity focused ultrasound applied to ventricles in frog[38], mouse[39], pig[40], and rat[41] resulted in mechanically-induced ventricular excitation (VE_M). On the other hand, to cause VE_M by using magnetic force, Rotenberg *et al*. injected magnetic microparticles into the blood stream of rats and pigs, which were collected in the right ventricle using an electromagnet. Electromagnetic pulses were applied to the right ventricle that caused movement of the microparticles towards the magnet, leading to stretch of the

tissue and VE_M. When repetitive stimulation was applied to pace the bradycardic heart, results demonstrated successful temporary pacing, however this lasted several seconds only. They related the loss of capture to the possibility of microparticles escaping due to the experimental setting.[37]

The results of the ultrasound studies show that mechanical stimulation can initiate excitation and contraction. The magnetic pulsing study demonstrates that repetitive VE_M can pace the heart for a short time. Collectively, the results of these studies raise the question as to whether the sustainability of mechanical pacing of the heart is feasible.

To address this question, Quinn *et al*. investigated the sustainability of pacing by mechanical stimulation in the Langendorff-perfused isolated rabbit heart. Local mechanical stimulation by direct epicardial tissue indentation was used to induce VE_M. The result of that study showed a frequency-dependent loss of VE_M, meaning that the higher the rate of pacing, the faster capture was lost. The loss of VE_M was not due to altered excitability of the tissue, since electrical stimulation after a mechanical stimulation that did not induce VE_M still caused excitation, and mechanically-induced excitability returned with time. It was also found that the maximum pacing rate was lower for mechanical pacing when compared to electrical pacing. The results of this study point to the fact that mechanical pacing is in fact not sustainable over long periods of time, even with direct contact of the heart.

The inability to mechanically pace the electrically excitable heart was related to the difference in refractoriness of the tissue in response to the different modes of pacing, meaning the tissue becomes insensitive to further mechanical stimulation for a period of time, while electrical stimulation will still cause an excitation at the same location, a

phenomena known as mechano-electric adaptation /refractory period. It appears there is a different mechanism of refractoriness between the two types. The mechanism of this difference was hypothesised to be "a depletable yet replenishable pool of mechano-electric mediator(s)". This is based on the idea that as 'the mediators' are 'depleted' there is a loss of capture, while after a period of rest the pool of 'mediators' is 'replenished', so that the ability to cause focal VE_M is restored.[42]

While the mediators and the mechanism responsible for the mechano-electric adaptation/refractory period are unknown, various factors have been suggested, including effects of mechanical stimulation on mechanical properties of the myocardium, mechano-sensitive channel activity, intracellular calcium handling, or other unknown factors. In the next section, I will describe these factors and how mechanical stimulation may affect them, leading to loss of VE_M.

1.6 Potential Factors Responsible for the Mechano-Electric Adaptation/Refractory Period

1.6.1 Mechanical Properties of the Myocardium

Mechanical properties of the myocardium contribute to the mechanical state of the organ as a whole and depend on intracellular and extracellular factors.

I) Intracellular Factors:

The sarcolemma, actin-myosin cross bridges, and the cell's cytoskeleton are the intracellular elements contributing to cell stiffness. The role of the sarcolemma is possibly least important, as skinned myocytes' resting stiffness is not substantially different than

the intact cells. Cytoskeleton elements such as titin, desmin and microtubules are the more obvious players in determining the mechanical stiffness of the cell.[43] Titin is located over the A band of the sarcomere and extends into the I-band to interact with the Z disk. It is proposed to be the main contributor to passive stiffness over normal working ranges of sarcomere length.[44,45] Desmin provides an interface between intracellular and extracellular elements.[46] Desmin's contribution to passive tension is less than titin and microtubules.[43] Microtubules are the most abundant filaments in cardiomyocytes. They consist of alpha and beta tubulin heterodimers, which assemble into a polymer to make the filament.[47] The role of microtubules in arrhythmogenesis has been demonstrated in hearts with pressure-overload hypertrophy. Destabilization of microtubules by depolymerization of the tubulin polymers has been shown to increase the vulnerability to arrhythmogenesis, whereas hyperpolymerization of the microtubules reduces arrhythmogenicity.[48,49] On the other hand, microtubule hyperpolymerization has been shown to increase the probability of stretch-induced arrhythmias, potentially through alteration of membrane channels, sarcoplasmic reticulum, or other organelles in the myocytes.[50] It has been demonstrated that the microtubule network becomes denser (up-regulation of polymerization) after increased wall stress, which may contribute to changes in mechanical properties following mechanical stimulation.[51,52] Polymerization of microtubules also decreases the free tubulin dimers in the cytosol, which interact with G-proteins and leads to their activation, which explains the indirect contribution of the microtubule network to intracellular signalling and stress control.[53,54]

Microtubules also play an important role in calcium signalling. A study by Gomes *et al*. showed that depolymerization of microtubules increased calcium current and SR

calcium release. This points to the importance of microtubule dynamics in excitation-contraction coupling.[48] Microtubules, however, do not appear to be the principal contributor to increased longitudinal passive stiffness in diseased heart models[55,56], but rather are involved in modulating the stiffness of myocytes in response to shear stress. This suggests microtubules may act as compression-resistant elements.[57] Thus, as mechanical stimulation, such as direct indentation of the tissue, applies shear stress to the tissue and myocytes, acute changes in the microtubule network may contribute to a loss of VE_M capture.

A study on the role of microtubules in the viscoelastic properties of isolated myocytes showed the importance of viscus drag. Hyperpolymerization of microtubules increases the viscosity of myocytes immediately after cell stretch. Surprisingly, depolymerization of microtubules did not have any effect on myocyte viscosity.[55] This may point to the mechanism of the changes in the microtubule network. In normal cardiomyocytes, the microtubule network is more concentrated in the perinuclear region and it may be extended to run along the myofibrils.[47] Therefore, hyperpolymerized microtubules will extend even longer to cover the length of the sarcomere (Z-line to Z-line), altering diastolic stiffness. The acute effects of repeated exposure to mechanical stimulus, by indentation pacing for instance, on increasing this viscus drag has not been addressed. It is possible that if viscosity is increased with each stimulus, the relaxation of the cytoskeleton and the other intracellular organelles may be impeded, such that the failure to reach complete cellular relaxation may result in loss of VE_M. Altogether, the role of changes in the microtubule network in the unsustainability of mechanical pacing needs to be investigated.

II) Extracellular Factors:

In addition to the intracellular factors described above, the extracellular matrix is another important contributor to passive tissue stiffness. Extracellular matrix components that are important in the heart are collagen, elastin and proteoglycan. Collagen I and III are the main types of extracellular matrix component in the heart and the ratio of these two types have been investigated during heart pathologies such as hypertrophy, failure, and infarct healing.[58–60] In normal hearts, collagen keeps myocytes aligned during systole and prevents extensive stretch of myocytes during diastolic filling.[61,62] In accord with stiffness of the heart, a non-linear positive relationship between stiffness and collagen content has been shown.[62] Many of the studies on the role of collagen in heart mechanics have used the chronic pressure overload model.[63] The relevance of these models for the role of collagen in mechanical pacing is minimal, however, as the turnover of collagen by matrix metalloproteinases take much longer (hours to days)[64] than the time to loss of capture during mechanical pacing . Alternatively, collagen can be degraded and the mechanical changes in the heart can be measured to determine its effect in the acute setting. However, this has proven more difficult. Collagenase treatment of intact hearts induces severe edema, which leads to changes in the mechanical properties of the heart and interpretation of these changes cannot be confidently associated with the role of collagen.[65,66] Because of that, the acute changes in collagen fibres after mechanical stimulation remain to be determined. Overall, collagen has significant effects on the mechanical properties of the heart at the tissue level, however it is highly unlikely to cause the changes that would lead to loss of capture after several seconds of repetitive mechanical stimulation.

The role of changes in cell stiffness in loss of VE_M during mechanical pacing could alternatively be explained by the phenomenon of 'strain softening'. Strain softening, first introduced by Mullins in 1947[67], is the softening of the elastomers when strain reaches a new maximum for the first time. Preconditioning of cardiac tissue by increased load has been shown to cause strain softening, such that with increased mechanical pressure tissue becomes softer, and this softening seems to be independent of time.[68] This could be relevant to loss of VE_M, because if the mechanically stimulated tissue becomes softer with each stimulus, then the sensitivity of the tissue may be reduced, such that the same amount of indentation has a reduced effect, causing a loss of excitation. Strain softening, however, is explained to be a long term effect[68,69], yet repetitive mechanical stimulation is re-gained after a minute of rest.[42] This contradictory point makes strain softening an unlikely mechanism of VE_M loss. The importance of strain softening in viable tissues is less pronounced[69], that being said, the effects of mechanical stimulation-induced strain softening of the tissue cannot be ignored and need to be investigated.

1.6.2 Mechano-Sensitive Channels

The translation of a mechanical event in the heart to a change in electrophysiology occurs primarily through mechano-sensitive ion channels. These channels can be divided into two groups. First, the ones whose main function is modulated by a mechanical event. Second, the ones whose main function is to respond to a mechanical event. In this thesis, I will be focusing on the second group. These mechanosensitive channels can be further broken down into two groups based on the type of stimulation that changes their open probability (i.e., activation). The ones that respond to increased volume are called volume-

activated channels (VAC), and the ones that respond to stretching of the cell are called stretch-activated channels (SAC).[70–72]

VAC activation occurs with an increase in cell volume, for instance swelling of the cell[73], resulting in increased conductance of potassium or chloride currents. Upon increase of the volume of the cell, inorganic ions such as chlorine and bicarbonate are released, which cause loss of water due to decrease of the cell osmolarity after release of the anions. This alleviates the pressure on the membrane as the volume decreases.[74] It is important to note that the activation of VAC occurs with a significant lag period[75], and during normal contraction-relaxation cycles the volume of the cell does not change. Therefore, the role of VAC as a mechanosensitive channel becomes less significant in acute beat-by-beat modulation of electrophysiology during repetitive mechanical stimulation.

On the other hand, SAC are activated by membrane deformation. Based on their ion selectivity, SACs can be subdivided into two groups: potassium-selective (SAC_K) and cationic non-selective (SAC_{NS}). SAC_K current is outwardly rectifying, meaning that the potassium ions flow out of the cell easier than they flow in. The opening of these channels allows efflux of potassium ions, which results in a hyperpolarization of membrane potential and thus hyperpolarization of the cell. Examples of SAC_K include TWIK-related K^+ channels (TREK), TWIK-related arachidonic acid-activated K^+ channels (TRAAK).[76–78] All these potassium channels have a reversal potential that is more negative than the membrane resting potential. Therefore, with regards to the cardiac action potential (AP), the activation of these channels will cause shortening of the action potential duration (APD) and faster repolarization.[79]

SAC_{NS} allow movement of more than one cation, including sodium, potassium and in some cases calcium.[80] The reversal potential of these channels lies somewhere near 0 mV.[81] Therefore, depending on the membrane potential, they may contribute to de- or hyperpolarization of the cell. When membrane potential is more positive than the reversal potential of SAC_{NS} (early repolarization phase of the AP), the activation of these channels will cause earlier repolarization of the membrane and shortening of AP.[82,83] However, once the membrane potential is more negative than the reversal potential of SAC_{NS} (late repolarization phase of the AP), the activation of SAC_{NS} will increase membrane potential and causes depolarization, which if it reaches threshold for fast sodium channels, can induce early afterdepolarization- like events.[84]

SAC_{NS}, in fact, have been shown to be the mechanism behind VE_M. As Quinn *et al*. demonstrated in their study of *Commotio cordis*, VE_M initiates at the point of mechanical contact, with the underlying mechanism involving SAC_{NS}, as it was prevented with the application of *Grammostola spatulata* MechanoToxin-4 (GsMTx-4; a specific SAC_{NS} blocker). Also of note, the downstream properties of excitation wave propagation were compared between local mechanical stimulation and same-site electrical stimulation and there were no significant differences observed, pointing to the fact that once excitation is initiated, propagation through the tissue is the same.[85]

As SAC_{NS} is the channel causing VE_M, properties of this channel may explain the loss of capture with repeated mechanical stimulation. It has been suggested that mechanical stimulation causes a decrease in SAC_{NS} current, such that repeated stimuli will cause a run-down of current, which may result in the loss of the ability to depolarize membrane potential to excitation threshold. Notably, increasing the time between each set of

mechanical stimuli to minutes seems to allow recovery of the channels, and the decrease in the current is no longer observed.[86]

There may also be an interaction between the cytoskeleton and SAC channels. The evidence comes from a study where destruction of tubulin and F-actin with cholchicine or cytochalasin D, respectively, reduced the efficiency of mechanical stimulation and activation of SAC channels coupling.[87]

1.6.3 Intracellular Calcium Handling

SR calcium load has been shown to be reduced with stretch[88,89] and interestingly, stretch increases the frequency of localized calcium release from the SR (calcium sparks), which might be the reason behind the reduction of SR calcium concentration.[90] The increase in calcium spark frequency with stretch is independent of SAC_{NS}, extracellular calcium and nitric oxide synthesis, as blocking them has no effect on spark frequency.[91] The increase in calcium sparks however, appears to depend on the direct transduction of the mechanical stimulus by the cytoskeleton.[90] Repetitive mechanical stimulation can increase the production of stretch-induced reactive oxygen species (X-ROS) via microtubule activation of NADPH oxidase in sarcolemma and t-tubule. X-ROS then can modulate ryanodine receptors to make them leakier, which further contributes to calcium handling dysregulation.[91]

It is noteworthy to mention that cell stretch also increases the sensitivity of troponin C for calcium and with increased calcium levels during stretch (explained by Frank-Starling mechanism), the cross-bridge formation between thin and thick filaments may be altered, which can contribute to alteration in tissue mechanical properties.[92] Stretch has

also been shown to increase intracellular cAMP concentration[86] which can activate PKA, and PKA causes phosphorylation of downstream effectors, such as ryanodine receptors, which may also explain the increased leakiness of these channels and increased calcium spark frequency.[93]

Another possible contributor is nitric oxide (NO). The postulated theory states that stretch can increase the production of NO via phosphatidylinositol-3-kinase dependent signalling pathway in myocytes. NO can then act as a secondary messenger, causing nitrosylation of ryanodine receptors, which modifies their open probability and results in increased calcium release.[94,95]

1.7 Conclusion

Mechanical pacing, as a readily available and well-tolerated means for non-invasive pacing, has attracted researchers to develop different methods to mechanically stimulate the heart. However, difficulties with sustainability of pacing have been constantly encountered, which up until now has been attributed to the experimental setting limitations. Recent investigations have demonstrated that mechanical pacing is in fact unsustainable for long periods of time, even with the most direct method of mechanical stimulation, i.e. direct tissue indentation. No clear mechanism is known to be the reason behind the unsustainability, however different mechanisms have been suggested. Those mechanisms include changes in tissue mechanical properties, mechano-sensitive ion channel activity, and/or intracellular calcium handling. In this thesis I will assess the effects of changes in stiffness, contraction, mechanical stimulation magnitude, baseline rate, and background

electrophysiology, by assessing whether alterations in these parameters affects the sustainability of mechanical pacing.

1.8 Hypotheses

- Hypothesis 1: Changes in mechanical properties of the heart, including stiffness and contraction will change the threshold for VE_M, thus affecting the sustainability of mechanical pacing.
- Hypothesis 2: Lower background rate will allow mechanical pacing at lower rates, therefore increasing the sustainability of mechanical pacing. Also, the rate prior to the initiation of mechanical pacing affects the sustainability.
- Hypothesis 3: Mechanical stimulation causes changes in action potential and/or calcium transient morphology.

1.9 Aims

- Aim 1: Use mechanical property altering agents, such as blebbistatin, paclitaxel, and colchicine, to assess the effect of changes in the mechanical properties of the myocardium on VE_M threshold and the sustainability of mechanical pacing.
- Aim 2: Reduce baseline heart rate and apply various baseline background rates to assess its effect on the sustainability of mechanical pacing.
- Aim 3: Optically map voltage and calcium to assess changes in action potential and calcium transient parameters with mechanical pacing.

Chapter 2: Methods

In this chapter of the thesis, I will first describe the reagents used in the project and then describe the rabbit isolated heart model. This will be followed by a description of the specific protocol and analysis for each experimental group.

2.1 Reagents

2.1.1 Krebs-Henseleit (KH) Solution

The KH solution consisted of NaCl (125 mM), KCl (4.7 mM), $NaHCO_3$ (24 mM), NaH_2PO_4 (1.4 mM), Glucose (10 mM), $MgCl_2$ (1 mM) and $CaCl_2$ (1.8 mM) mixed in double-distilled water. The solution was heated to 37 °C and bubbled with medical grade 95% O_2 - 5% CO_2 gas, to provide oxygen for the cell metabolism and carbon dioxide to adjust the pH. pH and osmolarity were measured to be 7.38 ± 0.00 and 299 ± 0.22 mOsm, respectively.

2.1.2 Blebbistatin (8 μM, in Dimethyl-Dulfoxide, DMSO)

Blebbistatin (B592490, Cedarlane) is an excitation-contraction uncoupler that functions by preventing cross-bridge formation between actin and myosin filaments. It was used to eliminate active tension generation.[96] Blebbistatin studies have shown minimal side effects on cardiac electrophysiology, thus making it the drug of choice to inhibit contraction.[97]

2.1.3 Paclitaxel (5 μM in DMSO)

Paclitaxel (ab120143, Abcam) is a microtubule hyperpolymerizer[98], that binds to the β-tubulin subunit of microtubules and prevents remodelling of the cytoskeleton.[99] It was used to increase passive tissue stiffness.[50]

2.1.4 Colchicine (100 μM in Double-Distilled Dater)

Colchicine (ab120663, Abcam) has been shown to depolymerize the microtubules in intact cardiomyocytes[49] and affect the rate of contraction and relaxation in whole hearts.[50] It was used to decrease passive tissue stiffness.

2.1.5 Ivabradine (Variable Concentration in Double-Distilled Water)

Ivabradine (148849-67-6, Sigma-Aldrich), a well-known funny-current blocker, was used to reduce heart rate. Ivabradine acts by blocking the pore of the HCN channels in the open state therefore reducing the slope of the diastolic depolarization.[100]

2.1.6 di-4-ANBDQPQ (27.4 mM Stock in 100% EtOH)

A voltage sensitive styryl-based potentiometric fluorescent dye, di-4-ANBDQPQ (di-4-PQ; acquired from the University of Connecticut Health Center, Farmington, CT), was used to measure epicardial electrical activity. di-4-PQ is incorporated into the cell membrane in a manner that the photosensitive chromophore is exposed to the extracellular space.[101] Changes in the membrane potential, i.e. depolarization and repolarization, cause a conformational shift in the dye, which is perceived as spectral shifts in the emitted

fluorescent light. This voltage dye was used specifically for its excitation and emission properties. di-4-PQ can be excited between ~450-700 nm and emits light at a wavelength in the near-infrared region.[102] Greater temporal stability and the ability to image deeper depth of the tissue due to the red-shifted excitation spectra are the notable advantages of di-4-PQ over other voltage dyes.[101]

2.1.7 Rhod-2-AM (0.89 mM Stock in DMSO)

To image intracellular calcium changes, a rhodamine-based calcium dye, Rhod-2-AM, was used (#142780, Abcam). This dye was used because of its longer excitation wavelength and 100-fold increase in emission intensity after binding to calcium.[103] This dye holds a BAPTA-based component, which is a calcium chelator, and an acetoxymethyl (AM) residue, that allows the dye to cross the membrane. Once intracellular, the AM residue is cleaved by esterases in the cell. This cleavage activates the dye. Thirty minutes of incubation with the dye was allowed for the dye to be taken up and cleaved at the physiological temperature for the optimal activity.[104] Rhod-2 was specifically chosen because even though the excitation wavelength of Rhod-2 excites the voltage dye as well, the changes in the membrane voltage do not change the emission fluorescence of the voltage dye at that Rhod-2's excitation wavelength, described as the "isosbestic point" of di-4-PQ.[105]

Since this dye chelates calcium in the process of indicating calcium levels, it may alter the effective amount of calcium. Control experiments were performed by Peter Baumeister in our lab to address this issue. He found that the levels we use do not significantly affect the calcium activity in the heart.

2.2 Rabbit Isolated Heart Model

Rabbits have been used as the most relevant model for cardiac electrophysiology research.[106] What makes rabbit's heart the most relevant small animal cardiac model are its similarities to the human heart. Those similarities include the regional patterns of myocardial deformation[107], cardiomyocyte electrophysiology (including the long calcium-dependent plateau phase in the action potential[108], and repolarizing currents[109]), heart size to excitation wave ratio (which is the indication of wave pattern and vulnerability to arrhythmogenesis[110]) and the coronary anatomy.[111]

Our experiments followed the guidelines put forth by the Canadian Council on Animal Care on using animal models for research. Female New-Zealand White rabbits (Charles River- Montreal, Canada) weighing 2192 ± 12 g were euthanized via injection of a lethal dose of pentobarbital (140 mg/kg) (Cerva Sante Animale) mixed with heparin (2000 units/Kg) (#SLBL4709V, Sigma-Aldrich) into the main marginal ear vein. Once the injection was successfully completed, the eye reflex to touch and pain withdrawal response to toe pinch were assessed to make sure the animal was non-responsive. The abdominal cavity inferior to the xiphoid process was surgically opened to expose the diaphragm. Then, access to the chest cavity was granted by cutting the diaphragm along the anterior wall of the chest cavity. The rib cage was cut along the lateral walls. The heart was rapidly excised and placed in a small dish containing KH solution and 0.1 mL of heparin. The ascending aorta was located and cut right below the branch of brachiocephalic trunk. Then, the aorta was securely cannulated via a 3-0 wax-coated silk suture to a Langendorff-apparatus. In all experiments, a minimum distance of 5-10 mm was allowed between the

ligation site of the ascending aorta and the aortic valve. This allowed unhindered perfusion of the coronaries and the heart.

The heart was perfused with 37 °C KH solution bubbled with 95% O_2 - 5% CO_2 gas. The solution was passed through an 11μm diameter nylon filter (#NY1102500, Millipore) to perfuse the heart in a retrograde fashion at a constant flow of 20 mL/min (Masterflex L/S, Cole-Parmer). The constant flow allowed constant perfusion of the heart regardless of the coronary resistance, whereas if we used constant pressure the perfusion of the heart could have been affected due to changes in resistance of the coronaries due to mechanical stimulation, and in extreme cases this could have caused ischemia. The flow rate was measured with a flowmeter (#FLR1001, Omega Engineering). The aortic perfusion pressure was measured with a pressure transducer (#MLT0699, ADInstruments) located at the cannula. The effluent solution was collected off of the heart via an in-house made dish and was pumped back into the main solution chamber throughout the experiment.

A drain made from 18G intravenous cannula was pushed into the left ventricle (LV) through a left atrial incision and across the mitral valve, then it was inserted into the apex to allow emptying of the coronary return from the Thebesian veins and prevent fluid build-up in the LV. A custom-made pre-stretched deflated polyethylene balloon, attached to a pressure transducer (#MLT0699, ADInstruments), was inserted into the left ventricle by the same route to measure the left ventricular pressure. The balloon was secured in the ventricle by the tip of the balloon anchoring to the apical drain, and a surgical tie around the left atrium at the mitral orifice. The balloon was filled with enough water to achieve a diastolic pressure of ~5 mmHg, then the opening was closed to allow isovolumetric

contraction. Pacing hook electrodes were placed at the apex to allow apical pacing. Two electrocardiogram (ECG) leads were placed on the LV, one near the base and one at the apex, to record the electrical activity of the heart. A super-fusion line was placed close to the heart to perfuse the surface with warm KH solution to prevent drying.

To achieve lower heart rates in order to be able to pace at lower rates, the sinoatrial node was removed by excising parts of the right atrium. A custom-made sylgard cradle was positioned in such a way that the heart was laying comfortably on it, and there was enough support to contain the heart from abrupt movement during mechanical pacing. Local mechanical stimuli were applied at the mid-LV free-wall, avoiding major coronary vessels. The epicardial indentation with a contact area of 7.8 mm^2 was accomplished by forward and reverse motion of a probe coupled to a DC-servomotor (LM 1247-02-01; Faulhaber Mini Motor SA). The indentation depth was controlled by a motion controller processor (MCLM 2006 S; Faulhaber Mini Motor SA) and manipulated by custom programs developed in Motion Manager (Faulhaber Mini Motor SA). All mechanical stimuli were applied at the highest possible speed. A sample image of the mechanical stimulation Langendorff apparatus is shown in Figure 1.

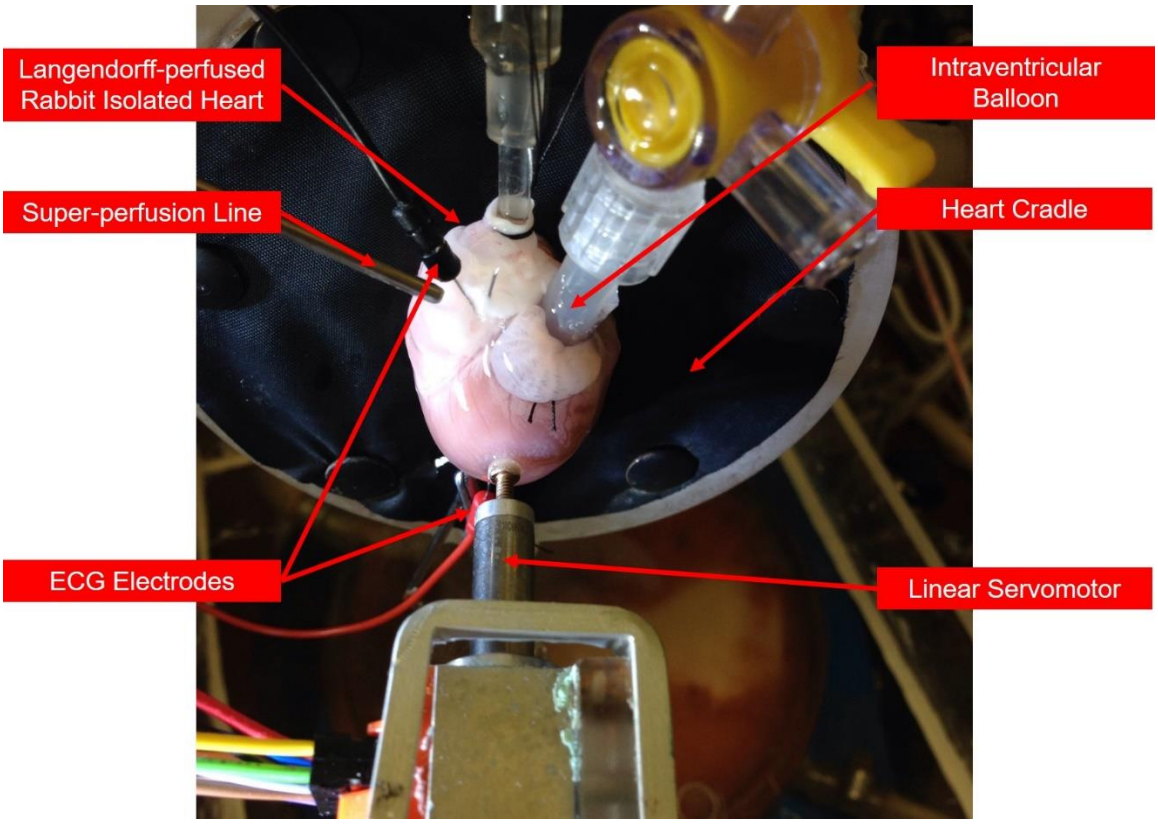

Figure 1. The Langendorff apparatus. Counter clockwise starting at the top left corner: the rabbit isolated heart attached to the cannula by the ascending aorta, the super-perfusion line dripping KH solution on the surface of the heart to keep it warm and moist, the ECG electrodes attached to the base and apex of LV, linear servomotor that mechanically stimulates the LV, heart cradle providing support for the heart from behind to prevent abrupt movement of the heart during mechanical stimulation, isovolumetric intraventricular balloon inserted in the LV through the left atrium and across the mitral valve, connected to a pressure transducer that monitors LV pressure.

2.3 Procedures

The protocol for each experimental group is described in detail below.

2.3.1 Blebbistatin

For these experiments (*n*=10), a total of four repeated measurements of mechanical pacing (m-pace) were applied. Two runs before and two runs after the incubation with blebbistatin. The protocol for each run is depicted in Figure 2. Each run consists of eight trains of stimuli from 2.5 Hz, with increasing rate in 0.5 Hz increments, to 6 Hz. 2 min of no pacing was allowed between each train as shown in figure 2. A 5 min rest period was allowed between each m-pace. The mechanical stimulation indentation was 4 mm in these experiments. This intensity was chosen because it caused VE_M every time, with no relation to the threshold. The train of stimuli were carried out for 50, 25, 12, 6, 5, 5, 5, 5 seconds for 2.5-6 Hz, respectively. In the case where the capture lasted more than the time specified, the pacing was allowed to continue until loss of capture. During the 30 min incubation period, 600 μL of blebbistatin (10 mM) was then added to 750 mL of re-circulating KH (for a final concentration of 8 μM). The number of beats to loss of capture before and after blebbistatin was measured offline using the LabChart software (ADInstruments).

2.3.2 Paclitaxel

Preliminary experiments (*n*=4) were carried out to determine the effects of paclitaxel on our whole heart model. 375 μL of 10 mM paclitaxel stock was added to 750 mL of re-circulating KH (5 μM final concentration). Force with indentation from 0-4 mm in 1 mm increments was measured by a force transducer every 15 min for three hours to assess stiffness.

The protocol for the paclitaxel experiments (*n*=7) is shown in Figure 3. For each mechanical pacing (m-pace) run, first, the stiffness was assessed by force-indentation, then the threshold for mechanical stimulation was determined. To determine the threshold, the heart was electrically paced at 2.5 Hz, and a mechanical stimulation was applied at 300 ms starting from 0.25 mm indentation, and was increased in 0.25 mm increments. Once three consecutive VE_M's were captured, that indentation depth was determined to be the threshold. A run of mechanical pacing until loss at rates 2.5-6 Hz in 0.5 Hz increments, at 1.5x the threshold with 2 min of normal rhythm in between the stimuli trains was applied, as shown in Figure 2. After the pacing protocol was completed, the mechanical stimulation threshold and stiffness were again measured. After 5 min of normal rhythm, the same was repeated at 2x the threshold of the previous run. 375 μL of 10 mM paclitaxel was added to 750 mL of re-circulating KH (5 μM final concentration). A 90 min incubation was allowed for the paclitaxel to act on the heart. During this incubation period, the stiffness was measured every 15 min. After the incubation period, the same protocol as the first run was repeated and the mechanical stimulation was applied at 1.5x the threshold measured during the first run.

The number of beats to loss of capture, as well as the stiffness measured from force-indentation and pressure hemodynamics (end diastolic pressure, maximum systolic pressure, developed pressure, pressure decay [LV tau], maximum rate of developed pressure [dP/dt_{max}], and perfusion pressure) were determined.

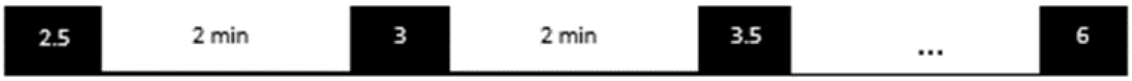

Figure 2. A typical mechanical pacing run protocol. Black boxes represent mechanical pacing and the white numbers in the boxes represent the rate of pacing (in Hz). The empty spaces between the boxes represent the normal rhythm periods. The pacing started at 2.5 Hz and was increased by 0.5 Hz each time up to 6.0 Hz, unless stated otherwise.

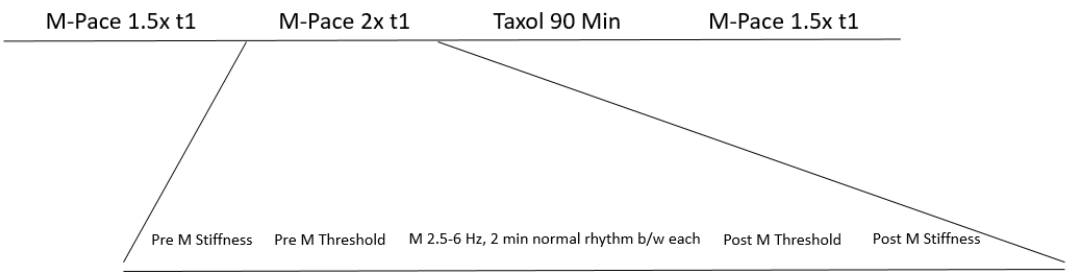

Figure 3. An example of the protocol for paclitaxel and no drug experiments. Each mechanical pacing period (m-pace) consisted of initial stiffness and threshold measurements, followed by a mechanical pacing run (M) as explained in Figure 2, and ended with threshold and stiffness measurements. The first m-pace was applied at 1.5x the pre first m-pace threshold (t1), the second was 2x t1, and third was 1.5x t1. Paclitaxel incubation was 90 min and stiffness was measured every 15 min during that period.

2.3.3 Colchicine

Preliminary experiments (*n*=3) were carried out to determine the effects of colchicine on the whole heart. 7.5 mL of 10 mM colchcine was added to 750 mL of re-circulating KH (for a final concentration of 100 μM). Stiffness by force-indentation was measured every 15 min for three hours. No further colchicine experiments were carried out as these experiments showed no evidence of reduced stiffness with colchicine application.

2.3.4 No Drug

Preliminary experiments (*n*=3) were carried out to determine the effects of time on the whole heart. 750 mL of KH was re-circulating. Stiffness by force-indentation was measured every 15 min for three hours.

The same experiment (*n*=7) as with paclitaxel was carried out, except no drug was added. The same measurements were determined for analysis. This experimental group is the control to the paclitaxel experiments.

2.3.5 Ivabradine

A total of three m-pace runs were applied in these experiments (*n*=9). The first run was applied as shown in Figure 2. Then, enough ivabradine was added to reduce the beating rate to less than 60 beats per minute, which allowed pacing at 1 Hz. The second m-pace was carried out in the same way as before, except the pacing rate started at 1 Hz, instead of 2.5 Hz. After 5 min of rest time, the third m-pace was carried out similar to the second m-pace, 1-6 Hz, except the heart was electrically paced during the 2 min rest periods between each train of stimuli. The rate of electrical pacing was determined to be the same

as the beating rate post SAN removal. This allowed beating rate matching prior to the mechanical stimuli.

2.3.6 Optical Mapping After Loss of Capture

A dual-parametric optical mapping technique was used to image voltage and calcium on the surface of the heart after loss of capture in these experiments (*n*=9). Excitation was alternated between green (Ex.1. 550 ± 10 nm) and red (Ex.2. 640 nm ± 10 nm) LED lights to excite Rhod-2 and di-4-PQ's isosbestic point or di-4-PQ, respectively. The emission light was filtered through a multi-bandpass filter (Em.1. 590 ± 20 nm; Em.2. 800 ± 100 nm) and captured at 500 frames/sec by a sCMOS camera (167 μm/pixel) with the image area of 350 x 550 pixels (Figure 4)

A 200 μL bolus of 0.89 mM Rhod-2 solution in DMSO was delivered in 4 μL increments over 2.5 min directly into the injection port of the aortic cannula, and the perfusate was collected to prevent re-circulation of the dye. Thirty minutes of incubation period was allowed. During this period, a 20 μL bolus of 27.4 mM di-4-PQ solution was delivered in 0.4 μL increments over 2.5 min. 600 μL of 10 mM blebbistatin (8 μm final concentration) was added to 750 mL of re-circulating KH in the incubation period as well, to eliminate motion artefact.

Once the incubation period was over, the threshold for mechanical stimulation was determined. A run of mechanical pacing until loss at rates of 2.5-6 Hz in 0.5 Hz increments, at 1.5x the threshold with 2 min of normal rhythm in between the stimuli trains was applied (Figure 2). Immediately after the termination of mechanical pacing, electrical pacing from the apex and imaging were initiated. Ten seconds videos were captured every 30 seconds

for 5 min. The pacing and imaging were repeated. A run of mechanical pacing until loss at 2.5 Hz at 1.5x the threshold was applied. Immediately, after the termination of mechanical pacing, electrical pacing from the apex and imaging were initiated. Ten seconds videos were captured every 30 seconds for 5 min. This was repeated for another two runs. Another three runs at 5 Hz were applied to investigate the effect of higher pacing rates.

To differentiate between the effects of mechanical and electrical pacing on the voltage and calcium activity of the heart, a separate experimental group (n=7) was designed. A run of mechanical pacing until loss at 2.5 Hz at 1.5x the threshold was applied. Immediately, after the termination of mechanical pacing, electrical pacing from the apex and imaging were initiated. Videos were captured for 10 seconds, every 30 seconds for 5 min. Then, the same was repeated, except with local electrical pacing from the same location that mechanical pacing was applied. The duration of electrical pacing was as long as mechanical pacing previously determined from the first run.

For all of the optical mapping experiments, data were analyzed using custom programs in Matlab (MathWorks). The pixels that did not contain fluorescence from the heart were eliminated. A region of interest was selected on the central section of the LV free-wall. The voltage signal was inverted because depolarization decreases the fluorescent emission signal intensity. The signals were temporally filtered using a 60 Hz low-pass filter. The images were smoothed by averaging 11x11 pixels window without erosion. The isochronal maps of upstroke velocity (first derivative of maximum change in fluorescence), duration to 80% repolarization (time from peak upstroke to 80% recovery; APD_{80} and calcium transient duration $CaTD_{80}$) and repolarization times for voltage and calcium were made.

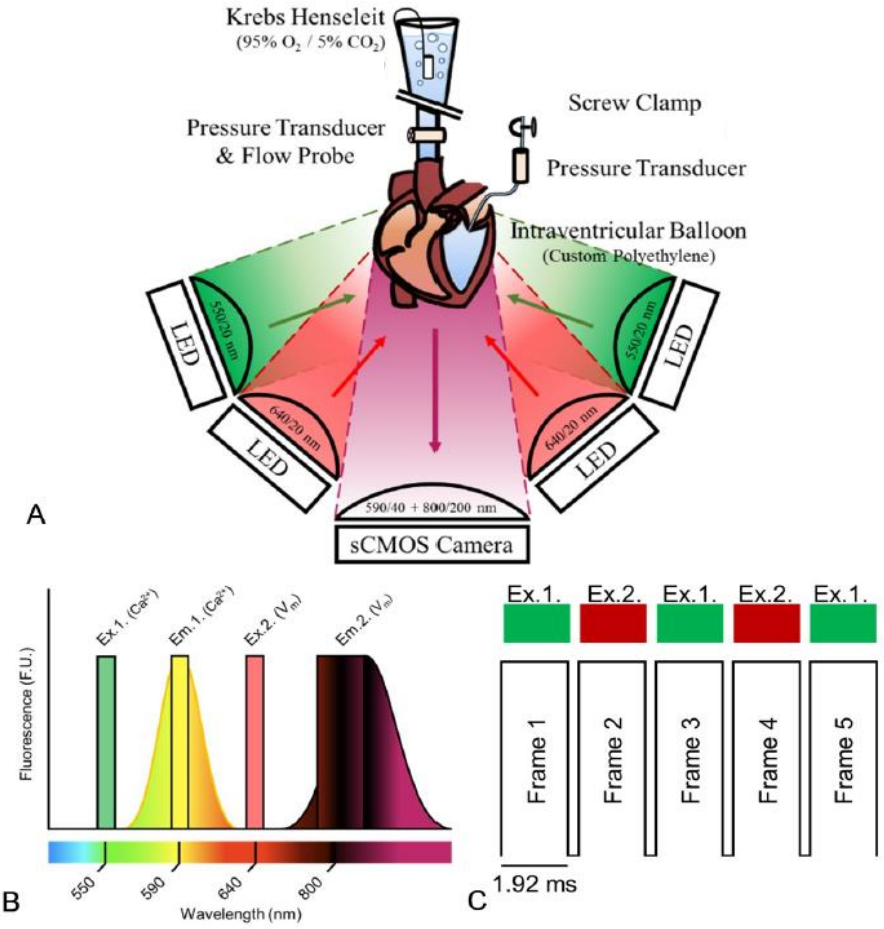

Figure 4. A schematic of the optical mapping setup. A) The red and green LED lights with their corresponding excitation wavelength are located on the sides and the camera with its corresponding multi band-pass filter is at the bottom. B) Illustration of excitation and emission spectra of Rhod-2 (Calcium) and di-4-PQ (Vm). C) Example of camera frames capturing alternate excitation lights.

2.3.7. Optical Mapping During Loss of Capture

Experiments with simultaneous imaging and mechanical pacing were carried out (n=7). The camera and the axis of the motor were 90^o apart, and a run of mechanical pacing until loss at 2.5 Hz at 1.5x the threshold and imaging were initiated, simultaneously. (Figure 5). The motion from the mechanical stimulation was captured as a sharp upwards signal. The delay between that sharp stimulation signal and initiation of action potential was observed to be increasing with every stimulation from the first to last beat captured (Figure 6).

A custom-made Matlab program was used to measure the delay between the mechanical/electric stimulation signal and initiation of the action potential.

At the end of the stimulation-excitation delay experiments, two additional experiments were carried out. First, the possibility of re-capture with increased indentation after the loss of capture, was investigated. A control run of mechanical pacing at 2.5 Hz at 1.5x the threshold was applied. After 2 min of normal rate rest period, the same was repeated however, once the capture was lost, the indentation was immediately increased to 2.0x the threshold.

In addition, the effect of sub-threshold pacing on refractoriness of the tissue to mechanical stimulation was investigated. The heart was paced at 0.5x the threshold for three times as long as the control run in the previous step, then immediately, the indentation depth was increased to 1.5x the threshold.

The number of beats captured was determined in both cases.

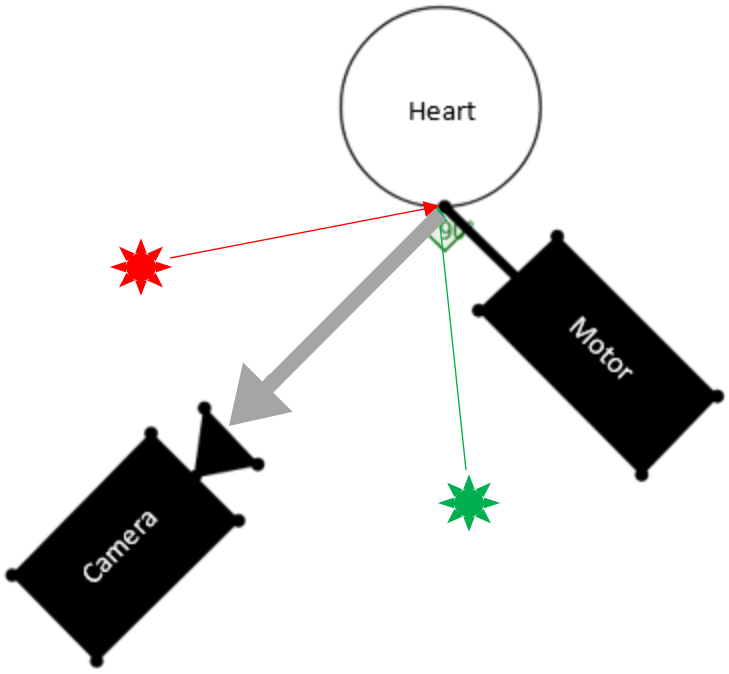

Figure 5. A top view schematic of the stimulation-delay experiment setup. The servomotor and its shaft are shown on the right and the shaft is touching the surface of the heart. The camera is shown on the left. The red and green LEDs, shown by red and green lights respectively, excite the heart and the emission light, shown in grey, is captured by the camera. The camera and the motor are 90^{o} apart, as shown by the right angle.

2.4 Statistical Analysis

To compare sustainability curves, the area under the curve (AUC) was calculated using custom-made programs in Matlab. To compare two paired measurements, 2-tailed paired t-test was used in Microsoft Excel. To compare multiple time point measurements within an experiment, One-way ANOVA, with Tukey post-hoc analysis was used in SPSS.

Chapter 3: Results

3.1 Effect of Blebbistatin (Reduced Active Force)

Blebbistatin was the first agent used to assess the role of active force generation, i.e. contraction, on the sustainability of repeated VE_M capture (*n*=10). Supra-threshold mechanical stimulation caused an excitation followed by a contraction. An increase in the rate of stimulation decreased the number of captured VE_M, as shown previously[42], meaning that the number of beats continuously captured is inversely proportional to the rate of stimulation. After the addition of blebbistatin, the amplitude of the generated LV pressure was decreased to ~1-3 mmHg (Figure 6). There was no significant reduction in the number of continuous VE_M captured with blebbistatin compared to the control setting (p=0.14) (Figure 7). The area under the curve was used for statistical comparison (Figure 8).

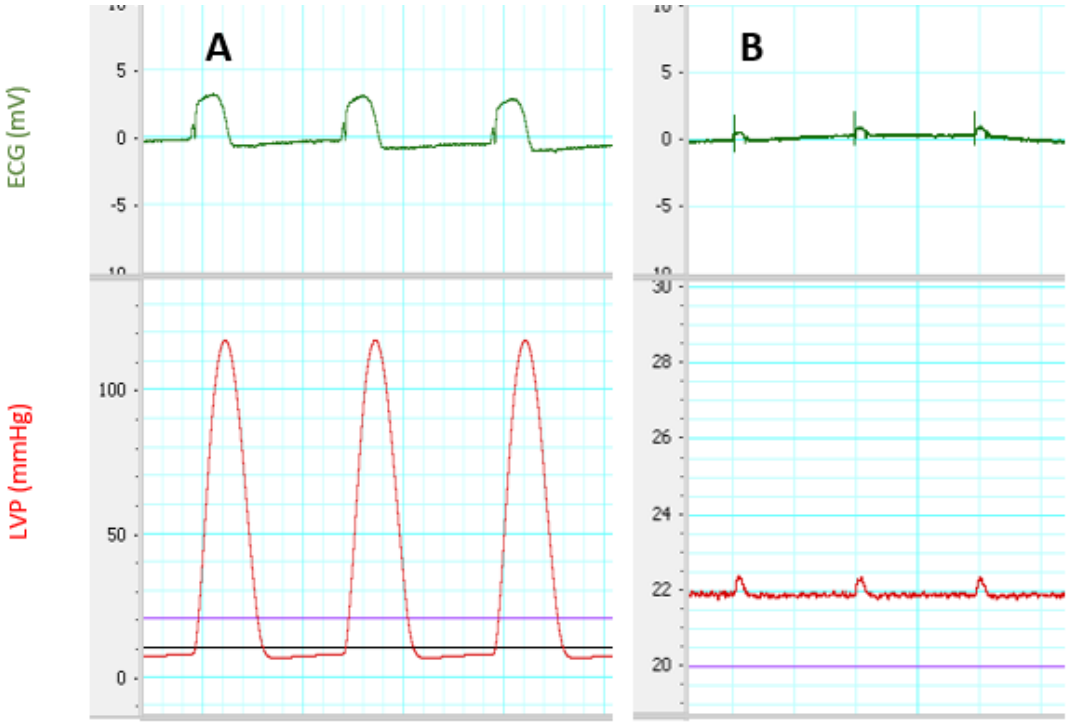

Figure 6. An example tracing of ECG and LVP during normal conditions and with blebbistatin. (A) Normal conditions: Top: ECG (green). Bottom: LVP (red) with the diastolic pressure of ~5 mmHg and systolic pressure of ~115 mmHg. (B) With blebbistatin: Top: ECG (green). Bottom: LV pressure (LVP) (red) with the diastolic pressure of ~22 mmHg and systolic pressure of ~22.5 mmHg.

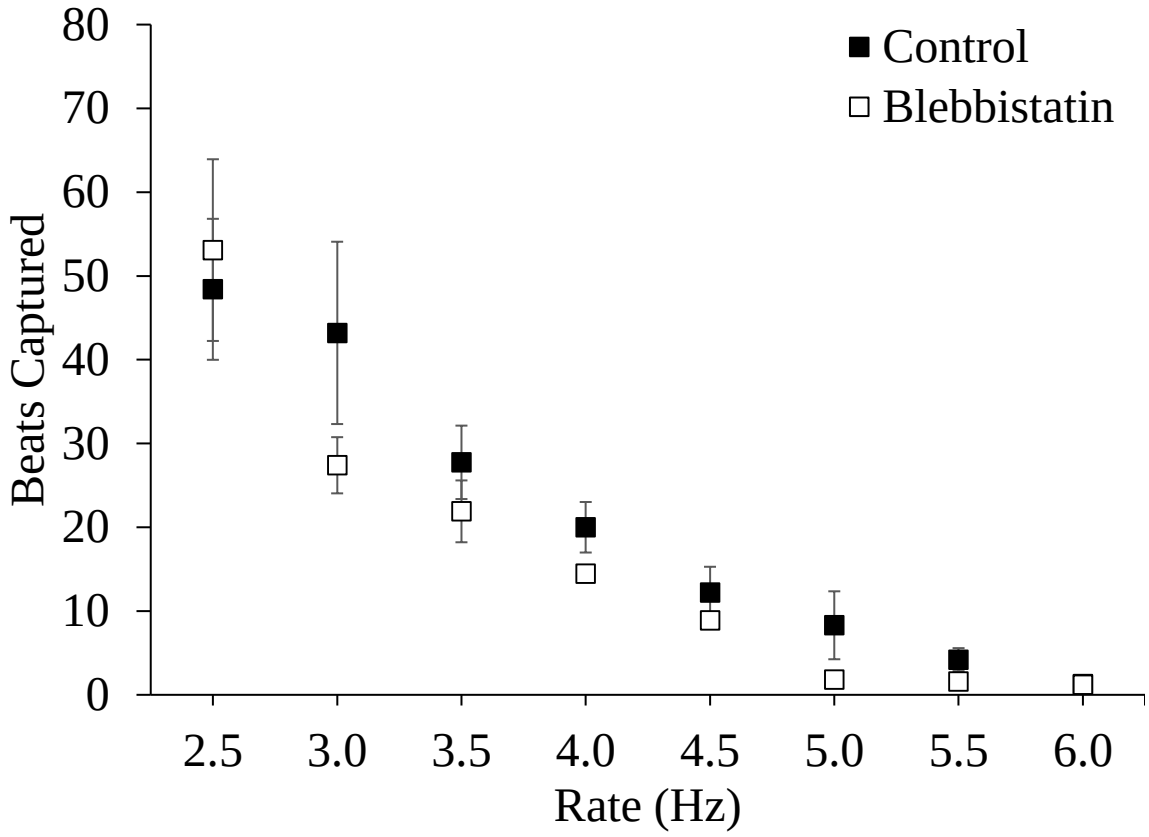

Figure 7. The number of beats to loss of capture with blebbistatin. The number of beats to loss of capture are shown at different frequencies, during control condition (white squares) and with blebbistatin (black squares). A decrease in the number of continuous beats captured is seen with an increase in the rate.

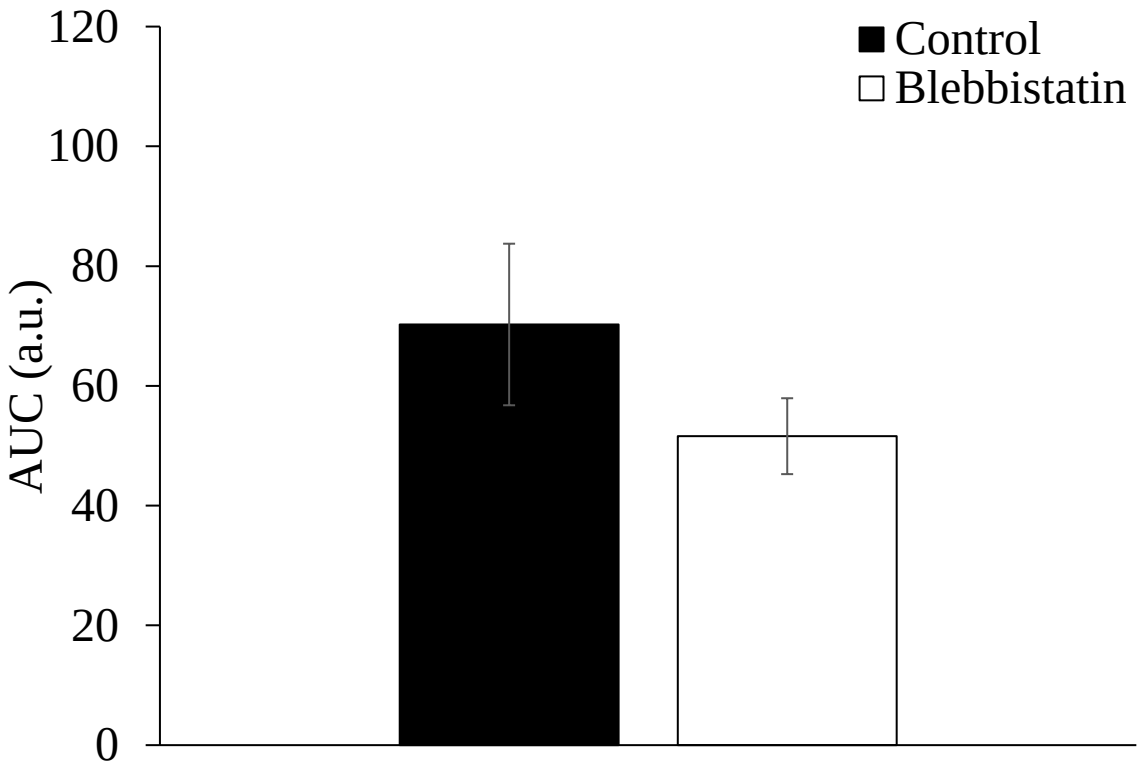

Figure 8. The average area under the curve (AUC) for data from Figure 7. The black bar shows the AUC of the 2.5-6 Hz VEM graph in control. The white bar shows the AUC of the 2.5-6 Hz VE_M graph with blebbistatin. The AUCs were not significantly different (*n*=10, p=0.14).

3.2 Effect of Paclitaxel (Increased Passive Stiffness)

Paclitaxel was used to increase the passive (diastolic) tension, i.e. stiffness. Preliminary experiments (n=4) were carried out, in which paclitaxel was added to the solution chamber and stiffness was measured every 15 min, for 3 hours. The stiffness of the tissue during diastole and systole over time with paclitaxel, estimated by measuring the force needed for 0-4 mm indentation, is shown in Figures 9 and 10, respectively. The diastolic force was qualitatively increased over time with paclitaxel (Figure 9). This qualitative pattern of increase was absent in systolic stiffness (Figure 10).

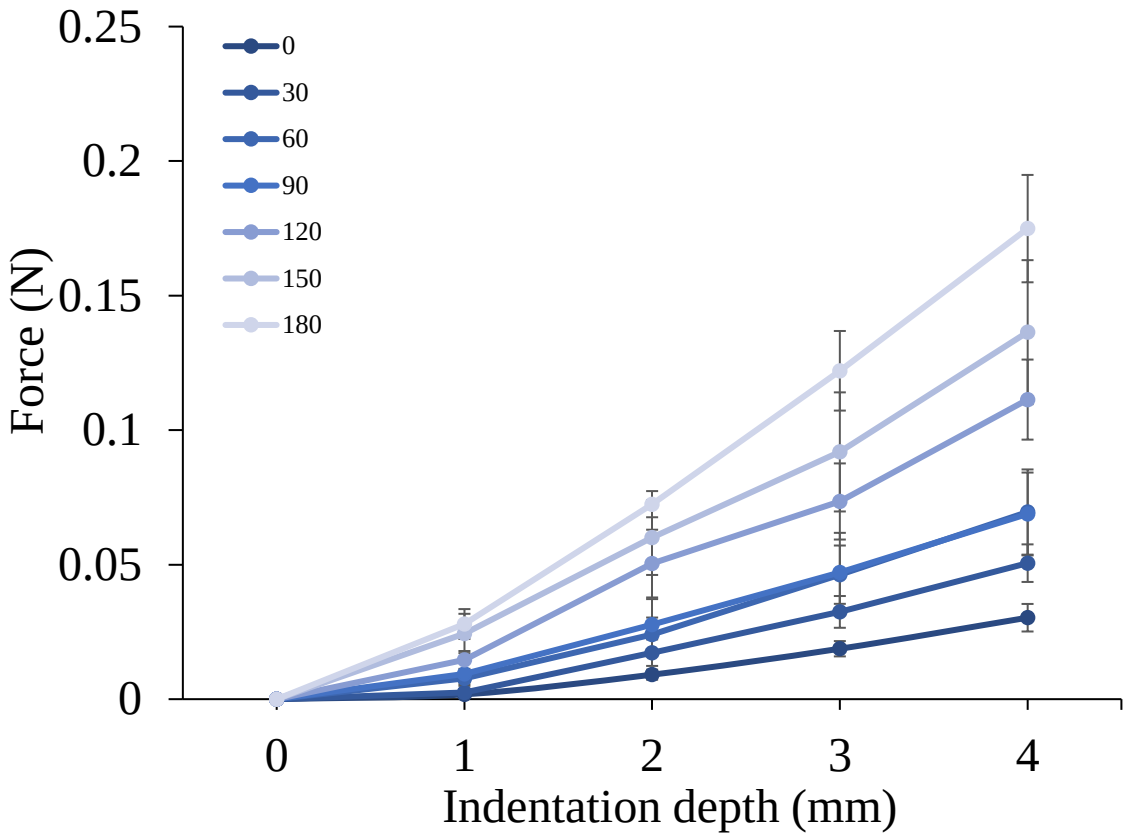

Figure 9. The diastolic force response to indentation in preliminary Paclitaxel experiments. The diastolic force response to indentation from 0 to 4 mm (stiffness), over 180 min with paclitaxel. The lines are coloured according to the time, so the light coloured lines represent later times and dark ones represent the earlier times. Stiffness was measured every 15 min (although the plot shows 30 min intervals). Stiffness was qualitatively increased over time with paclitaxel. (*n*=4)

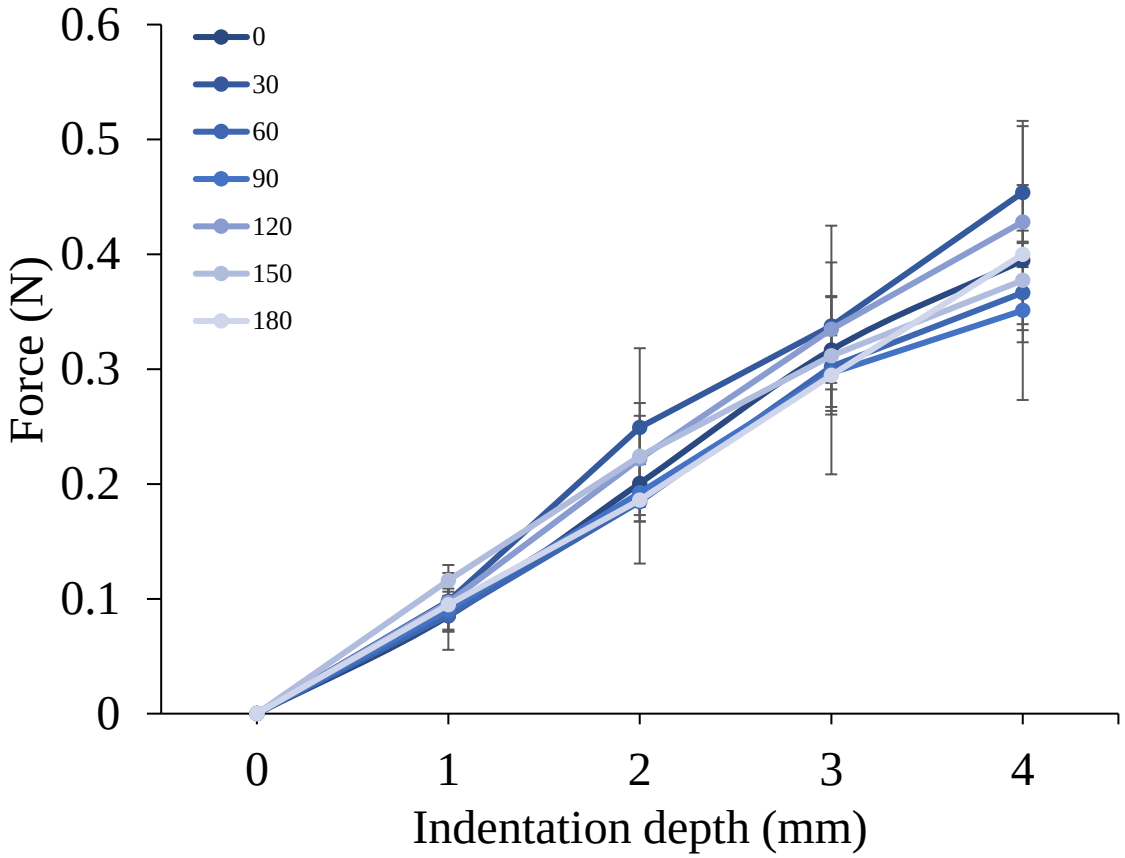

Figure 10. The systolic force response to indentation in preliminary Paclitaxel experiments. The systolic force response to indentation from 0 to 4 mm (stiffness), over 180 min with paclitaxel. The lines are coloured according to the time, so the light coloured lines represent later times and dark ones represent the earlier times. Stiffness was measured every 15 min (although the plot shows 30 min intervals). No obvious change in the stiffness is seen in response to paclitaxel.

Once an increase in tissue stiffness with paclitaxel was demonstrated in our preliminary experiments, experiments looking at the effect on VE_M were carried out (n=7). The force during diastole and systole was measured at 0-4 mm indentation, at two locations: the mechanical stimulation site on the free wall of LV and a remote location that was not affected by mechanical stimulation. With paclitaxel, diastolic stiffness at the mechanical stimulation site was increased significantly (Figure 11). There also appeared to be a small increase in diastolic (Figure 12) and systolic (Figure 13) stiffness immediately after mechanical pacing, however this was not significant.

Stiffness was also measured at a remote location after each mechanical pacing run as an internal control to remove the possible effect of mechanical stimulation on stiffness. The diastolic stiffness was significantly increased after the paclitaxel period (Figure 14 and 15), while systolic stiffness at the remote location did not change significantly (Figure 16 and 17).

Hemodynamic measurements were also analysed. The end diastolic pressure (EDP) was significantly increased with paclitaxel (Figure 18). The maximum systolic pressure (MSP) wasn't different after incubation with paclitaxel (Figure 18). The developed pressure (DP), which is the amount of pressure generated by the LV with contraction and is measured by MSP-EDP, was significantly reduced with paclitaxel (Figure 19). The maximum rate of change of pressure, measured as the first derivative of the pressure wave (dP/dt_{max}), was significantly lower with paclitaxel (Figure 20). The relaxation constant, LV tau, did not change with paclitaxel (Figure 21). Finally, the perfusion pressure was significantly increased with paclitaxel, pointing to the increased resistance of coronaries (Figure 22).

Paclitaxel caused a decrease in the indentation threshold for VE_M capture, while there was no change in the control group (Figure 23). Most importantly, paclitaxel did not change the capturing of continuous VE_M, meaning that with the same amount of indentation, the number of continuous successful VE_M was not different pre- and Paclitaxel (Pre Paclitaxel 1.5x vs. Paclitaxel 1.5x; Figure 24). On the other hand, an increase in indentation significantly increased the number of VE_M captured (Pre Paclitaxel 1.5x vs. Pre-Paclitaxel 2.0x). The statistical comparison was done using the area under the curves (Figure 25).

The fact that a larger indentation depth resulted in a larger number of beats captured suggested that the loss of pacing capture is due to 'relative' rather than 'absolute' refractoriness, and that capture could be re-established with a dynamic increase in indentation depth after loss of capture. This was investigated by increasing indentation depth immediately after loss of capture from 1.5x to 2.0x the threshold. This increase in stimulus strength resulted in additional VE_M. In this experiment (n=6), the number of beats to loss of capture at 1.5x the threshold was 26±8.5, with an additional 15.8±4.3 beats captured once indentation depth was increased.

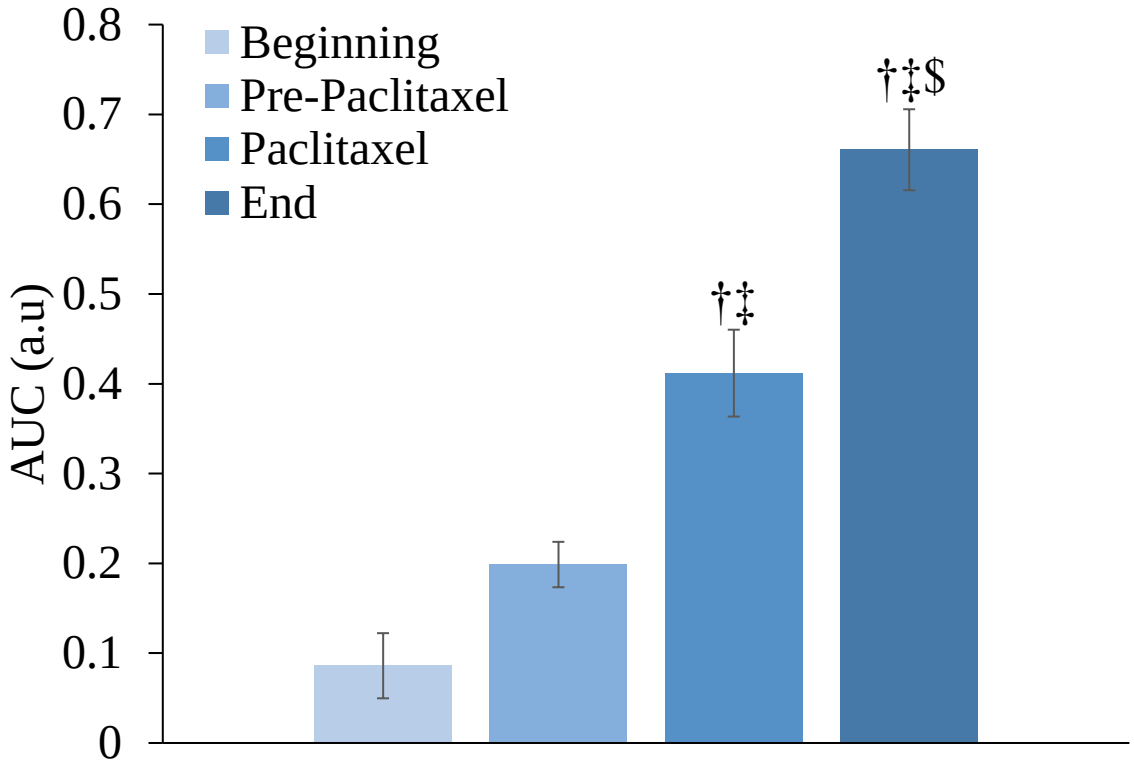

Figure 11. The area under the curve (AUC) of the diastolic stiffness curves in Paclitaxel experiments. The AUC of the stiffness curves measured by indentation force at 0-4 mm at four different time points throughout the experiments is used. The AUC was significantly increased with paclitaxel. †: vs. beginning. ‡: vs. pre-paclitaxel. $: vs. Paclitaxel. (One-way ANOVA, Tukey post-hoc test, $p < 0.05$) (n=7)

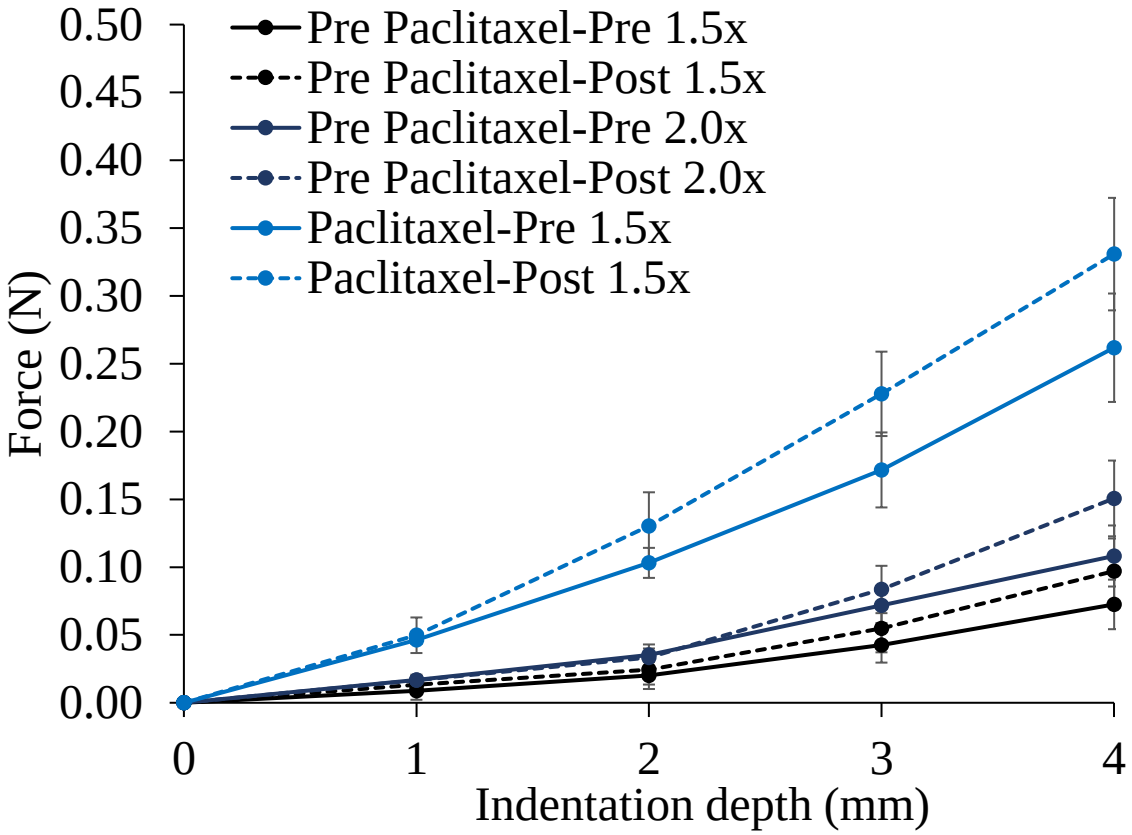

Figure 12. Mean diastolic stiffness before and after each mechanical run without and with paclitaxel. The solid lines represent the pre mechanical pacing measurements. The dashed lines represent the post mechanical pacing measurements. The dashed lines are always higher than their corresponding solid line, however this increase was not statistically significant. Post-drug measurements were all higher than pre-drug ones, which indicates qualitative increased stiffening of the tissue with paclitaxel. (*n*=7)

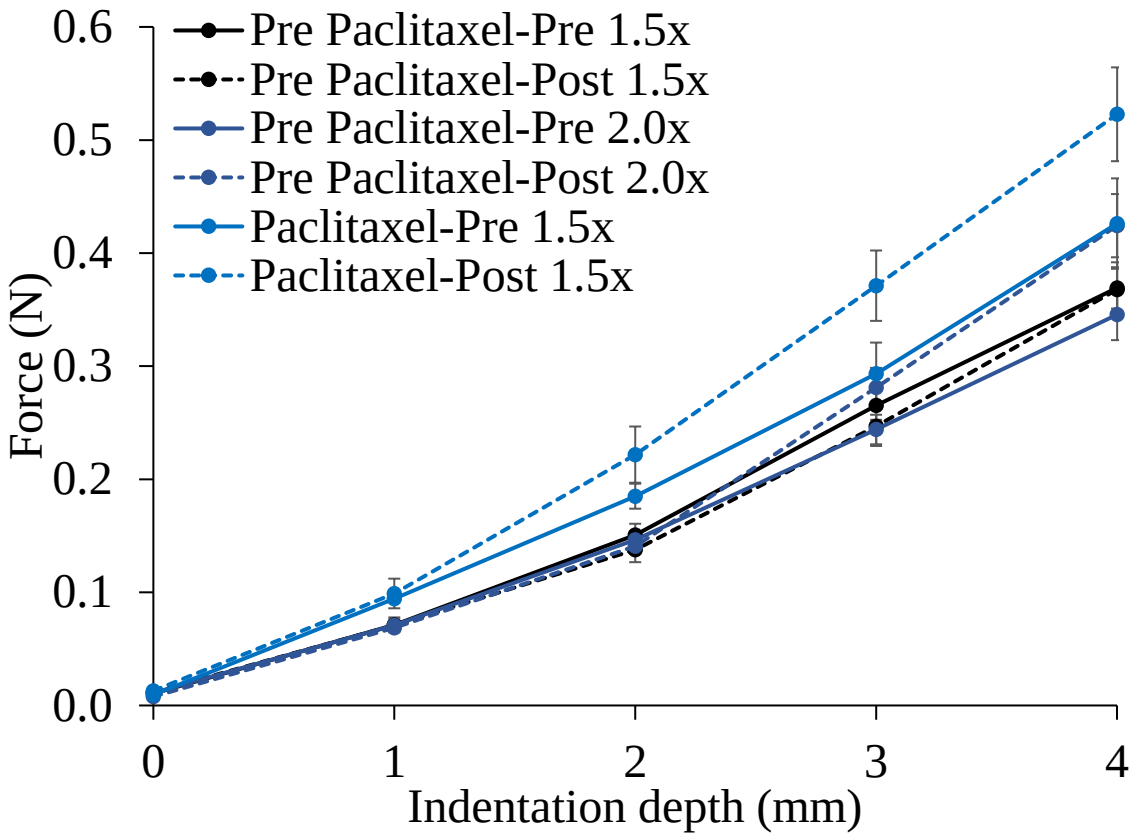

Figure 13. Mean diastolic stiffness before and after each mechanical run without and with paclitaxel. The solid lines represent the pre mechanical pacing measurements. The dashed lines represent the post mechanical pacing measurements. (*n*=7)

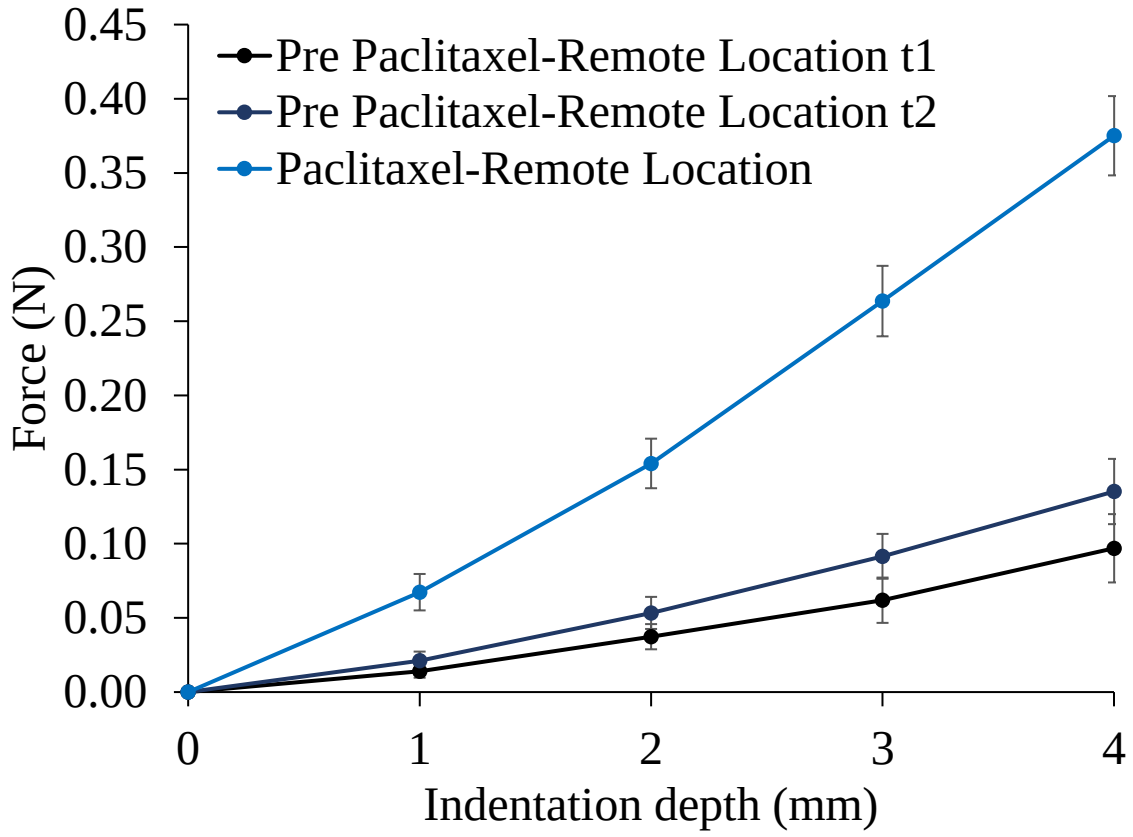

Figure 14. Mean diastolic stiffness at a remote location measured after each mechanical pacing run. The post-drug measurements were qualitatively increased compared to the pre-paclitaxel values at two different time points (t1 and t2), due to increased stiffness with paclitaxel. (*n*=7)

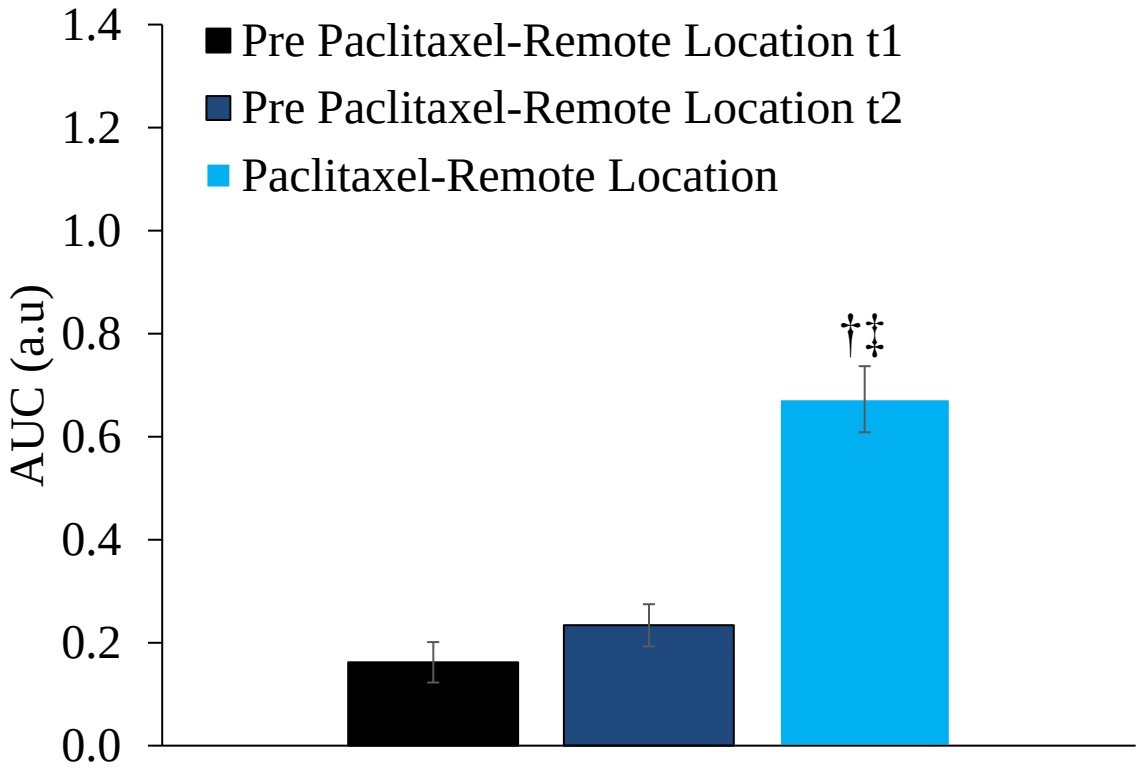

Figure 15. The AUC from figure 14. The diastolic stiffness of the remote location was significantly increased with paclitaxel compared to the two prior measurements without paclitaxel. †: vs. Pre-Paclitaxel remote location 1. ‡: vs. pre-Paclitaxel remote location 2. (One-way ANOVA, Tukey post-hoc test, $p < 0.05$) (*n*=7)

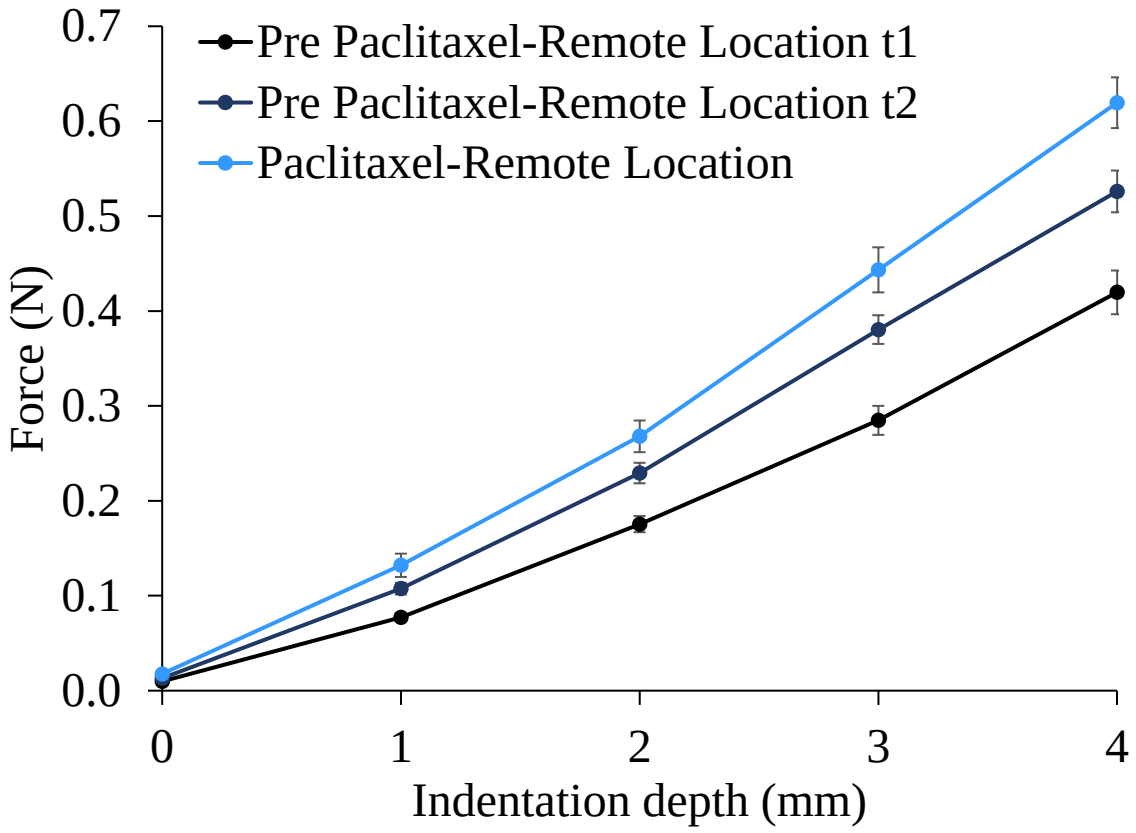

Figure 16. Peak systolic stiffness at a remote location measured after each mechanical pacing run. Qualitative increase of peak systolic stiffness over time at a remote location was observed, due to increased stiffness with paclitaxel. (*n*=7)

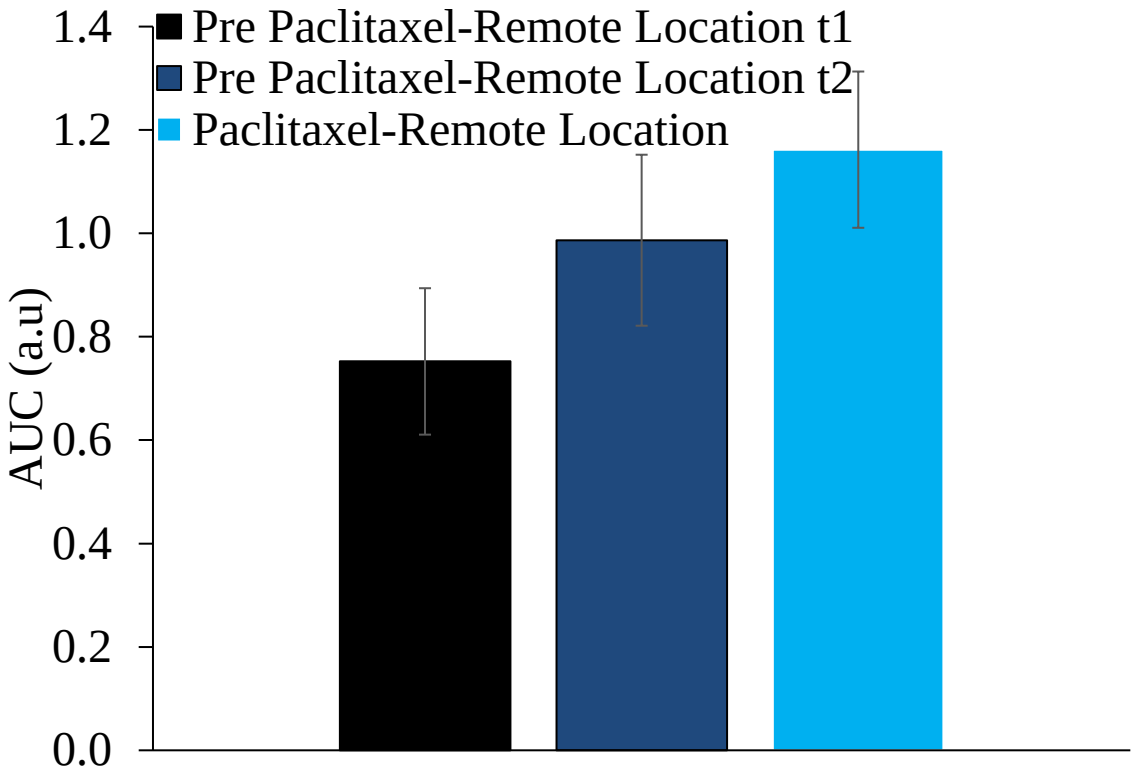

Figure 17. The AUC from figure 16. The systolic stiffness of the remote location was not significantly different with paclitaxel compared to the two prior measurements without paclitaxel. (p=0.19) (*n*=7)

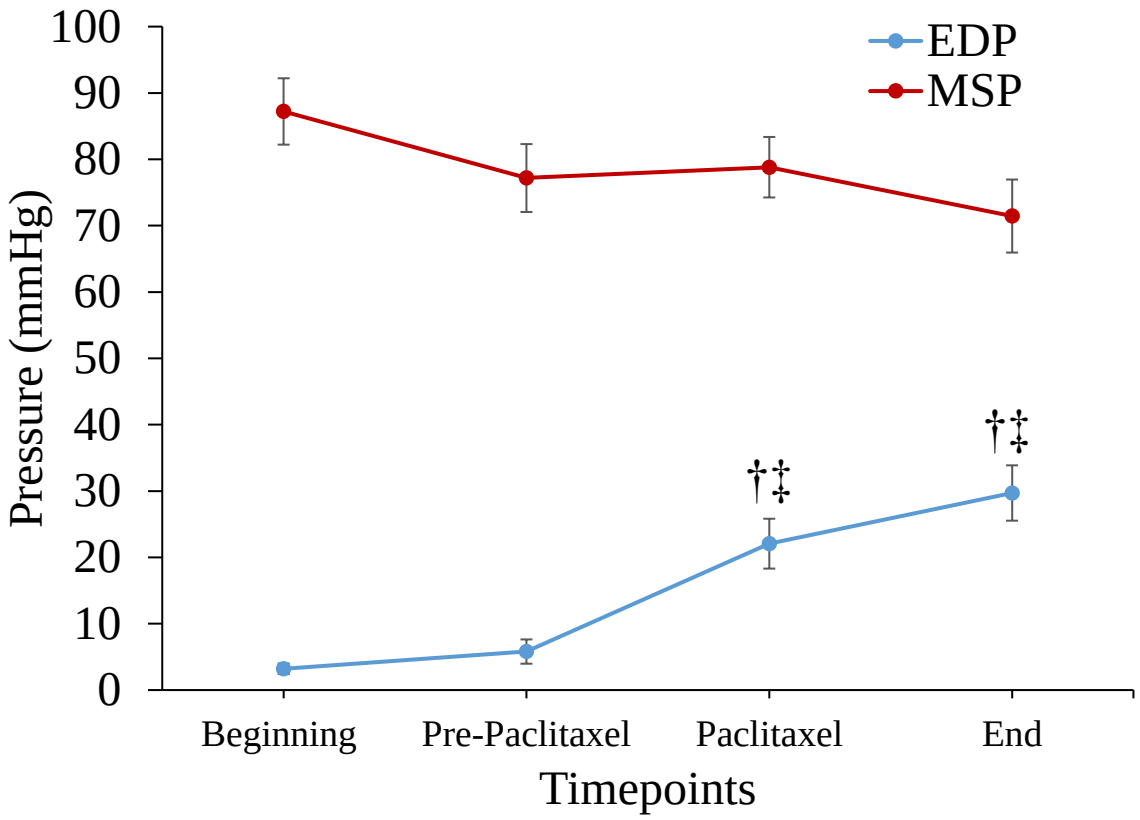

Figure 18. End diastolic pressures (EDP) and maximum systolic pressures (MSP) in paclitaxel experiments. The blue line represents the EDP and the red line represents the MSP. EDP significantly increase with paclitaxel, however the MSP did not change significantly. †: vs. beginning. ‡: vs. pre-paclitaxel. (One-way ANOVA, Tukey post-hoc test, $p < 0.05$) (n=7)

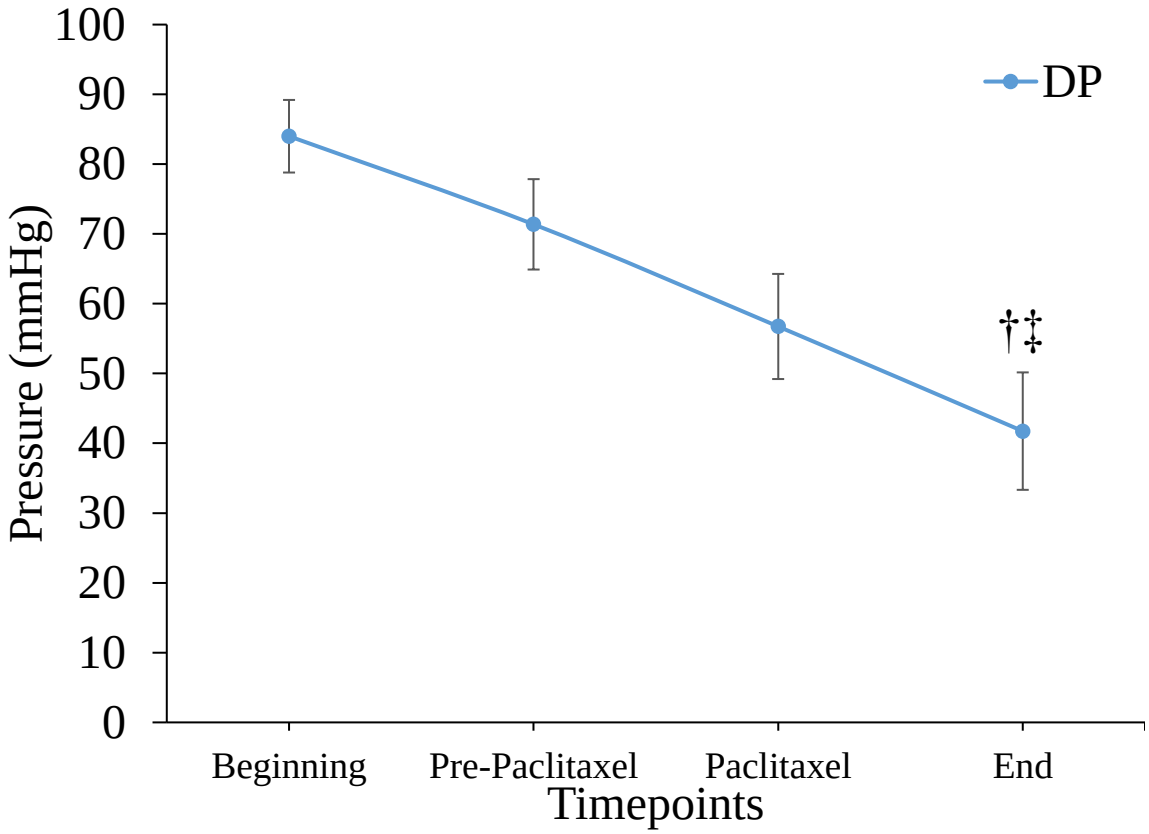

Figure 19. The developed pressure (DP) in paclitaxel experiments. The DP was significantly decreased by the end of the experiment. †: vs. beginning. ‡: vs. pre-paclitaxel. (One-way ANOVA, Tukey post-hoc test, $p < 0.05$) (n=7)

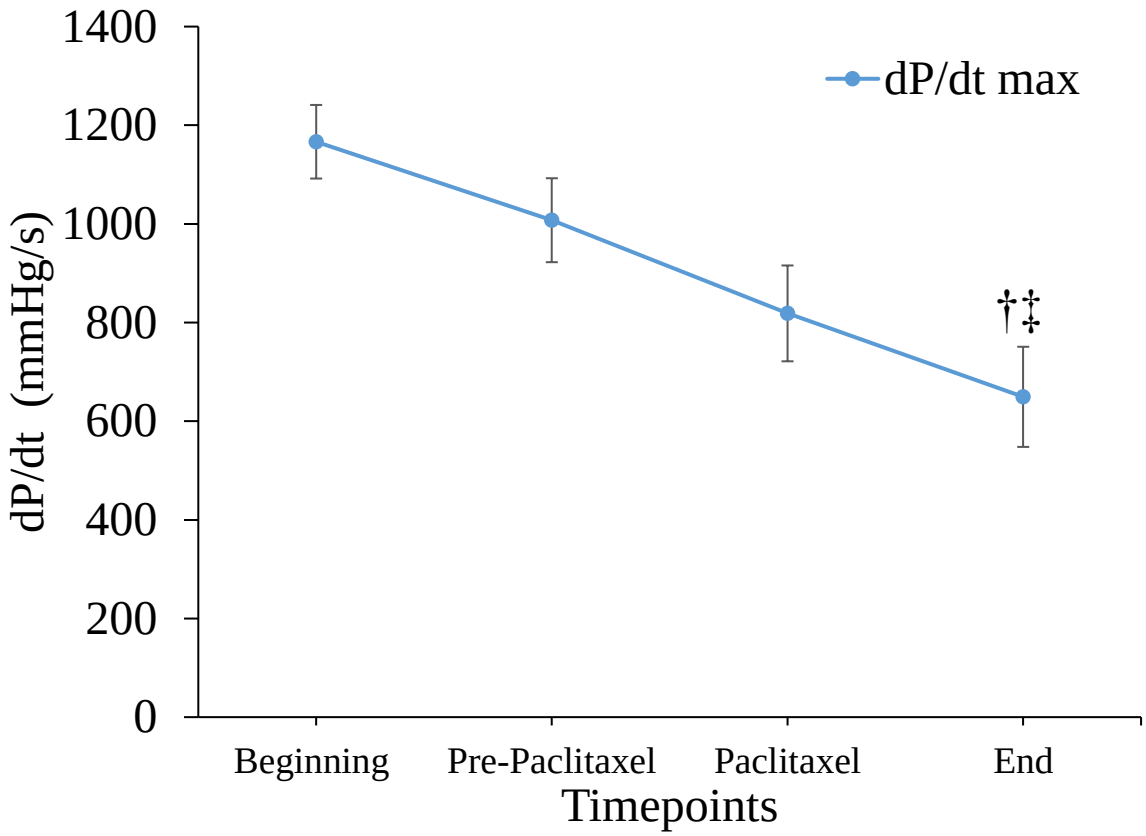

Figure 20. The maximum rate of pressure generation (dP/dtmax) in paclitaxel experiments. dP/dt max was significantly reduced with paclitaxel. †: vs. beginning. ‡: vs. pre-paclitaxel. (One-way ANOVA, Tukey post-hoc test, $p < 0.05$) (n=7)

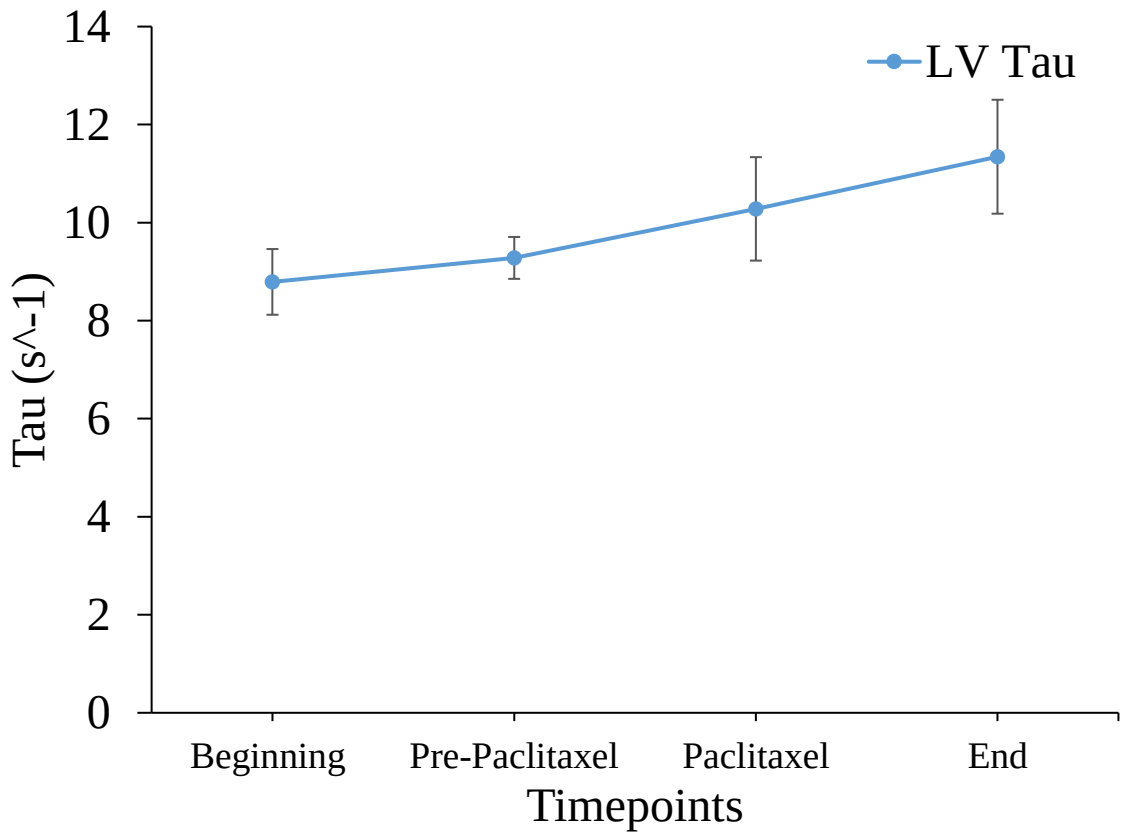

Figure 21. The rate of ventricular relaxation (LV tau) over time with paclitaxel experiments. No change is seen in tau with paclitaxel. (*n*=7, p=0.20)

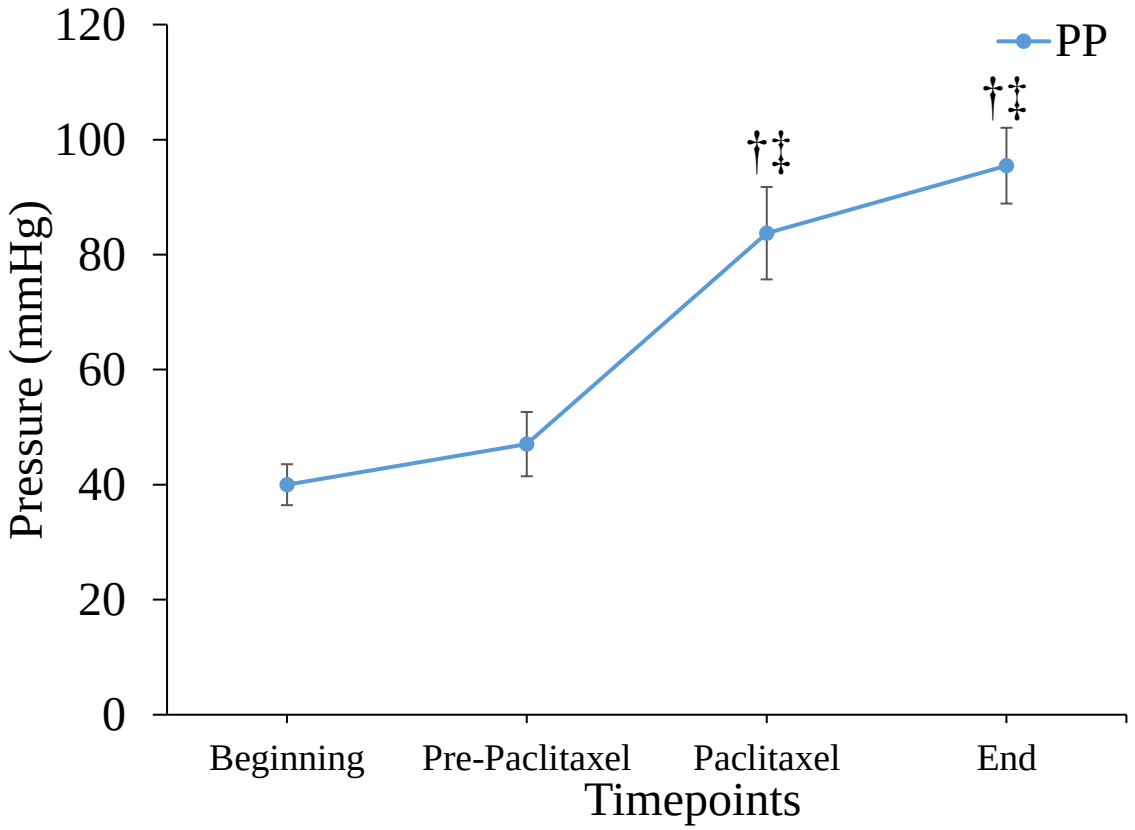

Figure 22. Perfusion pressure (PP) in paclitaxel experiments. The PP was significantly increased with paclitaxel. †: vs. beginning. ‡: vs. pre-paclitaxel. (One-way ANOVA, Tukey post-hoc test, $p < 0.05$) (n=7)

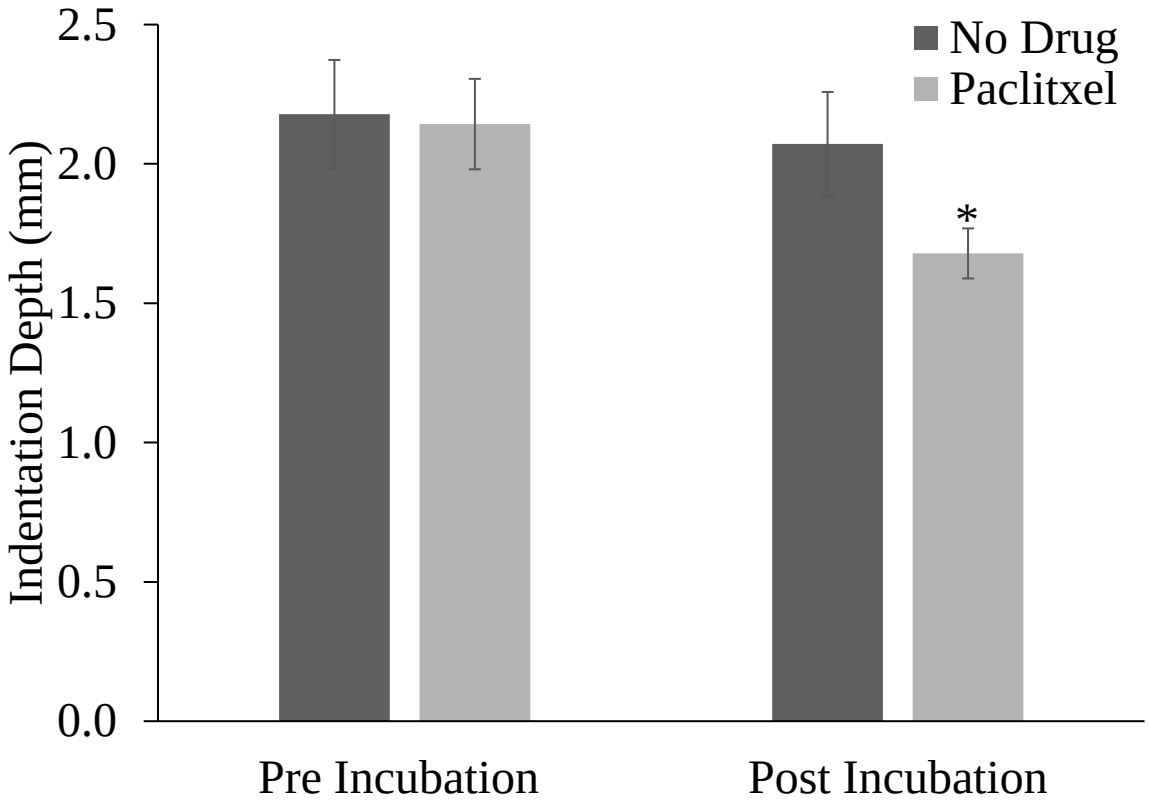

Figure 23. The threshold of VE_M Capture in paclitaxel and no drug experiments. Before the incubation period, the threshold was not significantly different at each testing time point between the two experimental groups. After the incubation period, the threshold of the paclitaxel group was significantly decreased compared to the pre-incubation value. (One-way ANOVA, Tukey post-hoc test, $p < 0.05$) (n=7)

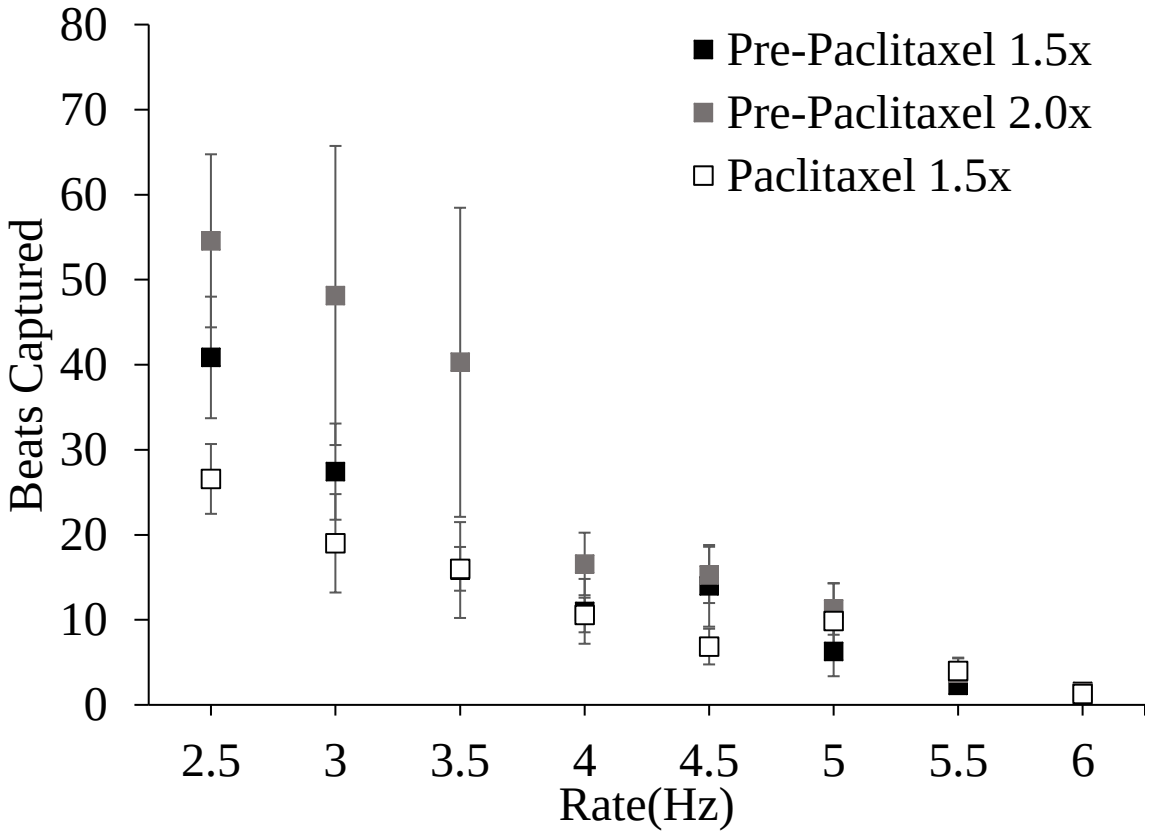

Figure 24. Number of beats continuously captured with increased indentation depth and with paclitaxel. The black squares represent the first run of mechanical pacing at 1.5x the threshold. The dark grey squares represent the second run of mechanical pacing at 2x the threshold. The light grey represents the similar run as the first run except with paclitaxel. (*n*=7)

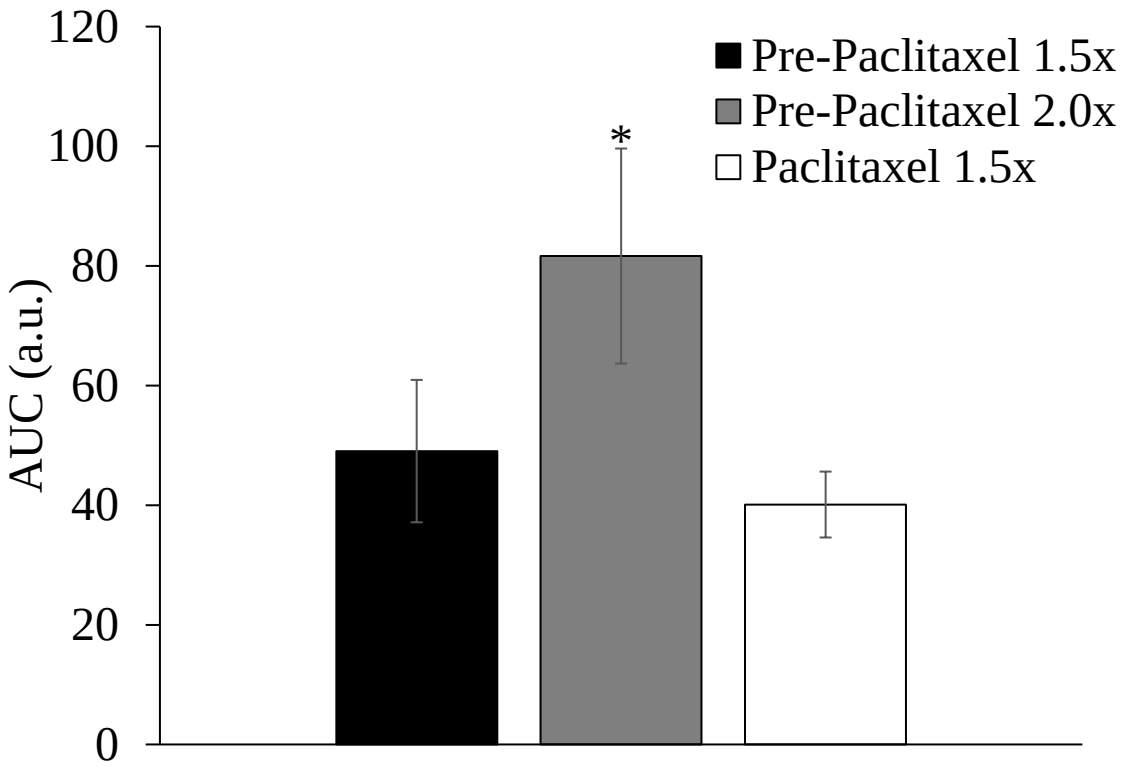

Figure 25. Area under the curves (AUC) for data from Figure 23. The black bar represents the m-pace at 1.5x the threshold. The dark grey bar represents the m-pace at 2x the threshold. The light grey bar represents the m-pace after paclitaxel incubation at 1.5x the original threshold. The AUC for pre-paclitaxel 2.0x was significantly greater that pre-paclitaxel 1.5x (One-way ANOVA, Tukey post-hoc test, $p < 0.05$). No significant change between pre- and Paclitaxel 1.5x was observed ($p=0.13$). ($n=7$)

3.3 Effect of Colchicine (Reduced Passive Stiffness)

Colchicine, a microtubule depolymerizer, was chosen as the agent to reduce the passive tension, i.e. stiffness, because it functions in the opposite way of paclitaxel. Preliminary experiments were carried out similar to paclitaxel preliminary experiments (n=3). Colchicine was added and the stiffness was measured every 15 min, over 180 min. Surprisingly, however, colchicine caused a qualitative increase in diastolic stiffness (rather than a decrease; Figure 26), without an effect on systolic stiffness (Figure 27), so further experiments using colchicine were not carried out.

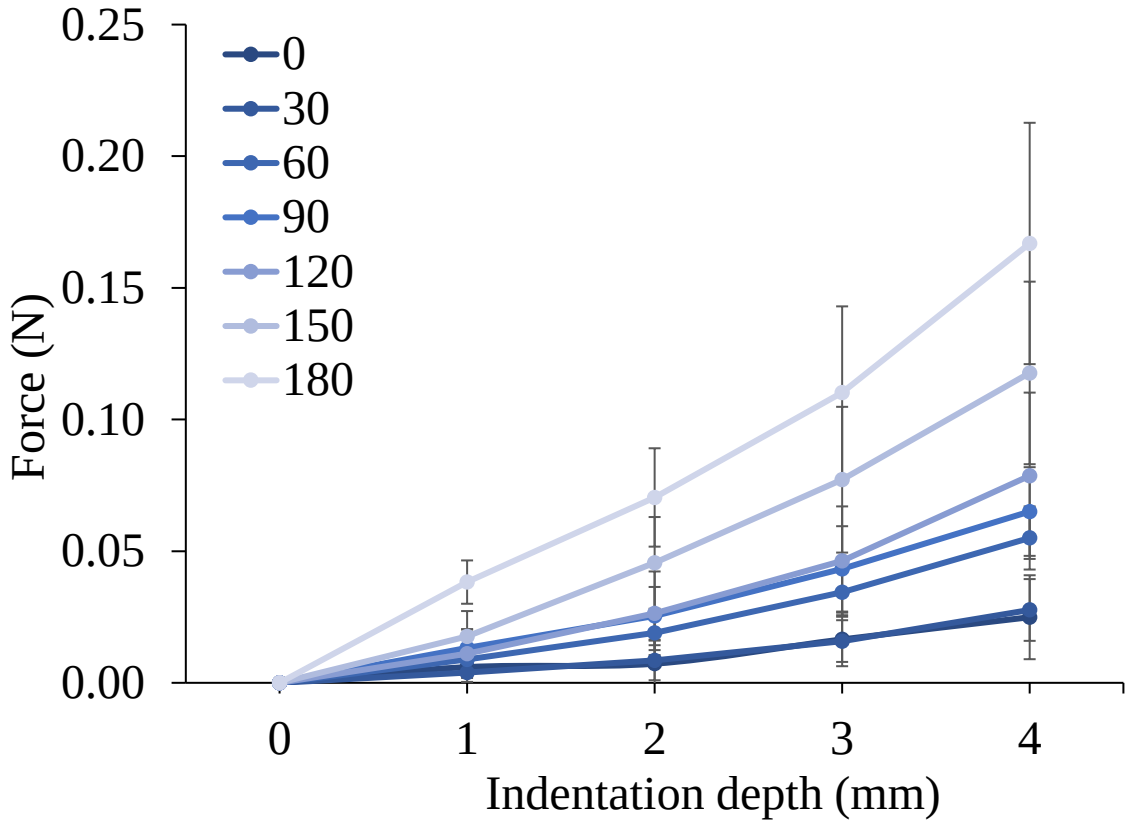

Figure 26. The diastolic stiffness with colchicine in preliminary experiments. The lines are coloured according to the time, so the light coloured lines represent later times and dark ones represent the earlier times. Stiffness was measured every 15 min (although the plot shows 30 min intervals). Diastolic stiffness was increased over time with colchicine.

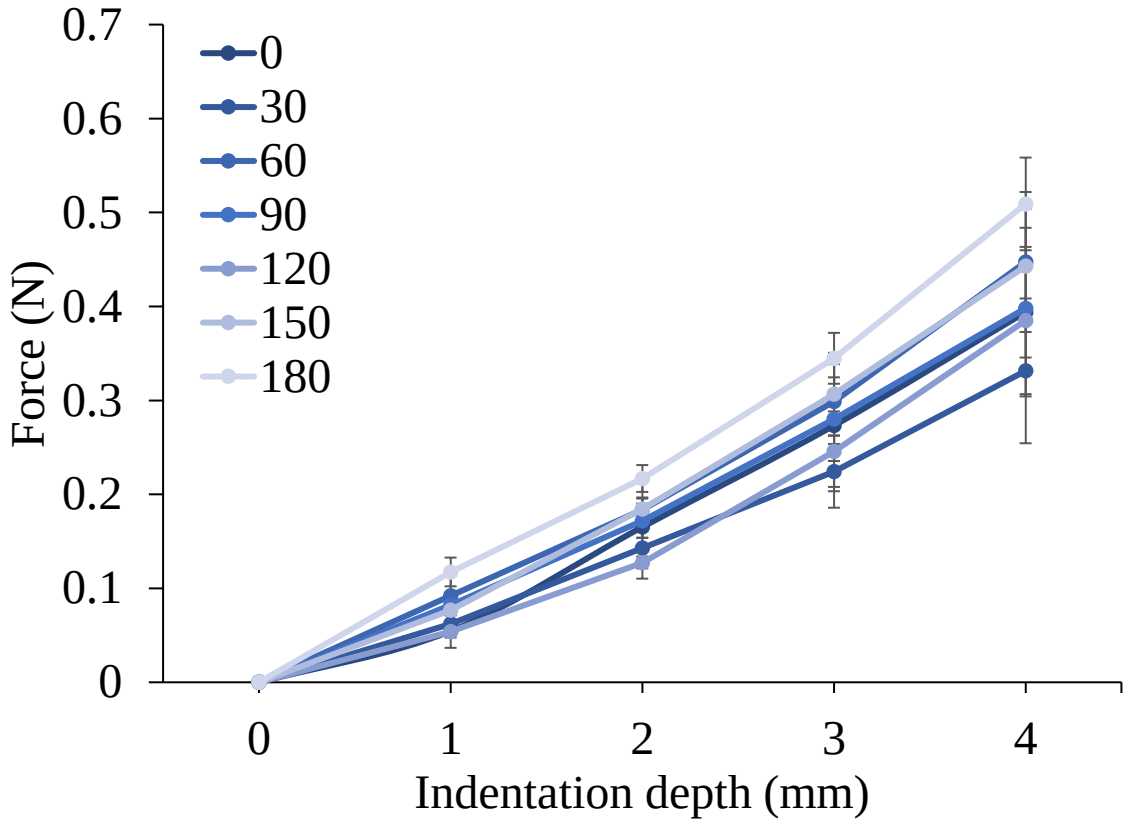

Figure 27. The systolic stiffness with colchicine in preliminary experiments. The lines are coloured according to the time, so the light coloured lines represent later times and dark ones represent the earlier times. Stiffness was measured every 15 min (although the plot shows 30 min intervals). No change in the systolic stiffness is seen in response to colchicine.

3.4 Effect of Time (Control)

In this experimental group, the same protocol as paclitaxel experiments was carried out except no drug was added (*n*=7). This way we could compare between the two experimental groups: one with an increase in stiffness (paclitaxel) and one without an increase (no drug).

First, the passive tension during diastole was investigated. There was an increase in diastolic stiffness by the end of the experiment (Figure 28), pointing to the possible effects of edema or mechanical stimulation. No significant change in diastolic (Figure 29) nor systolic stiffness (Figure 30) with each m-pace was observed. The diastolic (Figures 31 and 32) and systolic (Figure 33) stiffness of the remote location (as an internal control to remove the potential effect of mechanical stimulation on stiffness) did not change over the course of the experiment.

Hemodynamic measurements were also analysed. The end diastolic pressure was not increased (Figure 34). The maximum systolic pressure significantly decreased over the second half of the experiment (Figure 34), as did the developed pressure (Figure 35) and dP/dt_{max} (Figure 36). The LV tau did not change (Figure 37), while the perfusion pressure was significantly increased by the end of the experiment (Figure 38). Sustainability did not change with time (Figures 39 and 40).

The hemodynamic effects of paclitaxel and time were compared. The EDP was significantly increased with paclitaxel ($p=0.002$). The MSP was significantly decreased in no drug vs. paclitaxel experiments ($p=0.01$). The PP was significantly increased with paclitaxel compared to no drug control ($p=0.002$). The rest of the hemodynamic changes were not significantly different between the two experimental groups.

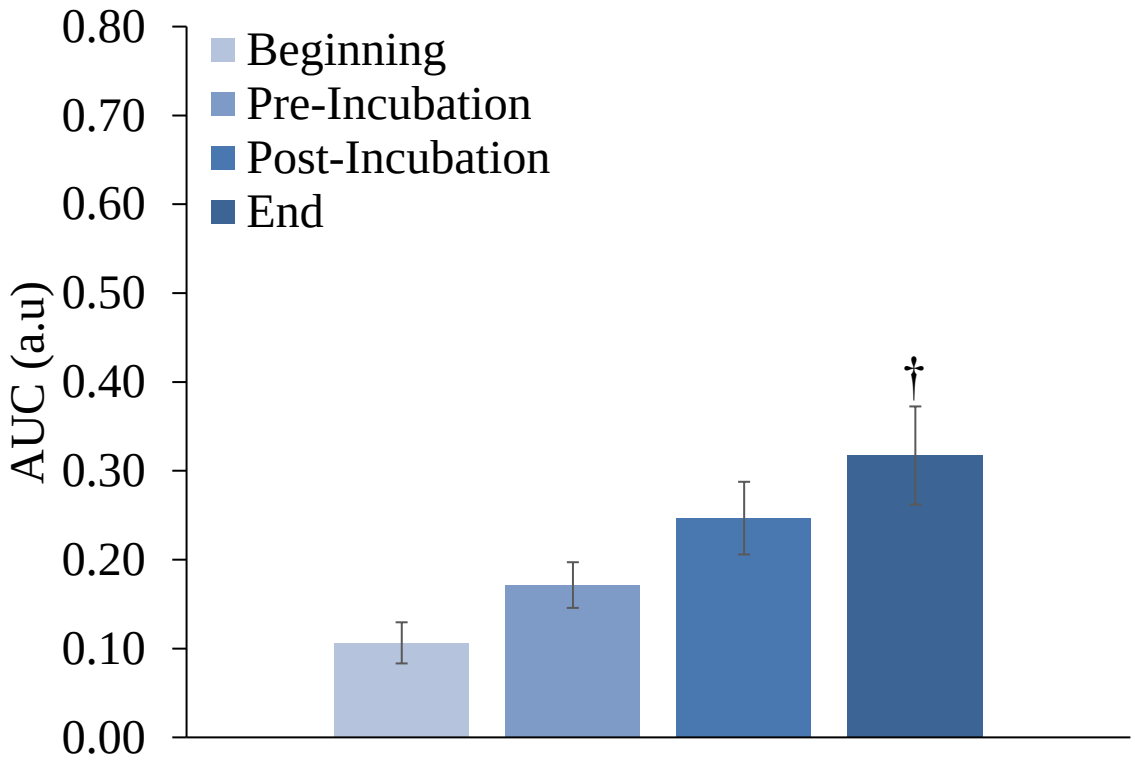

Figure 28. The area under the curve (AUC) of the diastolic stiffness curve in no drug experiments. The AUC of the diastolic stiffness curve measured by force indentation at 0-4 mm at four different time points throughout the no drug experiments. The AUC was significantly increased by the end of the experiment. †: vs. beginning. (One-way ANOVA, Tukey post-hoc test, $p < 0.05$) (n=7)

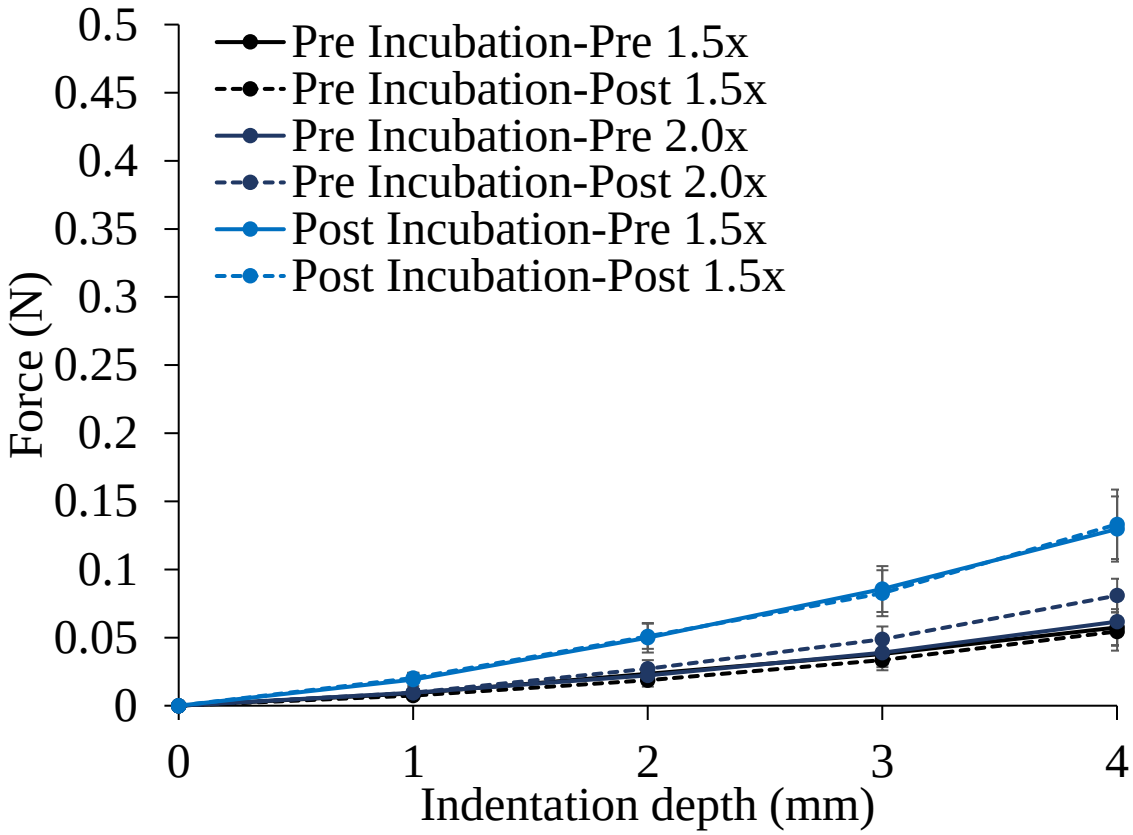

Figure 29. Mean diastolic stiffness before and after each run of mechanical pacing. The solid lines represent the pre mechanical pacing measurements. The dashed lines represent the post mechanical pacing measurements. (*n*=7)

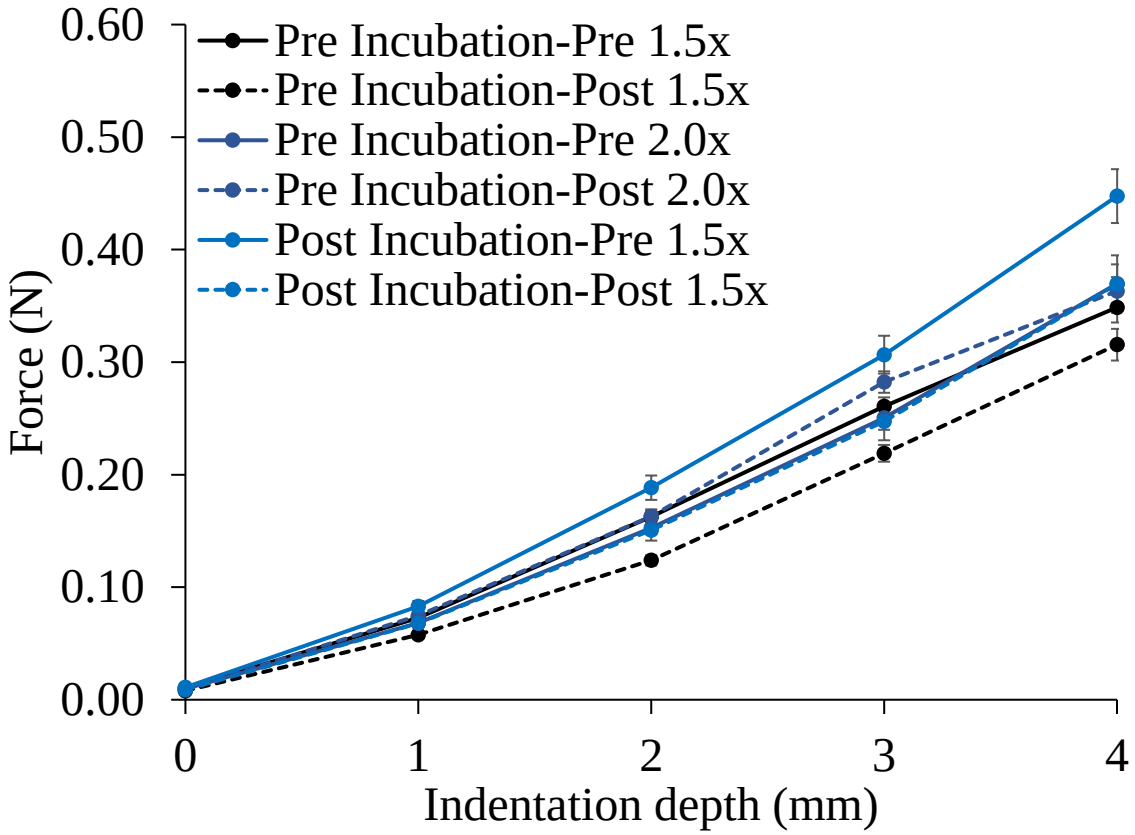

Figure 30. Peak systolic stiffness before and after each run of mechanical pacing. The solid lines represent the pre mechanical pacing measurements. The dashed lines represent the post mechanical pacing measurements. No clear change is visible. (*n*=7)

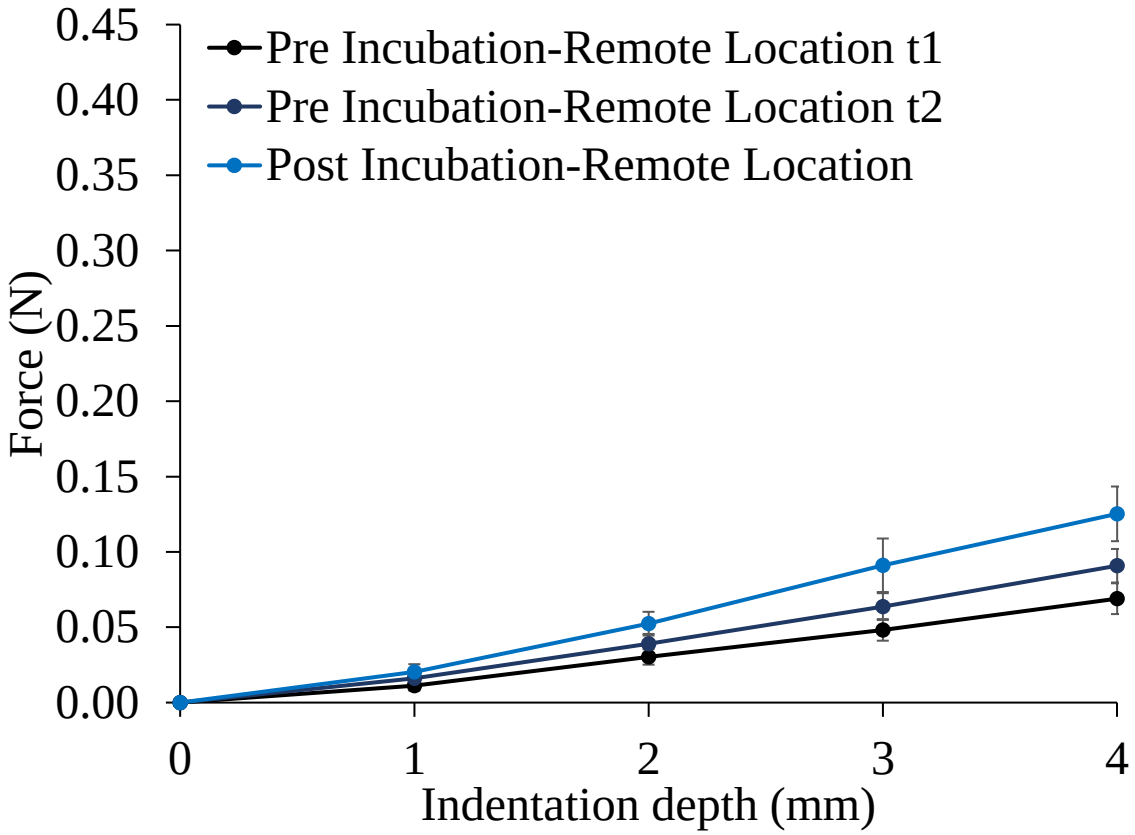

Figure 31. Mean diastolic stiffness at a remote location in no drug experiments. The response force to indentation was measured after each mechanical pacing run. (*n*=7)

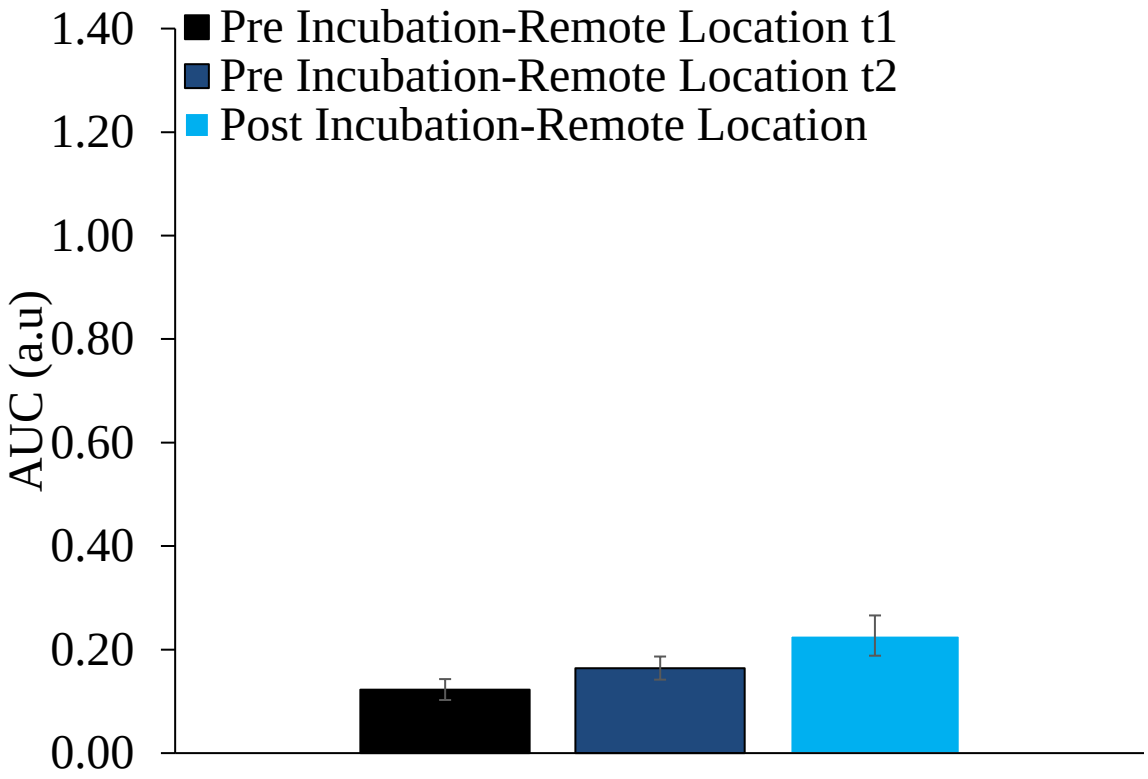

Figure 32. The AUC from figure 31. The diastolic stiffness of the remote location was not significantly different between the different time points measured throughout the experiments. (*n*=7, p=0.12)

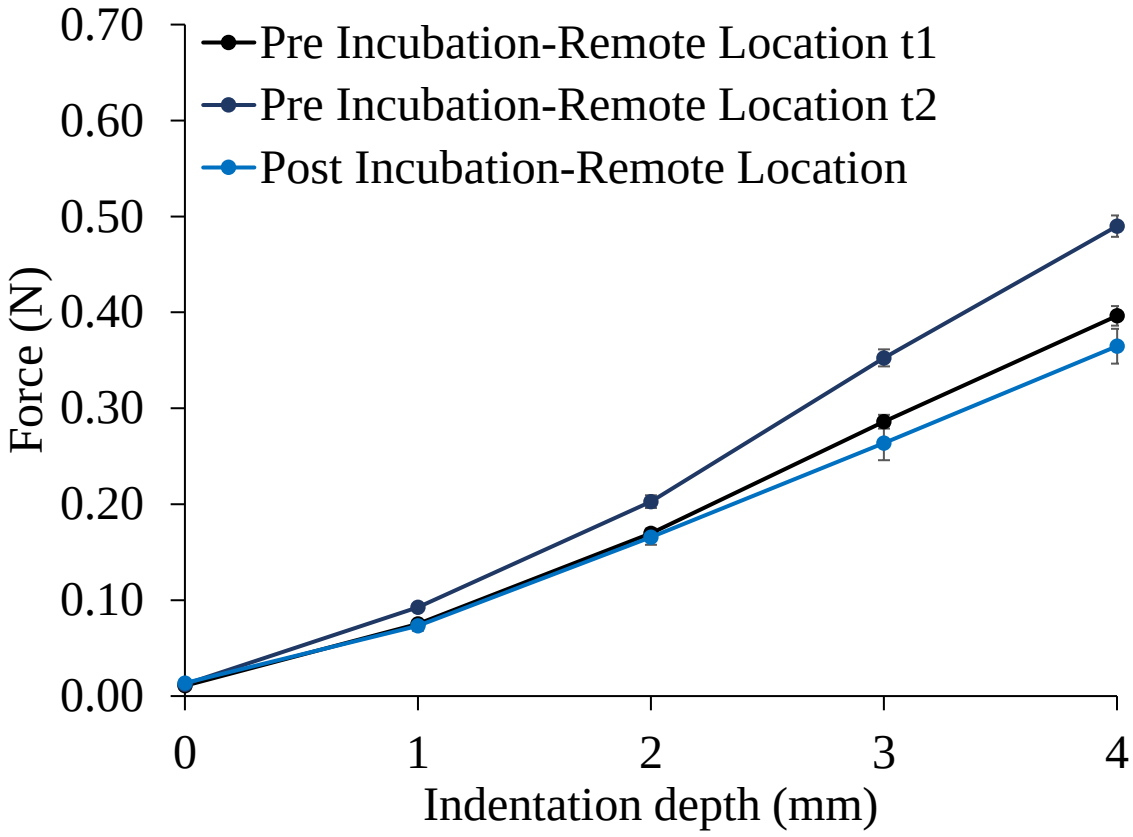

Figure 33. Peak systolic stiffness at a remote location in no drug experiments. The response force to indentation was measured after each mechanical pacing run. No clear pattern was observed. (*n*=7)

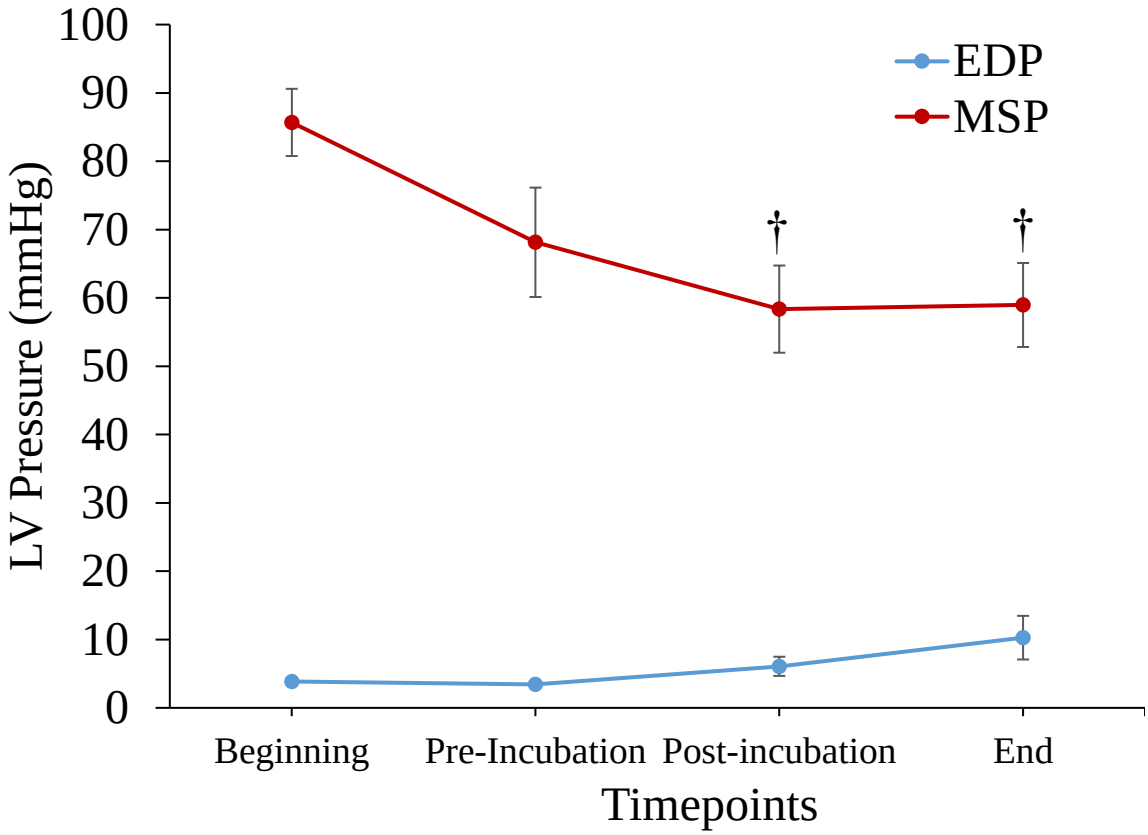

Figure 34. End diastolic pressures (EDP) and maximum systolic pressures (MSP) in no drug experiments. The blue line represents the EDP and the red line represents the MSP. EDP did not significantly change. However, the MSP was significantly reduced over the second half of the experiment. †: vs. beginning. (One-way ANOVA, Tukey post-hoc test, $p < 0.05$) (n=7)

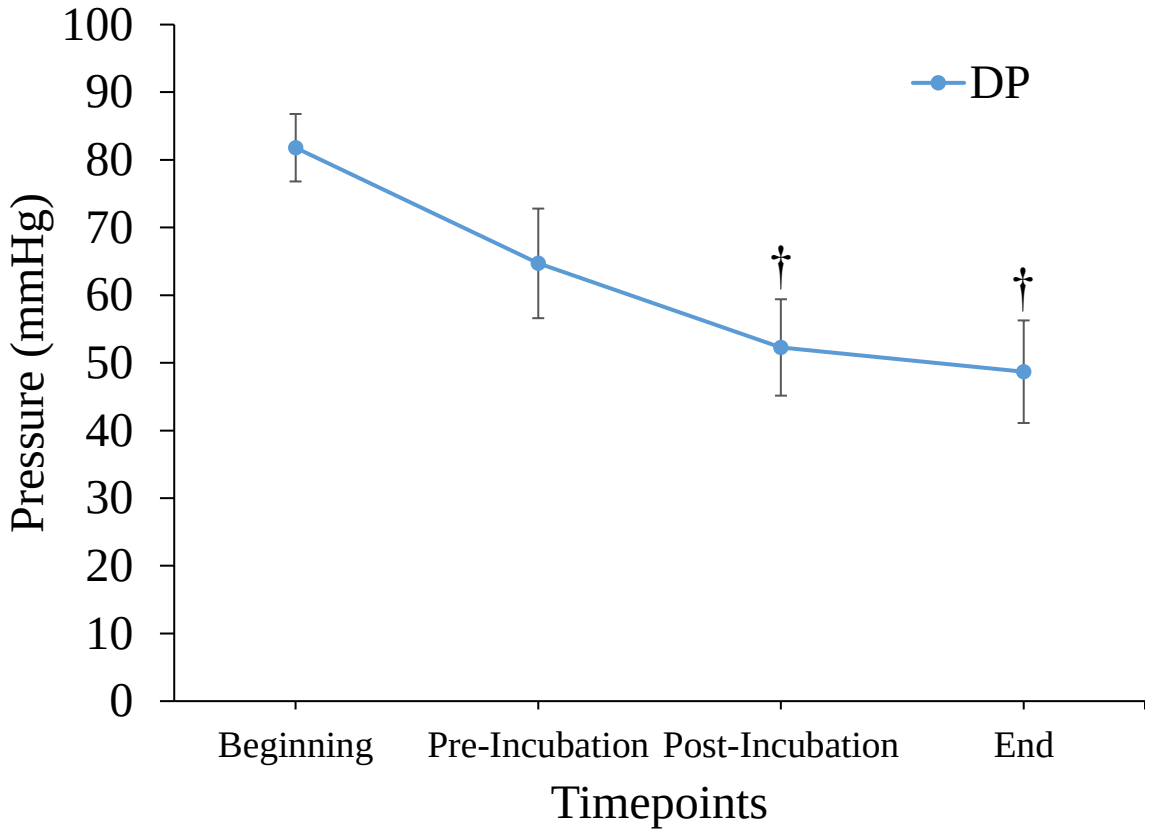

Figure 35. The developed pressure (DP) in no drug experiments. The DP significantly decreased over the second half of the experiment. †: vs. beginning. (One-way ANOVA, Tukey post-hoc test, $p < 0.05$) (n=7)

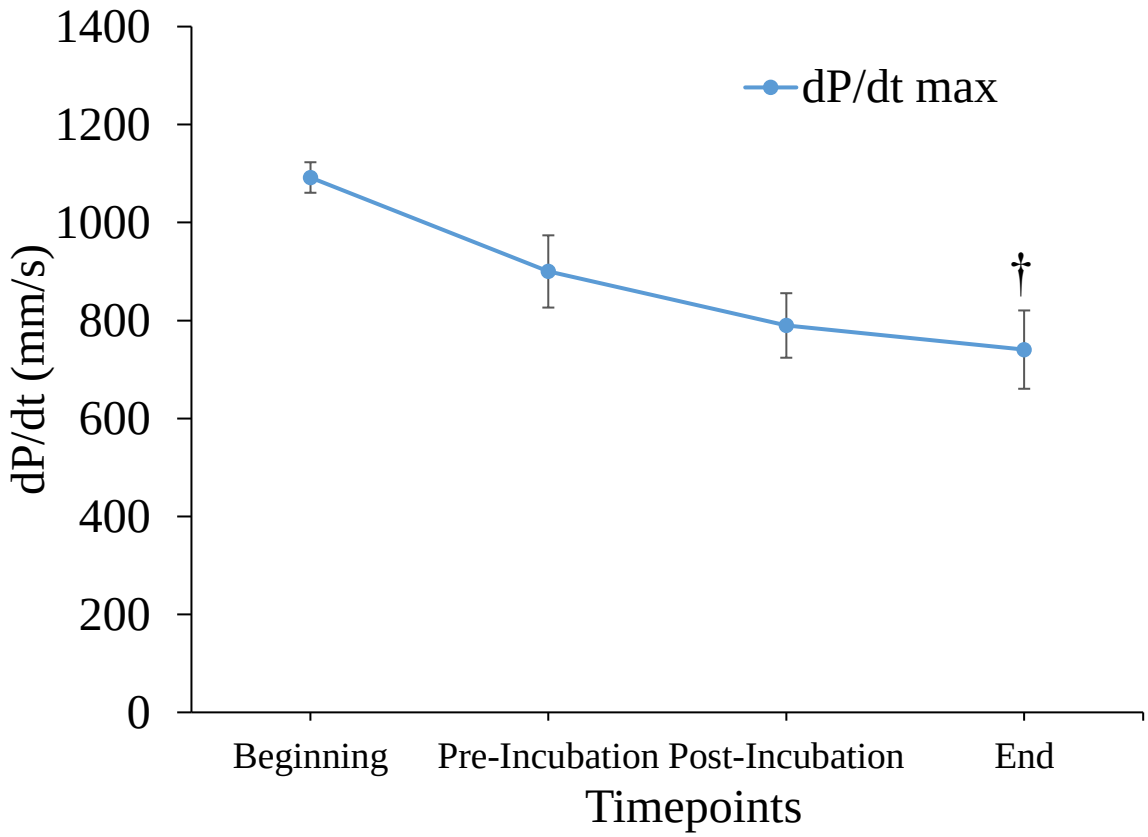

Figure 36. The maximum rate of pressure generation (dP/dt_{max}) in no drug experiments. dP/dt_{max} was significantly reduced by the end of the experiment. †: vs. beginning. (One-way ANOVA, Tukey post-hoc test, $p < 0.05$) (n=7)

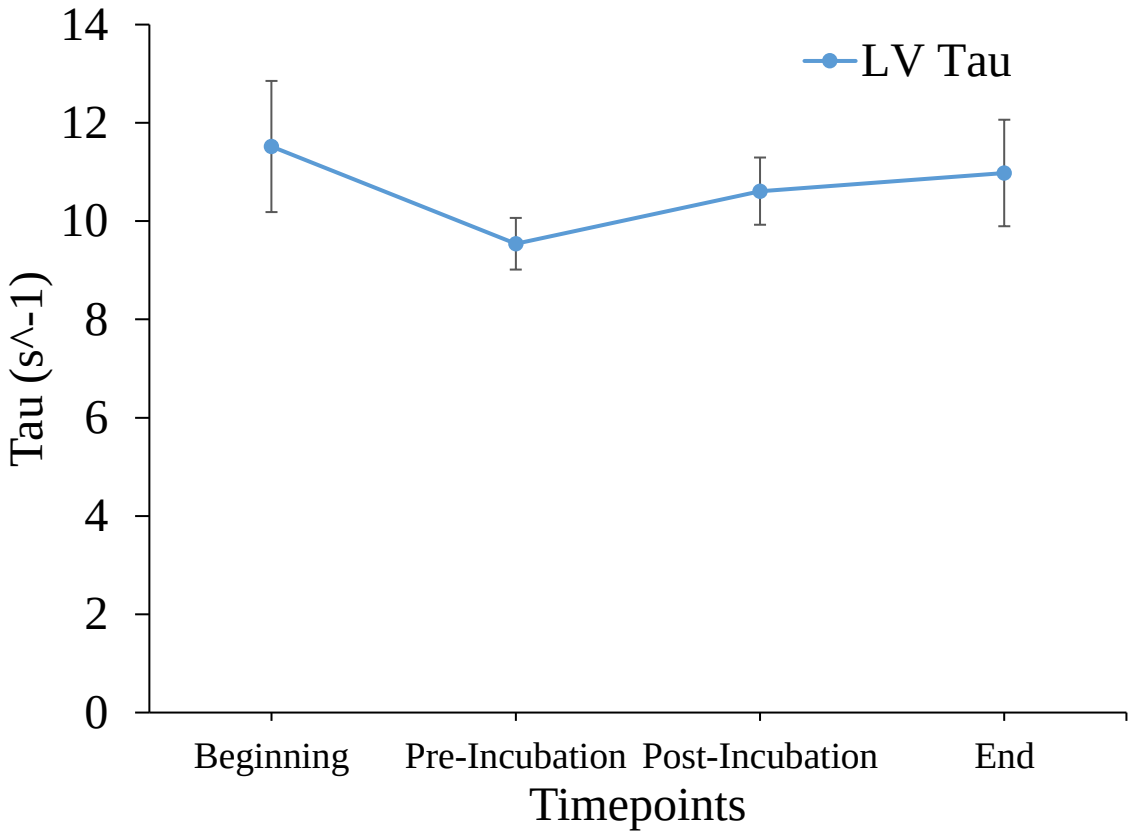

Figure 37. The rate of ventricular relaxation (LV tau) over time in no drug experiments. No change was seen. (*n*=7, p=0.54)

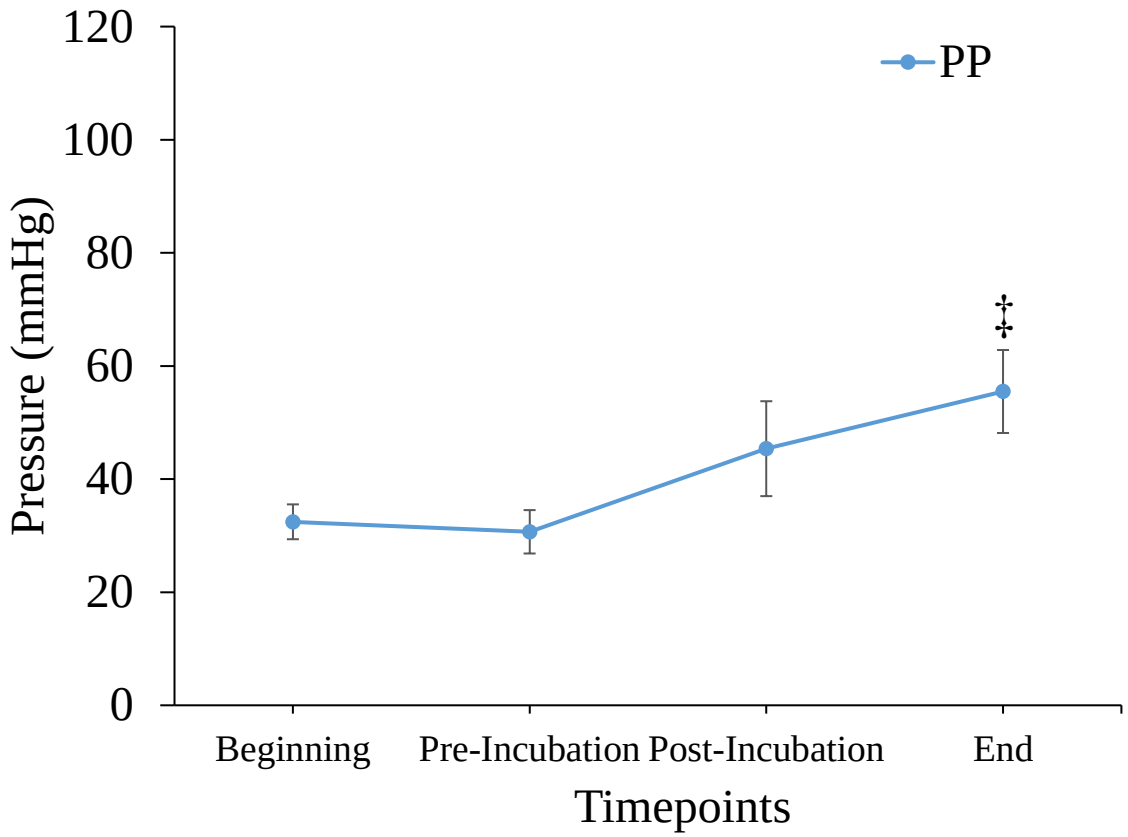

Figure 38. Perfusion pressure (PP) in no drug experiments. The PP was significantly increased by the end of the experiment. ‡: vs. pre-drug. (One-way ANOVA, Tukey post-hoc test, $p < 0.05$) (n=7)

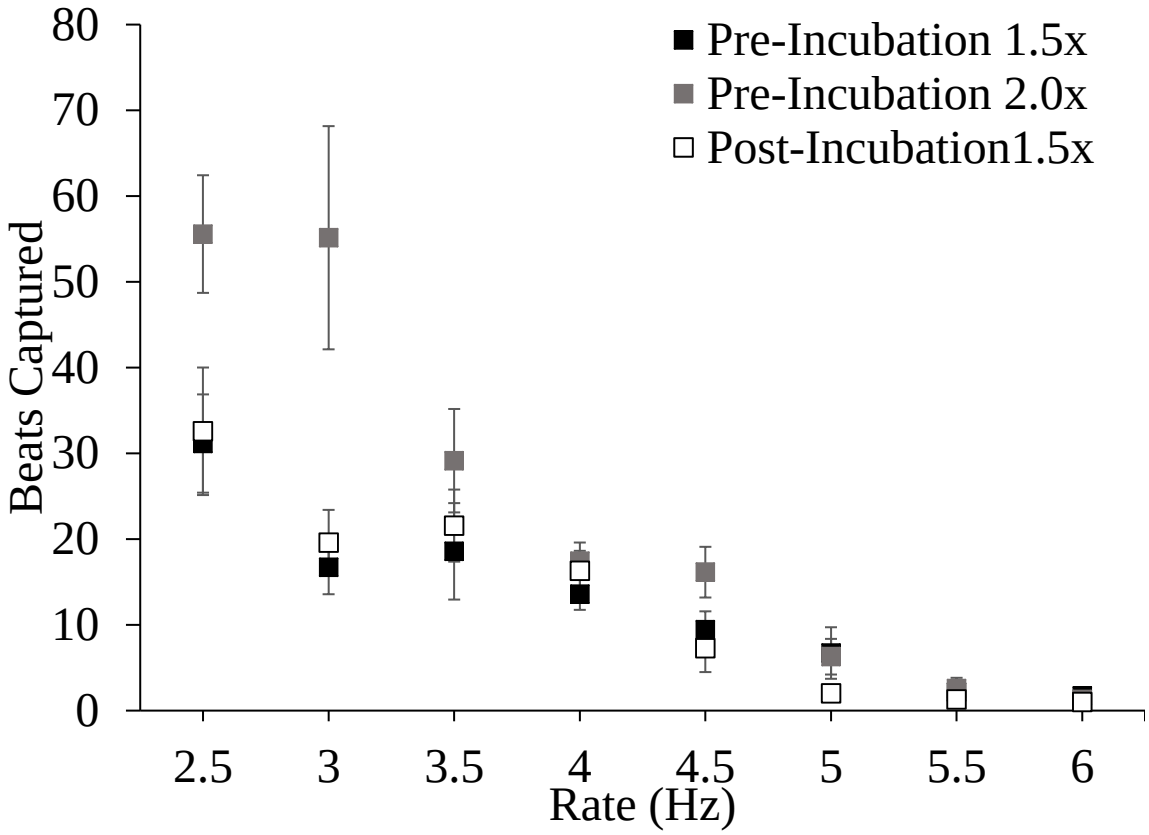

Figure 39. Number of beats continuously captured at different indentation depths and with time. The black squares represent the first run of mechanical pacing at 1.5x the threshold. The dark grey squares represent the second run of mechanical pacing at 2x the threshold. The light grey represents the similar run as the first run except after the incubation period. (*n*=7)

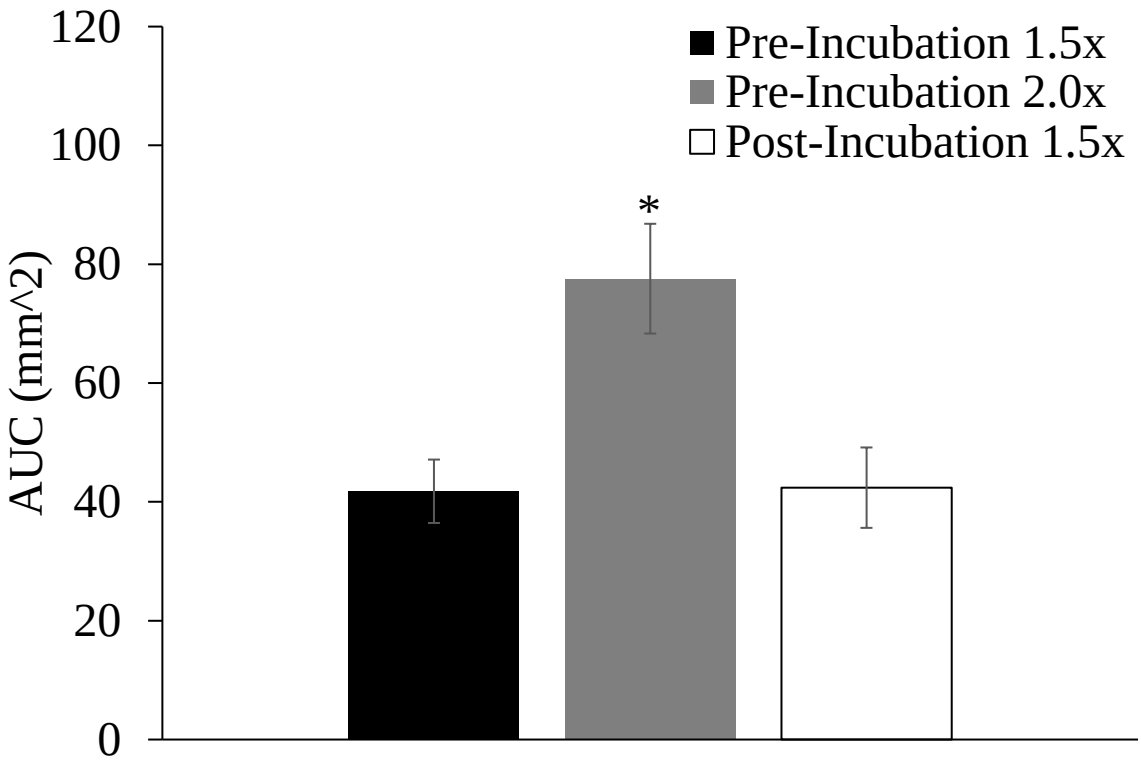

Figure 40. Area under the curves (AUC) for data from Figure 39. The black bar represents the m-pace at 1.5x the threshold (2.18±0.19 mm). The dark grey bar represents the m-pace at 2x the threshold. The light grey bar represents the m-pace at 1.5x the threshold after the incubation period. The AUC for pre-incubation 2.0x was significantly more that pre-incubation 1.5x. No significant change between pre- and post-incubation 1.5x was observed. (One-way ANOVA, Tukey post-hoc test, $p < 0.05$) (n=7)

3.5 Effect of Ivabradine (Reduced Rate)

From Figure 2, it can be implied that at a slow enough pacing rate, mechanical pacing might be sustainable. Ivabradine (an HCN channel blocker) was used to slow intrinsic rate, to allow for a reduced mechanical pacing rate (*n*=9). The ivabradine concentration was increased until heart rate was below 60 bpm. The amounts of ivabradine and the resulting heart rate in each experiment are shown in Figure 41. While the number of continuous VE_M was increased at lower pacing frequencies, it was found that mechanical pacing could still not be maintained. When designing the experiment, the effect of background heart rate between the periods of pacing was taken into account. To test for this effect, the heart was paced between pacing periods at the rate before ivabradine application. The sustainability graph of these experiments are shown in Figure 42. To determine the effect of ivabradine on sustainability, the AUCs of control and post-ivabradine + pacing (only from 2.5-6 Hz) were compared, since the background rate was the same in both settings. There was no significant difference between the AUCs of these two graphs, therefore the ivabradine did not affect sustainability (Figure 43). To determine the effect of background rate immediately prior to initiation of mechanical pacing, the AUCs of ivabradine and ivabradine + pacing were compared. There were no significant difference between the AUCs in these two settings either (Figure 44). Overall, ivabradine and the background rate do not affect mechanical pacing sustainability.

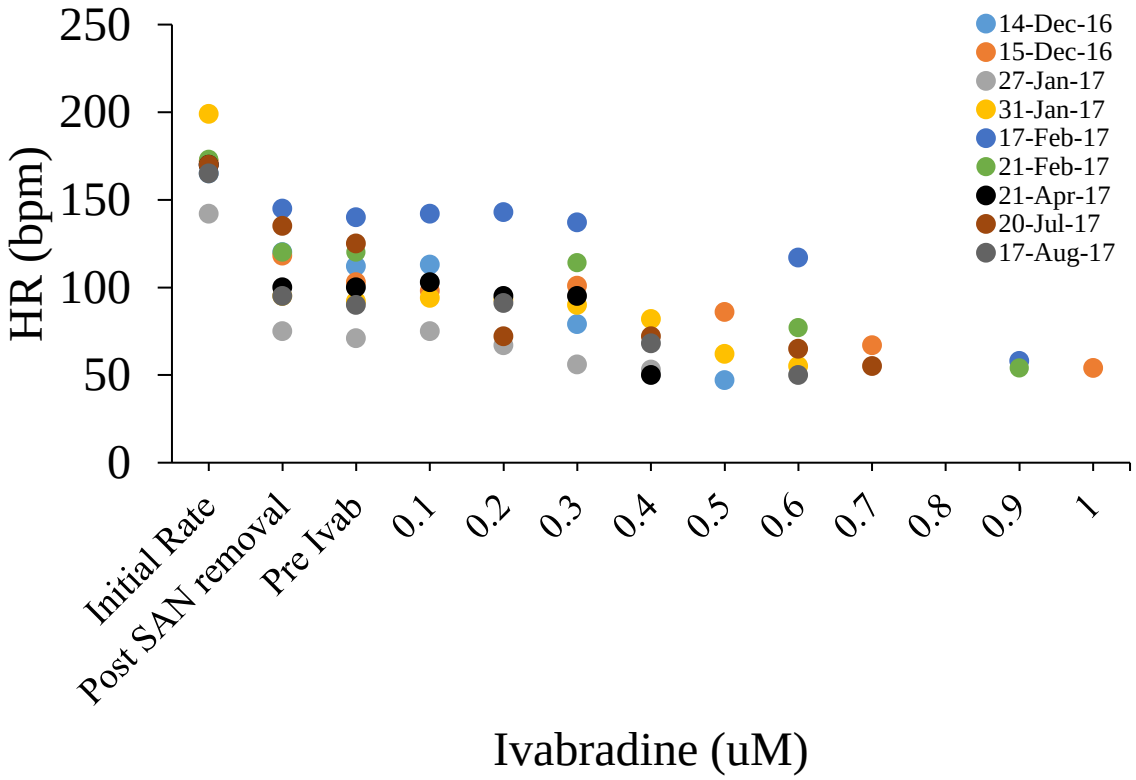

Figure 41. The HR in each ivabradine experiment. The HR in each ivabradine experiment, at different times have been shown. The amount of ivabradine used to reach a HR of <1 Hz was always less than or equal to 1 μM. (*n*=9)

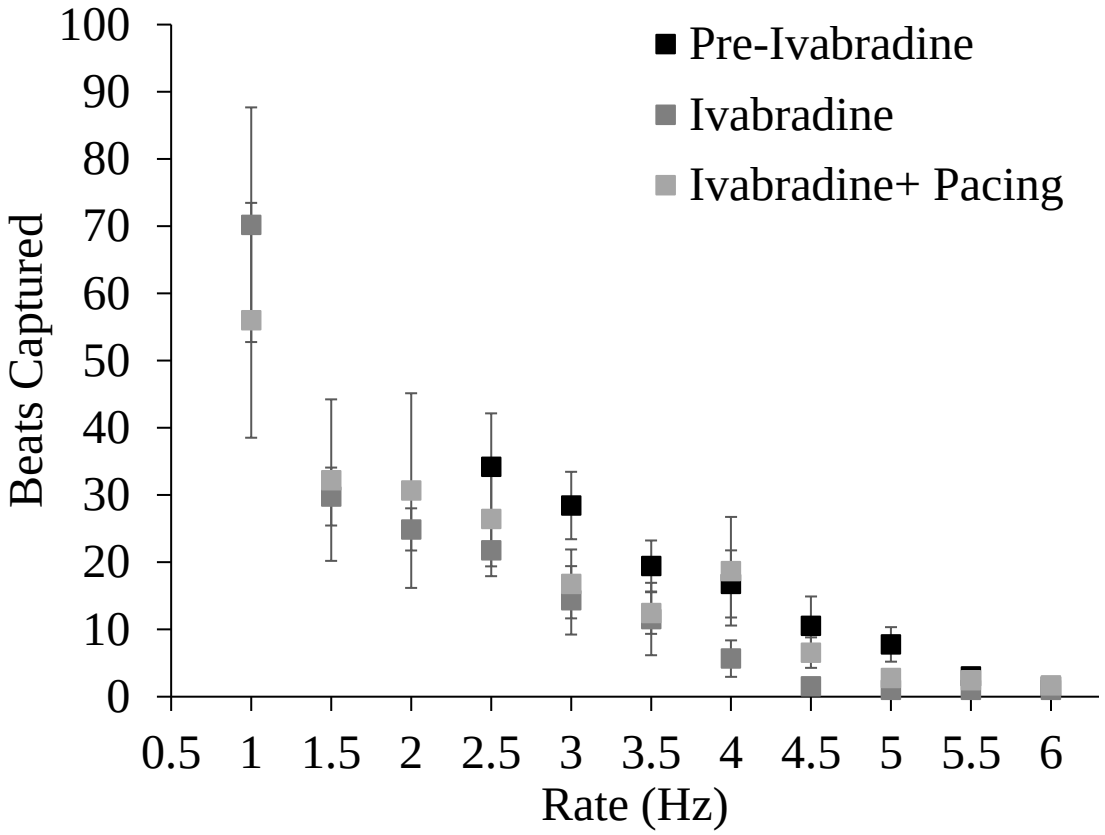

Figure 42. The sustainability graphs for the ivabradine experiments. The number of beats to loss of capture is shown at each pacing rate, in three different settings. The black squares represent the control setting. The dark grey squares represent the graph of ivabradine settings. The light grey squares represent the ivabradine and in-between paces pacing setting. (*n*=9)

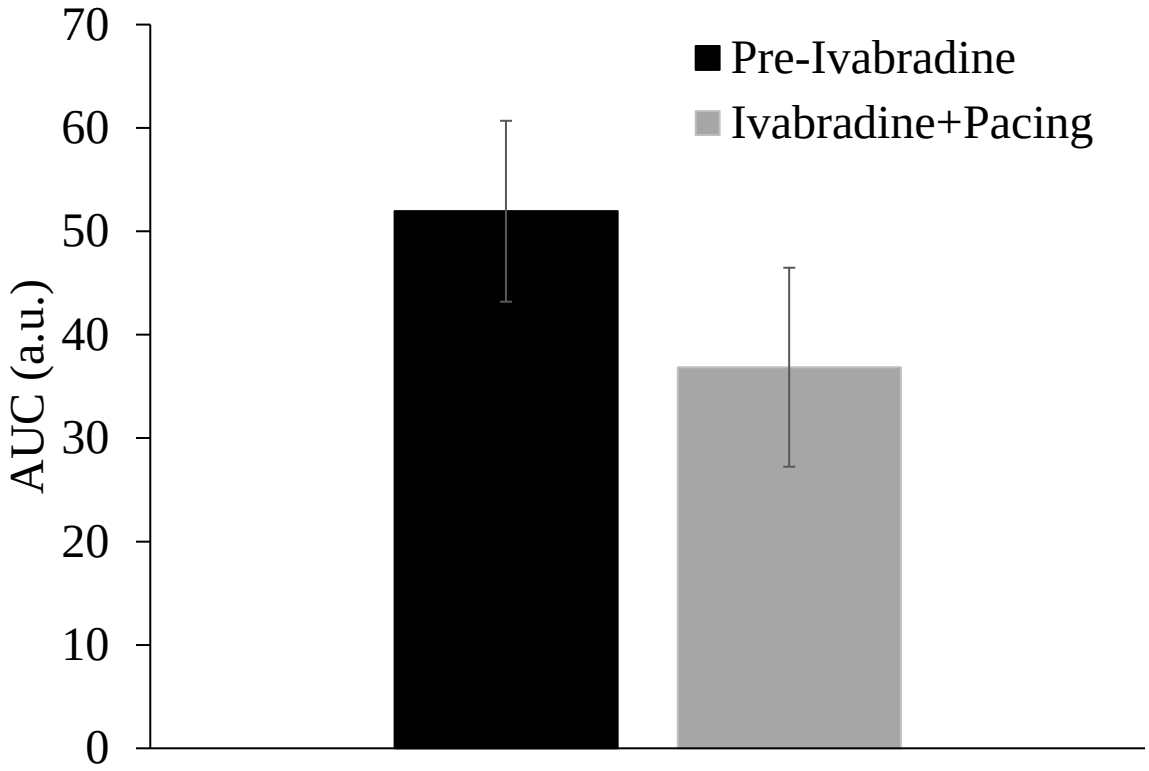

Figure 43. The AUCs of control and ivabradine + pacing from figure 42. The black bar represents the AUC of the pre-ivabradine (control) graph. The grey bar represents the AUC of a part of ivabradine + pacing graph (2.5-6 Hz). T-test was performed to compare these two bar graphs, and no significant difference was observed. (*n*=9, p=0.43)

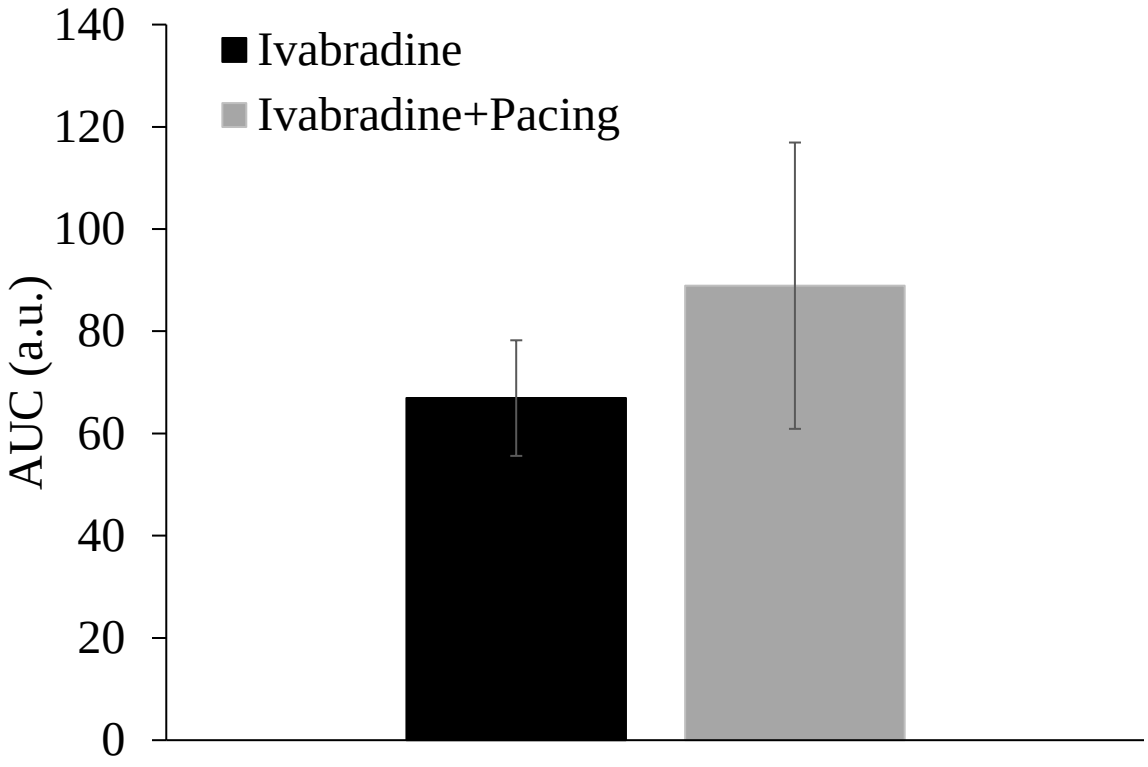

Figure 44. The AUCs of ivabradine and ivabradine + pacing from figure 42. The black bar represents the AUC of the ivabradine graph. The grey bar represents the AUC of the ivabradine + pacing graph. T-test was performed to compare these two bar graphs, and no significant difference was observed. (n=9, p=0.50)

3.6 Effect of Mechanical Stimulation on Membrane Voltage and Intracellular Calcium

Optical mapping was used to assess the effects of mechanical pacing on membrane voltage and intracellular calcium (*n*=9). Changes in action potential duration were observed, which revealed a fault in the experimental design. The heart rate difference between the period of lost capture and electrical pacing from the apex during imaging caused a prolongation of action potential duration due to restitution. This prolongation is shown in Figure 45. Changes in the calcium transient showed similar patterns to voltage.

The experiments were redesigned, so that mechanical pacing at 2.5 Hz was applied until loss of capture, after which imaging and apical pacing were immediately initiated (*n*=7). Point electrical pacing was then applied to the same location for the same period, followed by apical pacing and imaging for comparison. The first, middle and last beats during 30 sec of imaging were analyzed for both cases. In both cases, a similar uniform action potential duration shortening was seen between the first and last beat (Figure 46), which may represent effects of the change in activation sequence with apical pacing. Activation (Figure 47) and repolarization maps (Figure 48) are also shown, and there were no changes observable between the different modes of pacing.

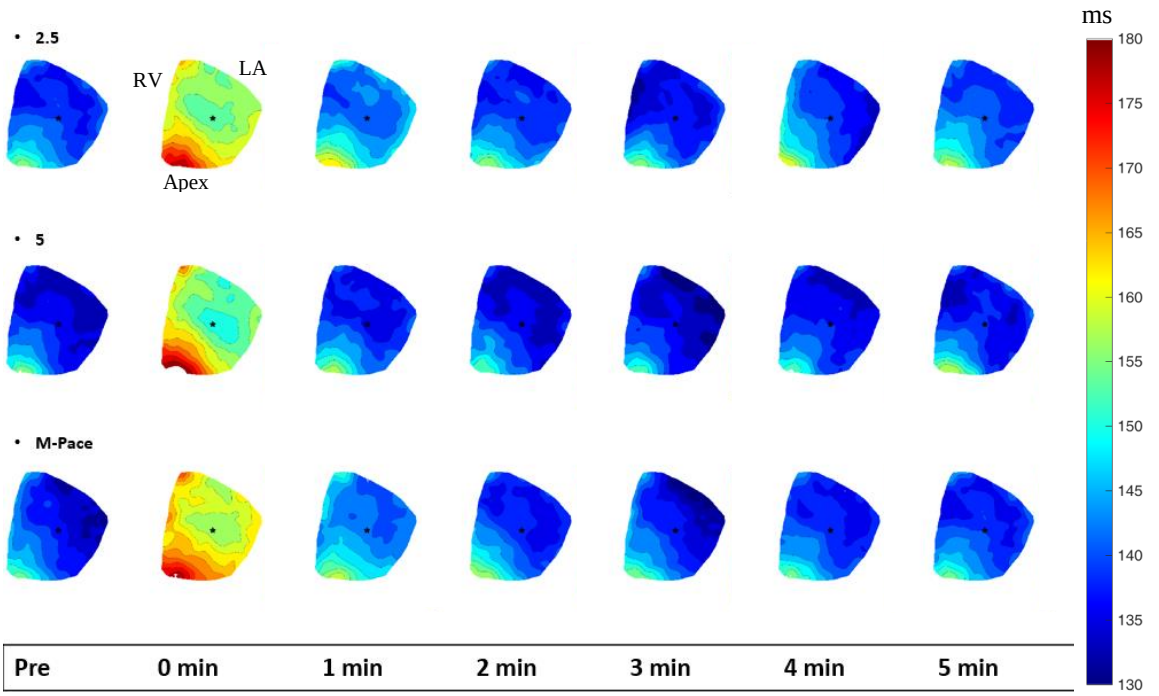

Figure 45. An example of APD_{80} after a period of lost mechanical pacing capture. 2.5 refers to the imaging after mechanical pacing at 2.5 Hz until loss. 5 refers to the imaging after mechanical pacing at 5 Hz until loss. M-Pace refers to the imaging after a mechanical pacing run of 2.5-6 Hz. A visible change is observed at 0 minute, which after the first minute goes back to pre-pacing durations. The dark blue represents the shortest APD and the dark red represents the longest APD. The black star represents the mechanical stimulation site. (*n*=9)

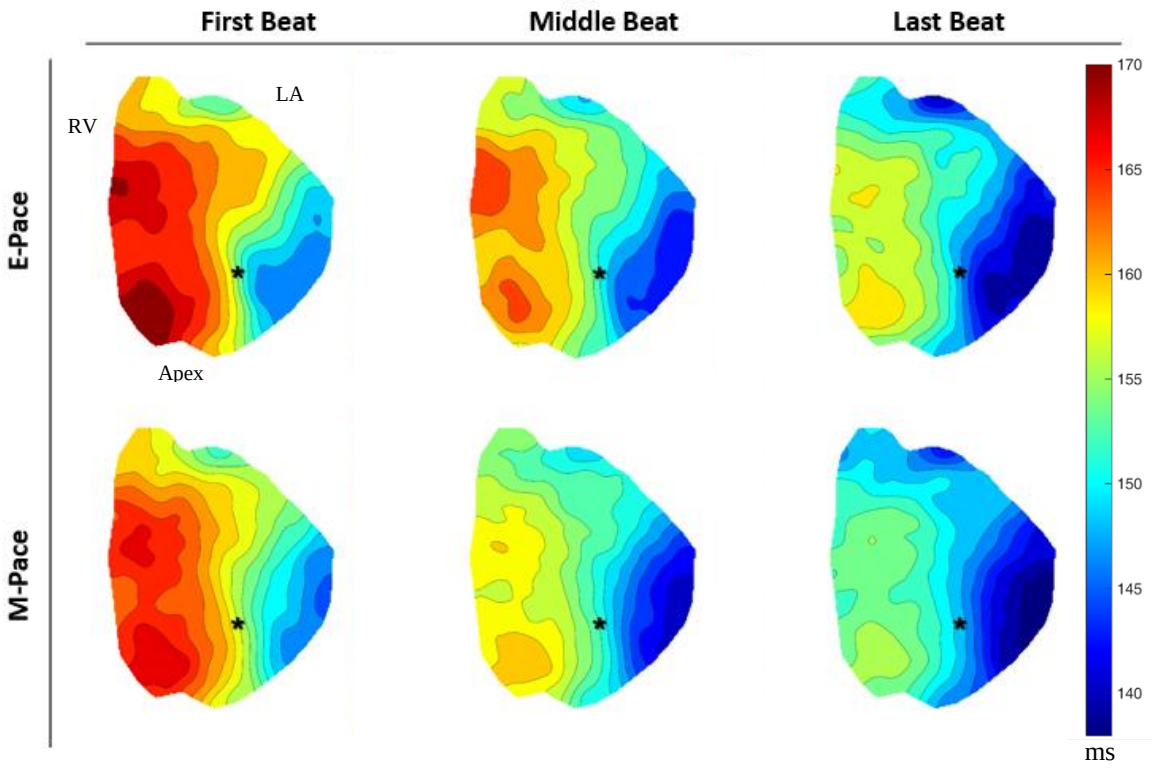

Figure 46. APD_{80} immediately after electrical and mechanical pacing. Top: the first, middle and last beats imaged right after electrical pacing at 2.5 Hz are shown, respectively. Bottom: the first, middle and last beats imaged right after mechanical pacing at 2.5 Hz are shown. In both settings, a similar uniform decrease was seen over time. The black star represents the local pacing location. (*n*=7)

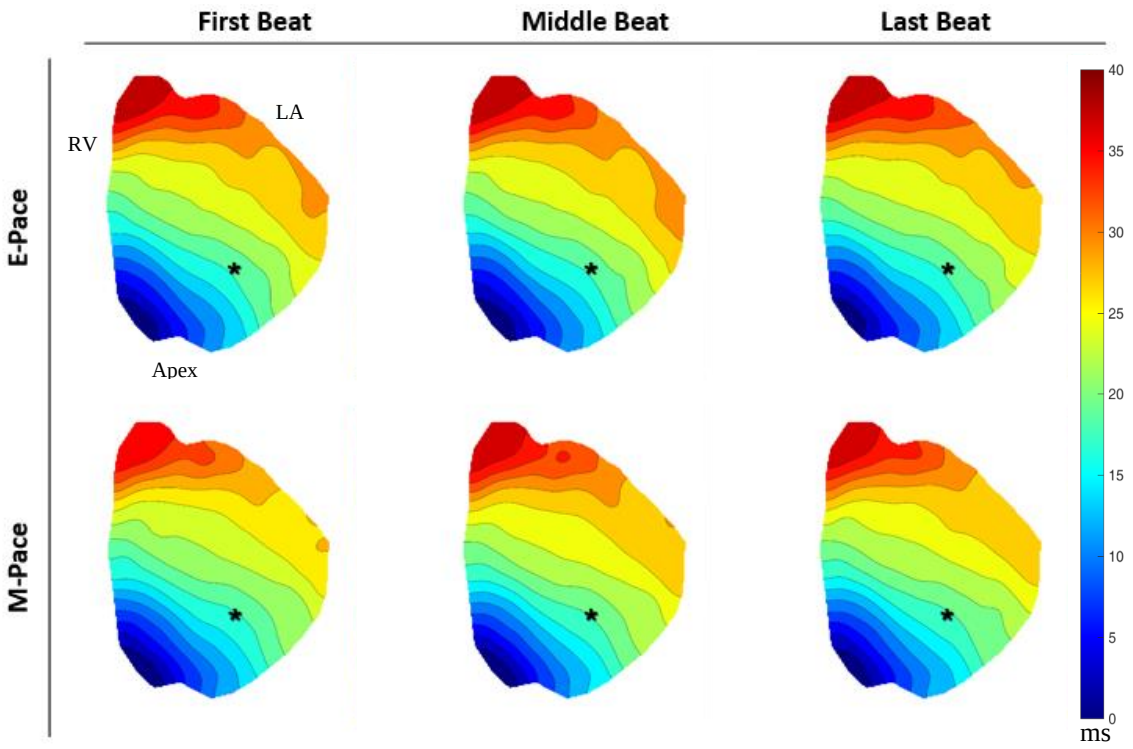

Figure 47. Activation immediately after electrical and mechanical pacing. Top: the first, middle and last beats imaged right after electrical pacing at 2.5 Hz are shown, respectively. Bottom: the first, middle and last beats imaged right after mechanical pacing at 2.5 Hz are shown. The black star represents the local pacing location. (*n*=7)

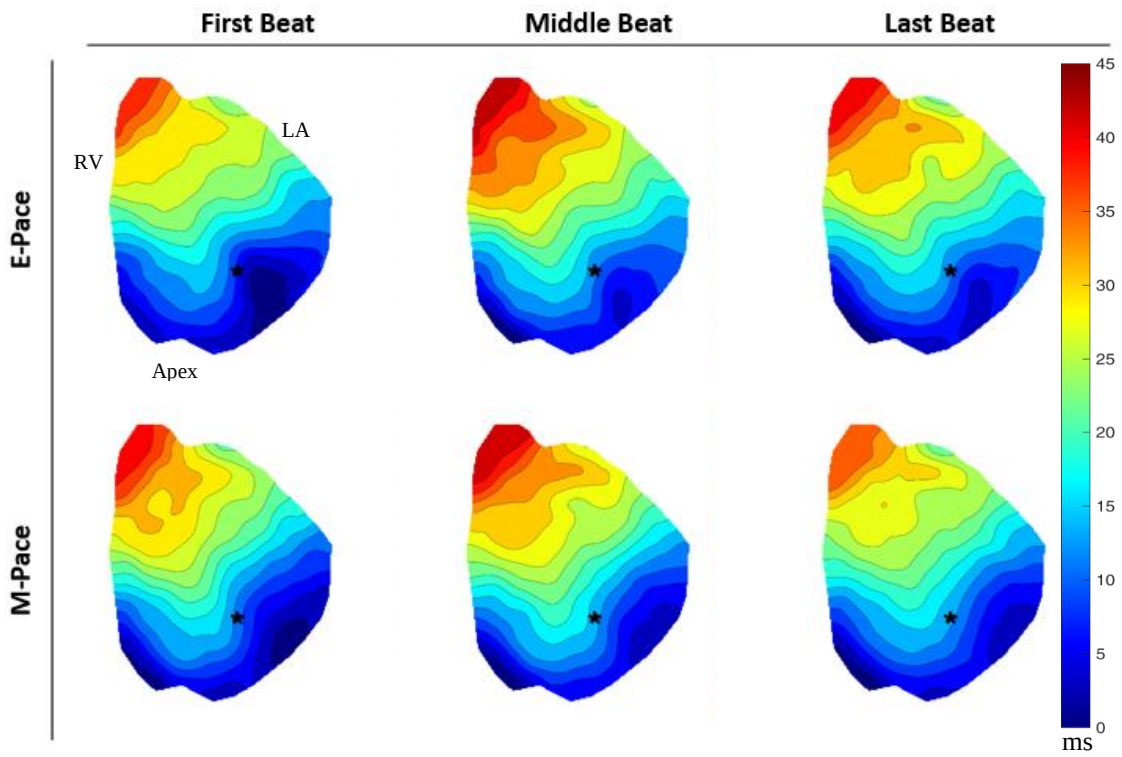

Figure 48. Repolarization immediately after electrical and mechanical pacing. Top: the first, middle and last beats imaged right after electrical pacing at 2.5 Hz are shown, respectively. Bottom: the first, middle and last beats imaged right after mechanical pacing at 2.5 Hz are shown. The black star represents the local pacing location. (*n*=7)

3.7 Effect of Mechanical Stimulation on Initiation of Excitation

To measure how mechanical stimulation might be affecting the initiation of excitation, simultaneous mechanical pacing and optical mapping was performed (n=7). A representative example of action potential measurements is shown in Figure 49. A continuous increase in the delay between stimulation and excitation was observed with each VE_M until loss of capture in all hearts. Two different techniques, one using optical mapping (Figure 50) and one using ECG timing (Figure 51), were used to measure this delay and in both cases, the delay was increased.

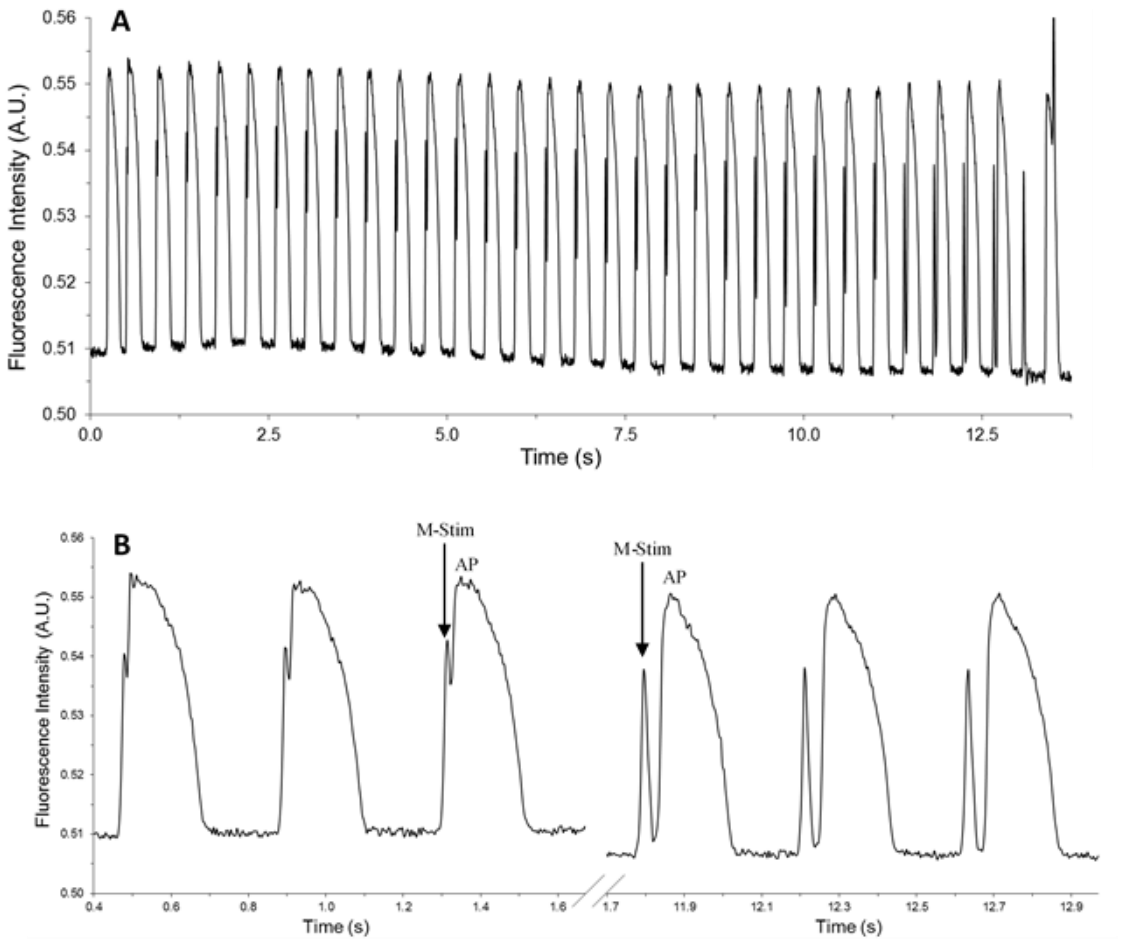

Figure 49. An example of stimulation-excitation delay. A) Action potential recordings, including an artefact from mechanical stimulation (m-stim), which separates from the action potential (AP) upstroke over time, indicating an increase in stimulation-excitation delay. B) A larger representation of the first and last three action potentials from (A) are shown, with the increase in the delay between mechanical stimulation and the initiation of the action potential being more obvious. (*n*=7)

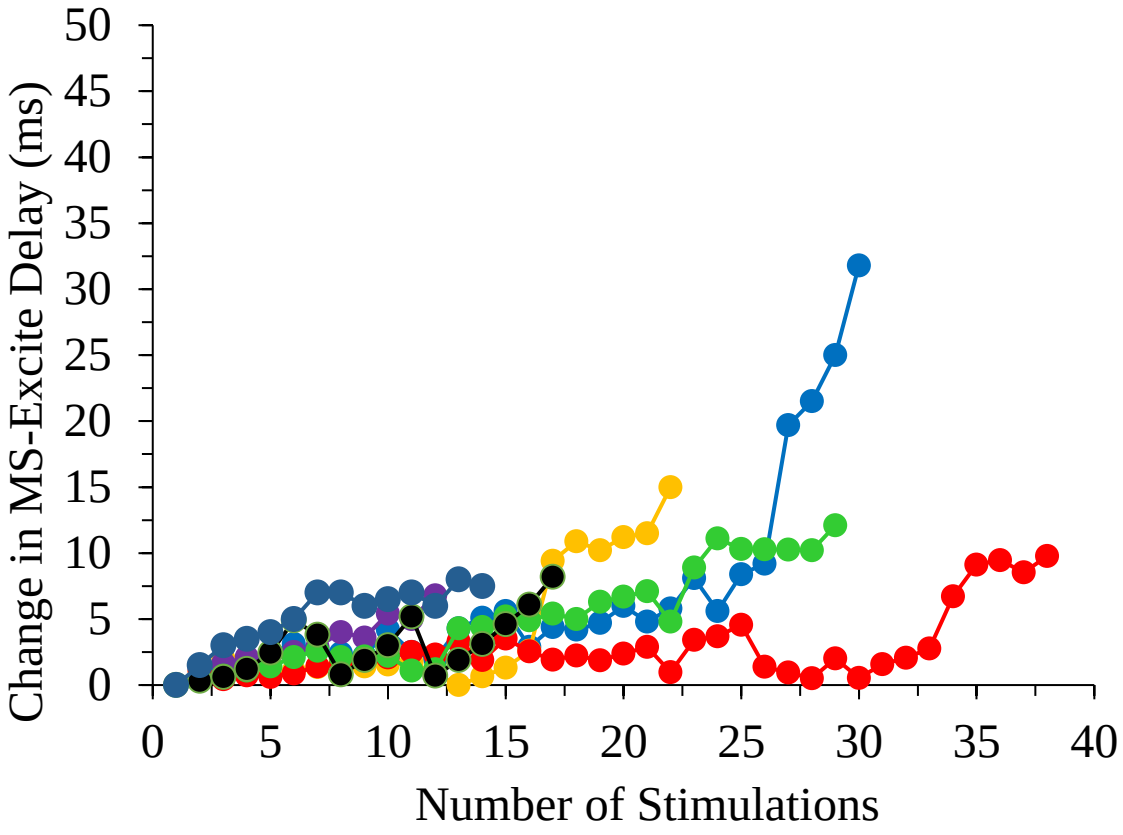

Figure 50. Increase in stimulation-excitation delay during mechanical pacing at 2.5 Hz measured by optical mapping. Each colour represents an experiment. In all experiments the delay between stimulation and excitation was continuously increased until loss of capture. (*n*=7)

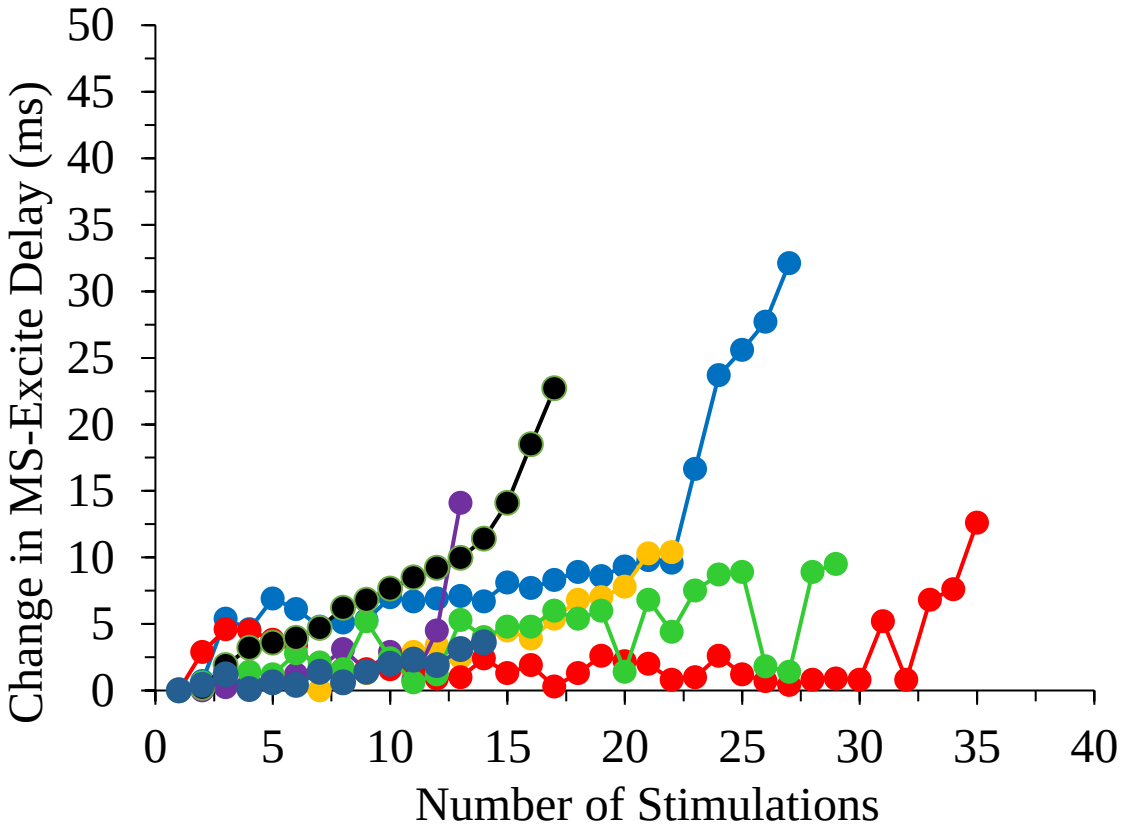

Figure 51. Increase in stimulation-excitation delay during mechanical pacing at 2.5 Hz measured by ECG. Each colour represents an experiment. In all experiments the delay between stimulation and excitation was continuously increased until loss of capture. (*n*=7)

3.8 Effect of Sub-Threshold Mechanical Stimulation on Pacing Sustainability

To test whether sub-threshold mechanical stimulation would affect pacing sustainability, a train of 2.5 Hz sub-threshold stimuli (0.5x threshold) were applied immediately before 2.5 Hz mechanical pacing (1.5x threshold; n=6). Compared to mechanical pacing alone, the number of beats to loss of capture was significantly lower when the tissue first experienced sub-threshold mechanical stimulation (Figure 52).

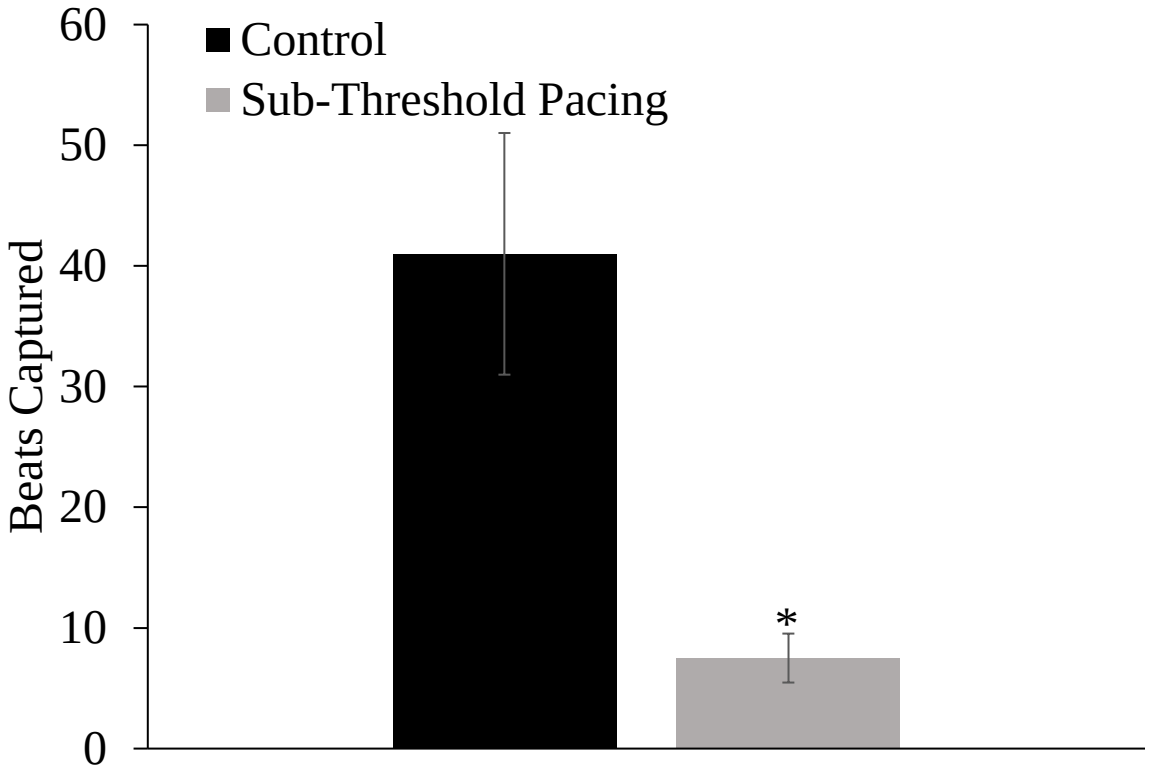

Figure 52. The effect of sub-threshold stimuli prior to mechanical pacing. The number of beats to loss of capture was significantly lower when sub-threshold pacing was carried out prior to the mechanical pacing. The black bar represents the number of beats captured in control mechanical pacing run. The light grey bar represents the number of beats captured after the tissue experience sub-threshold mechanical pacing. (*: vs. control; t-test, $p<0.05$) (n=6)

Chapter 4: Discussion

4.1 Summary

The main aim of this study was to identify factors that lead to unsustainability of mechanical pacing in isolated Langendorff-perfused rabbit hearts. As shown previously[42], local mechanical stimulation of the LV lead to focal VE_M. Consistent excitation with mechanical stimulation, however was lost after a finite number of stimuli, a number which decreased with increasing pacing rate. Relating to mechanisms, it was found that sustainability of mechanical pacing depends on the degree of tissue indentation. Increased tissue stiffness (with paclitaxel) decreased the indentation threshold for excitation but did not affect pacing sustainability. Elimination of active tension development (by excitation-contraction uncoupler blebbistatin) also had no effect. Reduced background heart rate (by ivabradine) did not change pacing sustainability. Optical mapping showed no change in ventricular activation, repolarisation, or action potential duration patterns with mechanical pacing, but did reveal an increasing delay between mechanical stimulation and excitation with each paced beat, suggesting that a continuous reduction in stretch-activated depolarising current may account for the loss of pacing capture. Each of these principal findings are discussed further, below.

4.2 Passive Tissue Mechanical Properties

As with mechanical pacing the means to pace the heart is applied through a mechanical effect, it is possible that stimulation of the tissue causes acute and reversible changes in mechanical properties that account for the loss of capture. Temporary acute mechanically-induced changes in cardiac tissue have been demonstrated previously, an

effect known as strain softening in which tissue becomes less stiff in response to a deformation, which resolves after some period of rest. This evidence comes from experiments in isolated arrested rat hearts in which hearts became less stiff with repeated cycles of LV balloon inflation and deflation, with stiffness restored after more than an hour of rest. By incorporating the theory proposed by Johnson and Beatty[112], this was explained as strain softening (rather than a viscoelastic property of the tissue).[68] In our experiments, since the ability to mechanically pace the heart was gained back after only two minutes of rest, strain softening seems an unlikely mechanism contributing to the loss of capture. A similar time scale as ours for the return of mechanical excitability was seen in a study utilizing intraventricular balloon inflation as the means to cause $VE_{M.}$[113] In that study a rest period of up to 1 minute was required for recovery of mechanically-induced excitation from balloon inflation. Furthermore, we did not measure a local reduction in stiffness at the site of mechanical stimulation, and in previous studies strain softening was not observed in viable tissue preparations, even in the presence of cross-bridge formation inhibitors (with similar effects of blebbistatin) that remove the active mechanical component.[28]

To directly determine whether changes in tissue stiffness affect the sustainability of mechanical pacing, paclitaxel (a microtubule hyperpolymerizer, also known as Taxol) was used to increase the tissue stiffness. Paclitaxel has been used previously by Parker *et al*. to assess the effect of tissue stiffness on mechanical excitation in rabbit isolated hearts. In that study they treated the hearts with either colchicine or paclitaxel, and increased the LV volume by a volume pump. The main goal of that study was to measure stretch induced arrhythmias, however the mechanical tissue properties, specifically stiffness, were also

assessed. The tissue was shown to be stiffer, demonstrated by a significant increase in LV dP/dt_{max}. We saw a similar increase in tissue stiffness with paclitaxel application, as measured by force indentation. In addition, we saw changes in pressure characteristics that indicated tissue stiffening, specifically an increase in EDP. In contrast, MSP was decreased in control (most likely reflecting preparation rundown) but not with paclitaxel, however in the case of paclitaxel the increase in EDP prevented a drop in MSP, as systolic function was clearly decreased in both groups, as shown by the similar reduction in developed pressure and dP/dt_{max}. Interestingly, the PP was increased in both experiment types, although the increase in no drug experiments was less than with paclitaxel. The increase in PP of the no drug experiments could have resulted from tissue edema over time, as our KH solution lacked protein and cellular components of blood. The increase in the PP in paclitaxel experiments, on the other hand, may have had an additional contribution of tissue stiffening and increased stiffness of smooth muscle cells of the coronary vessels.[114]

Yet, with the increase in tissue stiffness induced by paclitaxel, the sustainability of mechanical pacing did not change. This finding demonstrates that even if there is an acute temporary use-dependent change in the local tissue stiffness with mechanical pacing, it would not be expected to contributor to a loss of capture.

Sustainability is, however, directly related to the indentation depth. This was demonstrated in the paclitaxel and no drug experiments, where before the incubation period, the increase in indentation depth from 1.5x to 2.0x significantly increased the sustainability. Furthermore, additional beats were captured with an increase in indentation to 2.0x the threshold immediately after capture was lost at 1.5x the threshold. These findings point to the fact that the absolute indentation is more important for sustainability

than the relation of indentation depth to the indentation threshold. To explain this further, I will use the paclitaxel experiments as an example. The threshold for VE_M was reduced after paclitaxel. However, the indentation applied before and after paclitaxel was the same (1.5x the original indentation depth). As there was no difference between the pre- and Paclitaxel sustainability curves, the absolute amount of indentation was important, not how it compared to the threshold at that moment. With increased indentation depth, the extent of the stretch on the tissue is increased. Increased tissue stretch will affect more cells and activate a higher proportion of SAC_{NS}, thus maintaining an adequate depolarising current for longer and accounting for the increased sustainability of mechanical pacing with increased indentation.

Thus, the two key findings of the paclitaxel and no drug experiments are: 1. Changes in tissue stiffness do not affect the sustainability of mechanical pacing, so that the loss of capture under normal conditions is not related to changes in tissue stiffness. 2. The sustainability of mechanical pacing is directly related to the indentation depth, possibly due to more channels being involved.

4.3 Active Tissue Mechanical Properties

Active tension generation in the heart causes contraction. As reports of cases in which patients with asystolic hearts were kept alive for hours by chest thumping (a form of mechanical pacing), we wanted to investigate whether eliminating contraction, thus simulating conditions of asystole, might improve sustainability.

We used blebbistatin as a cross-bridge formation inhibitor to eliminate active force generation (i.e., contraction). We compared the sustainability of mechanical pacing before

and after the elimination of contraction. Elimination of contraction did not significantly change the number of beats before loss of capture. It should be noted that blebbistatin changed some pressure characteristics, such as EDP. While we did not measure stiffness in those hearts (our method does not work reliably in non-contracting hearts), it felt stiffer to the touch. These changes are similar to what occurred with placitaxel, which did not affect sustainability, so even though the tissue stiffening with blebbistatin occurs by a different mechanism that with paclitaxel, the sustainability was not affected with increased in stiffness nor with blebbistatin

In summary, the key finding of the blebbistatin experiment is that elimination of contraction does not change the sustainability of mechanical pacing.

4.4 Background Rate and Ivabradine

The sustainability curve in the blebbistatin, paclitaxel, and no drug experiments, and the reports on patients with severe bradycardia kept alive for extended periods of time with chest thumping suggest that there may be a slow pacing rate at rate at which mechanical pacing is sustainable. Removal of the sinus node in our experiments only reduced the beating rate to ~2 Hz, which allowed us to start overdrive mechanical pacing at 2.5 Hz. To further reduce heart rate, we used ivabradine, a well-known HCN channel blocker. Ivabradine was added in small doses to reduce the heart rate to < 1 Hz. Mechanical pacing was tested before and after ivabradine, as well as after ivabradine with electrical pacing at the pre-ivabradine heart rate in between periods of mechanical pacing. These two combinations allowed us to determine the effect of rate and of ivabradine. By comparing the results of pre-ivabradine and post-ivabradine with electrical pacing in between (which

allows us to determine the effect of ivabradine on sustainability, as the background rates are matched), it was found that ivabradine does not affect the mechanical pacing sustainability. The concern here was that ivabradine might have off-target effects that could affect sustainability. One off-target ion channel on which the effect of ivabradine has been studied is hERG. It has been shown that the IC_{50} of ivabradine on different isoforms of hERG is 2.07 and 3.31 μM[115]. In our study, the amount of ivabradine used in each experiment was well below the amount that has been reported to affect hERG. However, this does not eliminate the possibility of ivabradine affecting other channels. By comparing the result of post-ivabradine and post-ivabradine with pacing in between (which allows us to determine the effect of background rate on sustainability), it was found that the background rate has no significant effect on sustainability of mechanical pacing. The concern here was that a difference in rate would affect the ionic concentrations and sub-cellular compartmentations, which could affect sustainability. For instance, calcium dynamics are dependent on the beating rate, and has additionally been shown to be affected by mechanical effects such as stretch, including increased SR calcium release, leading to a reduction in SR calcium levels[88,91,116]. Overall, the two key findings of the ivabradine experiments are: 1. Ivabradine does not affect the sustainability of mechanical pacing. 2. Background rate has no effect on sustainability of mechanical pacing, which suggests that changes in ion concentrations and calcium handling may not affect the sustainability of mechanical pacing.

4.5 Optical Mapping

We used dual-parametric optical mapping to measure myocardial voltage and intracellular calcium, to determine whether they were affected by mechanical pacing. While mechanical pacing had no obvious effect on activation, repolarisation, or action potential duration patterns, it was observed that with each mechanical stimulus, the time to excitation appeared to be prolonged. Further experiments confirmed this finding, demonstrating that the stimulus-excitation delay continuously increased until loss of capture. It has been shown that local mechanically-induced excitation in the isolated heart is due to the activation of SAC_{NS}[85]. Furthermore, in isolated cell studies, ion channel current, including mechanosensitive ones, has been shown to decrease with repeated mechanical stimulation[117,118]. If this occurs in SAC_{NS} and in the whole heart with mechanical pacing, then the decrease in depolarising current will result in slower depolarization, causing an increase in the time between stimulation and excitation. Moreover, if the depolarising current continues to be diminished, it will eventually be overcome by the source-sink relation, causing loss of capture. We believe that this indeed underlies the lack of sustainability of mechanical pacing.

A recent study in fact supported the speculation from above. Piezo 1 and 2, which are the candidates for stretch activated channels, were expressed in human embryonic kidney cells. These channels were then mechanically stimulated with patch-clamp pipette suction. The stimulation pattern was either sinusoidal or square stimulation. The current from these channels was measured and shown to be reduced with every mechanical stimulation. This is in fact what we speculated from our optical mapping results. This current decrease seemed to be more apparent in the squared stimulation at all stimulation

rate, however with sinusoidal stimulation pattern, this decrease in current was absent at low frequency rate, pointing to the possibility of sustainable mechanical pacing under specific circumstances. They further showed that with increased frequency, the same decrease in the current happens in lower number of stimuli. This explains the lower number of beats captured at higher stimulation rates we observed in all of the sustainability curves. Another interesting experiment they performed was direct mechanical stimulation of neurons and they observed a loss of capture in the neuronal cells after a period of consistent capture, just the same way we saw loss of capture in our model. This point to the universal presence of loss of capture beyond the mechanical pacing of the heart.[119] We can show whether these channels are also responsible for what we saw in our model by using a Piezo activator on inhibitor and determine the changes in the stimulation-excitation delay and the overall changes on the sustainability.

This is supported by an additional experiment in which we preceded supra-threshold mechanical pacing with a period of sub-threshold (0.5x threshold) mechanical stimuli and compared the number of captured beats to supra-threshold mechanical pacing alone. The number of beats to loss of capture was significantly less when the tissue first experienced sub-threshold stimuli. This suggest that even in the absence of excitation, mechanical stimuli causes SAC_{NS} current run-down. Related to this, we also ran experiments in which indentation depth was increased to 2x threshold immediately after a loss of capture, which re-established excitation for a period of additional beats, presumably by affecting additional tissue and a higher proportion of SAC_{NS} channels. This is maybe unsurprising as we also showed that indentation depth is a significant determining factor for sustainability, as 2x threshold pacing captured more beats than pacing at 1.5x threshold.

Thus, the key findings from the optical mapping experiments are: 1. Mechanical pacing has no effects on activation, repolarisation, or action potential duration patterns. 2. Mechanical pacing leads to an increase in stimulation-excitation delay, which relates to the loss of capture.

4.6 Limitations

The limited reports of "successful" mechanical pacing to keep patients alive in emergency settings seem to contradict the results of this study. This could be due in part to limitations of our experimental model. We used isolated rabbit hearts, and as similar as they are to the human heart in some respects, difference in ion channels or tissue properties could play a role. In addition, having the heart in ex vivo conditions and detached from the central nervous system could alter the effects of mechanical stimulation. Related to that¸ our studies involved direct contact of the stimulation probe with the epicardial surface of the heart, which could give a different result than extracorporeal impact. That said, our results agree with recent in vivo studies reporting loss of mechanical pacing capture[36–39,41,120], so may indeed apply.

4.7 Future Directions

Understanding the reason(s) behind the observed increase in excitation-stimulation delay with mechanical pacing, effects of background rate and ionic concentration balance on sustainability, and other factors that might be affecting pacing capture require further investigation. To determine whether SAC_{NS} current run down is involved in the increased

excitation-stimulation delay, experiments should involve current recording from cardiomyocytes subjected to repeated mechanical stimulation, including time for recovery. In addition, a similar set of experiments can be designed where sub-threshold mechanical stimuli are performed and the current of SAC_{NS} is measured in cardiomyocytes. Experiments where Piezo channel activator or inhibitors are used should be performed to determine if these channels are the ones responsible for VE_M, and asses how the changes on the Piezo channels affect the mechanical pacing sustainability. To further address the role of current run down and the importance of the stimulation location, experiments involving two mechanical stimulation locations that will be stimulated alternatively should be carried out. In these experiments the stimulation rate is reduced by half at each location but the overall rate of pacing will stay the same. Theoretically, this method should allow the number of captured beats to be doubled. Other studies to investigate cross-species differences, influence of disease settings and other pathophysiological states are necessary to fully understand the reason(s) for the unsustainability and the utility of mechanical pacing.

References

1. Larsson, B., Elmqvist, H., Rydén, L. & Schüller, H. Lessons from the first patient with an implanted pacemaker: 1958-2001. *Pacing Clin. Electrophysiol.* **26,** 114–124 (2003).
2. Kirkfeldt, R. E., Johansen, J. B., Nohr, E. A., Jorgensen, O. D. & Nielsen, J. C. Complications after cardiac implantable electronic device implantations: an analysis of a complete, nationwide cohort in Denmark. *Eur. Heart J.* **35,** 1186–1194 (2014).
3. Palmisano, P. *et al.* Rate, causes, and impact on patient outcome of implantable device complications requiring surgical revision: large population survey from two centres in Italy. *EP Eur.* **15,** 531–540 (2013).
4. Mallela, V. S., Ilankumaran, V. & Rao, S. N. Trends in cardiac pacemaker batteries. *Indian Pacing Electrophysiol. J.* **4,** 201–212 (2004).
5. Difrancesco, D. The role of the funny current in pacemaker activity. *Circ. Res.* **106,** 434–446 (2010).
6. Brown, H. F., DiFrancesco, D. & Noble, S. J. How does adrenaline accelerate the heart? *Nature* **280,** 235–236 (1979).
7. Maltsev, V. A., Vinogradova, T. M. & Lakatta, E. G. The emergence of a general theory of the initiation and strength of the heartbeat. *J. Pharmacol. Sci.* **100,** 338–369 (2006).
8. Torrente, A. G. *et al.* L-type Cav1.3 channels regulate ryanodine receptor-dependent Ca2+release during sino-atrial node pacemaker activity. *Cardiovasc. Res.* **109,** 451–461 (2016).

9. Lakatta, E. G., Vinogradova, T. M. & Maltsev, V. A. The Missing Link in the Mystery of Normal Automaticity of Cardiac Pacemaker Cells. *Ann. N. Y. Acad. Sci.* **1123,** 41–57 (2008).

10. Bakker, M. L., Moorman, A. F. M. & Christoffels, V. M. The Atrioventricular Node: Origin, Development, and Genetic Program. *Trends Cardiovasc. Med.* **20,** 164–171 (2010).

11. Shacklock, P. S., Wier, W. G. & Balke, C. W. Local Ca2+ transients (Ca2+ sparks) originate at transverse tubules in rat heart cells. *J. Physiol.* **487 (Pt 3,** 601–8 (1995).

12. Soeller, C. & Cannell, M. B. Numerical simulation of local calcium movements during L-type calcium channel gating in the cardiac diad. *Biophys. J.* **73,** 97–111 (1997).

13. Keizer, J. & Levine, L. Ryanodine Receptor Adaptation and Ca2+-lnduced Ca2+ Release- Dependent Ca2+ Oscillations. *Biophys. J.* **71,** 3477–3487 (1996).

14. Nakai, J. *et al.* Functional nonequality of the cardiac and skeletal ryanodine receptors. *Proc. Natl. Acad. Sci. U. S. A.* **94,** 1019–22 (1997).

15. Dotson, D. G. & Putkey, J. A. Differential recovery of Ca2+ binding activity in mutated EF-hands of cardiac troponin C. *J. Biol. Chem.* **268,** 24067–73 (1993).

16. Potter, J. D., Sheng, Z., Pan, B. S. & Zhao, J. A direct regulatory role for troponin T and a dual role for troponin C in the Ca2+ regulation of muscle contraction. *J. Biol. Chem.* **270,** 2557–62 (1995).

17. Patchell, V. B. *et al.* The inhibitory region of troponin-I alters the ability of F-actin to interact with different segments of myosin. *Eur. J. Biochem.* **269,** 5088–100 (2002).

18. Piazzesi, G. & Lombardi, V. Simulation of the rapid regeneration of the actin-myosin working stroke with a tight coupling model of muscle contraction. *J. Muscle Res. Cell Motil.* **17,** 45–53 (1996).

19. Bers, D. M. Cardiac excitation–contraction coupling. *Nature* **415,** 198–205 (2002).

20. Kohl, P., Bollensdorff, C. & Garny, A. Effects of mechanosensitive ion channels on ventricular electrophysiology: experimental and theoretical models. *Exp. Physiol.* **91,** 307–321 (2006).

21. Quinn, T. A., Kohl, P. & Ravens, U. Cardiac mechano-electric coupling research: Fifty years of progress and scientific innovation. *Prog. Biophys. Mol. Biol.* **115,** 71–75 (2014).

22. Quinn, T. A. & Kohl, P. Rabbit models of cardiac mechano-electric and mechano-mechanical coupling. *Prog. Biophys. Mol. Biol.* **121,** 110–122 (2016).

23. Peyronnet, R., Nerbonne, J. M. & Kohl, P. Cardiac Mechano-Gated Ion Channels and Arrhythmias. *Circ. Res.* **118,** 311–329 (2016).

24. Bainbridge, F. A. The Influence of Venous Filling Upon the Rate of the Heart. *J. Physiol.* **50,** 65–84 (1915).

25. Katz, A. M. Ernest Henry Starling, His Predecessors, and the "Law of the Heart." *Circulation* **106,** 2986–2992 (2002).

26. Lab, M. J. Depolarization produced by mechanical changes in normal and abnormal myocardium. *J. Physiol.* **284,** 143P–144P (1978).

27. White, E., Boyett, M. R. & Orchard, C. H. The effects of mechanical loading and changes of length on single guinea-pig ventricular myocytes. *J. Physiol.* **482 (Pt 1),** 93–107 (1995).

28. Franz, M. R., Cima, R., Wang, D., Profitt, D. & Kurz, R. Electrophysiological effects of myocardial stretch and mechanical determinants of stretch-activated arrhythmias. *Circulation* **86,** 968–78 (1992).

29. Lee, J. C. *et al.* ICD lead proarrhythmia cured by lead extraction. *Hear. Rhythm* **6,** 613–8 (2009).

30. Zoll, P. M. Resuscitation of the Heart in Ventricular Standstill by External Electric Stimulation. *N. Engl. J. Med.* **247,** 768–771 (1952).

31. Zoll, P. M., Belgard, A. H., Weintraub, M. J. & Frank, H. A. External Mechanical Cardiac Stimulation. *N. Engl. J. Med.* **294,** 1274–1275 (1976).

32. Kohl, P., Nesbitt, A. D., Cooper, P. J. & Lei, M. Sudden cardiac death by Commotio cordis : role of mechano – electric feedback. *N. Engl. J. Med.* **50,** 280–289 (2001).

33. Qu, Z., Garfinkel, A. & Weiss, J. N. Vulnerable window for conduction block in a one-dimensional cable of cardiac cells, 1: single extrasystoles. *Biophys. J.* **91,** 793–804 (2006).

34. Levine, J. H. *et al.* Changes in myocardial repolarization in patients undergoing balloon valvuloplasty for congenital pulmonary stenosis: Evidence for contraction-excitation feedback in humans. *Circulation* **77,** 70–77 (1988).

35. Pennington, J. E., Taylor, J. & Lown, B. Chest thump for reverting ventricular tachycardia. *N. Engl. J. Med.* **283,** 1192–5 (1970).

36. Livneh, A., Kimmel, E., Kohut, A. R. & Adam, D. Extracorporeal acute cardiac pacing by High Intensity Focused Ultrasound. *Prog. Biophys. Mol. Biol.* **115,** 140–153 (2014).

37. Rotenberg, M. Y., Gabay, H., Etzion, Y. & Cohen, S. Feasibility of Leadless Cardiac Pacing Using Injectable Magnetic Microparticles. *Sci. Rep.* **6,** 24635 (2016).

38. Dalecki, D., Keller, B. B., Raeman, C. H. & Carstensen, E. L. Effects of pulsed ultrasound on the frog heart: I. Thresholds for changes in cardiac rhythm and aortic pressure. *Ultrasound Med. Biol.* **19,** 385–90 (1993).

39. MacRobbie, A. G., Raeman, C. H., Child, S. Z. & Dalecki, D. Thresholds for premature contractions in murine hearts exposed to pulsed ultrasound. *Ultrasound Med. Biol.* **23,** 761–5 (1997).

40. Towe, B. C. & Rho, R. Ultrasonic cardiac pacing in the porcine model. *IEEE Trans. Biomed. Eng.* **53,** 1446–1448 (2006).

41. Hersch, A. & Adam, D. Premature Cardiac Contractions Produced Efficiently By External High-Intensity Focused Ultrasound. *Ultrasound Med. Biol.* **37,** 1101–1110 (2011).

42. Quinn, T. A. & Kohl, P. Comparing maximum rate and sustainability of pacing by mechanical vs. electrical stimulation in the Langendorff-perfused rabbit heart. *Europace* **18,** iv85-iv93 (2016).

43. Sequeira, V., Nijenkamp, L. L. A. M., Regan, J. A. & Van Der Velden, J. The physiological role of cardiac cytoskeleton and its alterations in heart failure. *Biochim. Biophys. Acta - Biomembr.* **1838,** 700–722 (2014).

44. Fürst, D. O., Osborn, M., Nave, R. & Weber, K. The organization of titin filaments in the half-sarcomere revealed by monoclonal antibodies in immunoelectron microscopy: a map of ten nonrepetitive epitopes starting at the Z line extends close to the M line. *J. Cell Biol.* **106,** 1563–72 (1988).

45. Maruyama, K. *et al.* Connectin filaments link thick filaments and Z lines in frog skeletal muscle as revealed by immunoelectron microscopy. *J. Cell Biol.* **101,** 2167–72 (1985).

46. Watkins, S. C., Samuel, J. L., Marotte, F., Bertier-Savalle, B. & Rappaport, L. Microtubules and desmin filaments during onset of heart hypertrophy in rat: a double immunoelectron microscope study. *Circ. Res.* **60,** 327–36 (1987).

47. Rappaport, L. & Samuel, J. L. Microtubules in Cardiac Myocytes. *Int. Rev. Cytol.* **113,** 101–143 (1988).

48. Gómez, A. M., Kerfant, B. G. & Vassort, G. Microtubule disruption modulates Ca(2+) signaling in rat cardiac myocytes. *Circ. Res.* **86,** 30–6

49. Tsutsui, H., Ishihara, K. & Cooper, G. Cytoskeletal role in the contractile dysfunction of hypertrophied myocardium. *Science* **260,** 682–7 (1993).

50. Parker, K. K., Taylor, L. K., Atkinson, B., Hansen, D. E. & Wikswo, J. P. The effects of tubulin-binding agents on stretch-induced ventricular arrhythmias. 131–140 (2001).

51. Cooper, G. Cardiocyte cytoskeleton in hypertrophied myocardium. *Heart Fail. Rev.* **5,** 187–201 (2000).

52. Cooper, G. Cytoskeletal networks and the regulation of cardiac contractility: microtubules, hypertrophy, and cardiac dysfunction. *AJP Hear. Circ. Physiol.* **291,** H1003–H1014 (2006).

53. Wang, N., Yan, K. & Rasenick, M. M. Tubulin binds specifically to the signal-transducing proteins, Gs alpha and Gi alpha 1. *J. Biol. Chem.* **265,** 1239–42 (1990).

54. Palmer, B. M., Valent, S., Holder, E. L., Weinberger, H. D. & Bies, R. D. Microtubules modulate cardiomyocyte beta-adrenergic response in cardiac hypertrophy. *Am. J. Physiol.* **275,** H1707-16 (1998).

55. Yamamoto, S. *et al.* Role of microtubules in the viscoelastic properties of isolated cardiac muscle. *J. Mol. Cell. Cardiol.* **30,** 1841–1853 (1998).

56. Kato, S., Koide, M., Cooper, G. & Zile, M. R. Effects of pressure- or volume-overload hypertrophy on passive stiffness in isolated adult cardiac muscle cells. *Am. J. Physiol.* **271,** H2575-83 (1996).

57. Nishimura, S. *et al.* Microtubules modulate the stiffness of cardiomyocytes against shear stress. *Circ. Res.* **98,** 81–87 (2006).

58. Chapman, D., Weber, K. T. & Eghbali, M. Regulation of fibrillar collagen types I and III and basement membrane type IV collagen gene expression in pressure overloaded rat myocardium. *Circ. Res.* **67,** 787–94 (1990).

59. Pauschinger, M. *et al.* Dilated cardiomyopathy is associated with significant changes in collagen type I/III ratio. *Circulation* **99,** 2750–6 (1999).

60. Cleutjens, J. P., Verluyten, M. J., Smiths, J. F. & Daemen, M. J. Collagen remodeling after myocardial infarction in the rat heart. *Am. J. Pathol.* **147,** 325–38 (1995).

61. Granzier, H. L. & Irving, T. C. Passive tension in cardiac muscle: contribution of collagen, titin, microtubules, and intermediate filaments. *Biophys. J.* **68,** 1027–1044 (1995).

62. Villari, B. *et al.* Influence of collagen network on left ventricular systolic and diastolic function in aortic valve disease. *J. Am. Coll. Cardiol.* **22,** 1477–84 (1993).

63. Fomovsky, G. M., Thomopoulos, S. & Holmes, J. W. Contribution of extracellular matrix to the mechanical properties of the heart. *J. Mol. Cell. Cardiol.* **48,** 490–496 (2010).

64. Bishop, J. E. & Laurent, G. J. Collagen turnover and its regulation in the normal and hypertrophying heart. *Eur. Heart J.* **16 Suppl C,** 38–44 (1995).

65. MacKenna, D. A., Omens, J. H., McCulloch, A. D. & Covell, J. W. Contribution of collagen matrix to passive left ventricular mechanics in isolated rat hearts. *Am. J. Physiol.* **266,** H1007-18 (1994).

66. Todaka, K. *et al.* Functional consequences of acute collagen degradation studied in crystalloid perfused rat hearts. *Basic Res. Cardiol.* **92,** 147–158 (1997).

67. Mullins, L. Effect of Stretching on the Properties of Rubber. *Rubber Chem. Technol.* **21,** 281–300 (1948).

68. Emery, J. L. & Mcculloch, A. D. Strain Softening in Rat Left Ventricular IVIyocardium. **119,** 6–12 (2017).

69. Kirton, R. S., Taberner, A. J., Nielsen, P. M. F., Young, A. A. & Loiselle, D. S. Strain softening behaviour in nonviable rat right-ventricular trabeculae, in the presence and the absence of butanedione monoxime. *Exp. Physiol.* **89,** 593–604 (2004).

70. McBride, D. W. & Hamill, O. P. Pressure-clamp: a method for rapid step perturbation of mechanosensitive channels. *Pfl*[illegible]*gers Arch. Eur. J. Physiol.* **421,** 606–612 (1992).

71. Hurwitz, C. G. & Segal, A. S. Application of pressure steps to mechanosensitive channels in membrane patches: A simple, economical, and fast system. *Pflugers Arch. Eur. J. Physiol.* **442,** 150–156 (2001).

72. Coste, B. *et al.* Piezo1 and Piezo2 Are Essential Components of Distinct Mechanically Activated Cation Channels. *Science (80-.).* **330,** 55–60 (2010).

73. Baumgarten, C. M., Browe, D. M. & Ren, Z. *Swelling- and Stretch-activated Chloride Channels in the Heart: Regulation and Function*. *Mechanosensitivity in Cells and Tissues* (Academia, 2005). at <http://www.ncbi.nlm.nih.gov/pubmed/21290764>

74. Kim, D. A mechanosensitive K+ channel in heart cells. Activation by arachidonic acid. *J. Gen. Physiol.* **100,** 1021–40 (1992).

75. Gomis, A., Soriano, S., Belmonte, C. & Viana, F. Hypoosmotic- and pressure-induced membrane stretch activate TRPC5 channels. *J. Physiol.* **586,** 5633–49 (2008).

76. Berrier, C. *et al.* The Purified Mechanosensitive Channel TREK-1 Is Directly Sensitive to Membrane Tension. *J. Biol. Chem.* **288,** 27307–27314 (2013).

77. Brohawn, S. G., Su, Z. & MacKinnon, R. Mechanosensitivity is mediated directly by the lipid membrane in TRAAK and TREK1 K^+ channels. *Proc. Natl. Acad. Sci.* **111,** 3614–3619 (2014).

78. Van Wagoner, D. R. Mechanosensitive gating of atrial ATP-sensitive potassium channels. *Circ. Res.* **72,** 973–83 (1993).

79. Link, M. S. *et al.* Selective activation of the K(+)(ATP) channel is a mechanism by which sudden death is produced by low-energy chest-wall impact (Commotio cordis). *Circulation* **100,** 413–8 (1999).

80. Inoue, R., Jian, Z. & Kawarabayashi, Y. Mechanosensitive TRP channels in cardiovascular pathophysiology. *Pharmacol. Ther.* **123,** 371–385 (2009).

81. Craelius, W. Stretch-activation of rat cardiac myocytes. *Exp. Physiol.* **78,** 411–423 (1993).

82. White, E. *et al.* The effects of increasing cell length on auxotonic contractions; membrane potential and intracellular calcium transients in single guinea-pig ventricular myocytes. *Exp. Physiol.* **78,** 65–78 (1993).

83. Quinn, T. A. Cardiac mechano-electric coupling: a role in regulating normal function of the heart? *Cardiovasc. Res.* **108,** 1–3 (2015).

84. Zeng, T., Bett, G. C. & Sachs, F. Stretch-activated whole cell currents in adult rat cardiac myocytes. *Am. J. Physiol. Heart Circ. Physiol.* **278,** H548-57 (2000).

85. Quinn, T. A., Jin, H., Lee, P. & Kohl, P. Mechanically Induced Ectopy via Stretch-Activated Cation-Nonselective Channels Is Caused by Local Tissue Deformation and Results in Ventricular Fibrillation if Triggered on the Repolarization Wave Edge (Commotio Cordis). *Circ. Arrhythmia Electrophysiol.* **10,** e004777 (2017).

86. Hu, H. & Sachs, F. Stretch-activated ion channels in the heart. *J. Mol. Cell. Cardiol.* **29,** 1511–23 (1997).

87. Isenberg, G. *et al.* Differential effects of stretch and compression on membrane currents and [Na+]c in ventricular myocytes. *Prog. Biophys. Mol. Biol.* **82,** 43–56 (2003).

88. Iribe, G. & Kohl, P. Axial stretch enhances sarcoplasmic reticulum Ca2+ leak and cellular Ca2+ reuptake in guinea pig ventricular myocytes: Experiments and models. *Prog. Biophys. Mol. Biol.* **97,** 298–311 (2008).

89. Gamble, J., Taylor, P. B. & Kenno, K. A. Myocardial stretch alters twitch characteristics and Ca2+ loading of sarcoplasmic reticulum in rat ventricular muscle. *Cardiovasc. Res.* **26,** 865–870 (1992).

90. Iribe, G. *et al.* Axial stretch of rat single ventricular cardiomyocytes causes an acute and transient increase in Ca2+ spark rate. *Circ. Res.* **104,** 787–795 (2009).

91. Prosser, B. L., Khairallah, R. J., Ziman, A. P., Ward, C. W. & Lederer, W. J. X-ROS signaling in the heart and skeletal muscle: Stretch-dependent local ROS regulates [Ca2+]i. *J. Mol. Cell. Cardiol.* **58,** 172–181 (2013).

92. Isenberg, G. & Wendt-Gallitelli, M.-F. Binding of calcium to myoplasmic buffers contributes to the frequency-dependent inotropy in heart ventricular cells. *Basic Res. Cardiol.* **87,** 411–417

93. Todaka, K. *et al.* Characterizing ventricular mechanics and energetics following repeated coronary microembolization. *Am. J. Physiol.* **272,** H186-94 (1997).

94. Petroff, M. G. V. *et al.* Endogenous nitric oxide mechanisms mediate the stretch dependence of Ca2+ release in cardiomyocytes. *Nat. Cell Biol.* **3,** 867–873 (2001).

95. Shim, A. L. *et al.* Kinetics of Mechanical Stretch-Induced Nitric Oxide Production in Rat Ventricular Cardiac Myocytes. *Bull. Exp. Biol. Med. Transl. from Byulleten' Eksp. Biol. i Meditsiny* **163,** 532–535 (2017).

96. Swift, L. M. *et al.* Properties of blebbistatin for cardiac optical mapping and other imaging applications. *Pflügers Arch. - Eur. J. Physiol.* **464,** 503–512 (2012).

97. Fedorov, V. V. *et al.* Application of blebbistatin as an excitation–contraction uncoupler for electrophysiologic study of rat and rabbit hearts. *Hear. Rhythm* **4,** 619–626 (2007).

98. Schiff, P. B., Fant, J. & Horwitz, S. B. Promotion of microtubule assembly in vitro by taxol. *Nature* **277,** 665–7 (1979).

99. Rowinsky, E. K. & Donehower, R. C. Paclitaxel (Taxol). *N. Engl. J. Med.* **332,** 1004–1014 (1995).

100. Yaniv, Y., Maltsev, V. A., Ziman, B. D., Spurgeon, H. A. & Lakatta, E. G. The "funny" current (I(f)) inhibition by ivabradine at membrane potentials encompassing spontaneous depolarization in pacemaker cells. *Molecules* **17,** 8241–54 (2012).

101. Loew, L. M. Potentiometric dyes: Imaging electrical activity of cell membranes. **68,** 1405–1409 (1996).

102. Matiukas, A. *et al.* Near-infrared voltage-sensitive fluorescent dyes optimized for optical mapping in blood-perfused myocardium. *Hear. Rhythm* **4,** 1441–1451 (2007).

103. Del Nido, P. J., Glynn, P., Buenaventura, P., Salama, G. & Koretsky, A. P. Fluorescence measurement of calcium transients in perfused rabbit heart using rhod 2. *Am. J. Physiol.* **274,** H728-41 (1998).

104. Trollinger, D. R., Cascio, W. E. & Lemasters, J. J. Selective Loading of Rhod 2 into Mitochondria Shows Mitochondrial Ca2+Transients during the Contractile Cycle in Adult Rabbit Cardiac Myocytes. *Biochem. Biophys. Res. Commun.* **236,** 738–742 (1997).

105. Lee, P. *et al.* Single-sensor system for spatially resolved, continuous, and multiparametric optical mapping of cardiac tissue. *Hear. Rhythm* **8,** 1482–1491 (2011).

106. Janse, M. J., Opthof, T. & Kléber, A. G. Animal models of cardiac arrhythmias. *Cardiovasc. Res.* **39,** 165–77 (1998).

107. Jung, B. *et al.* A quantitative comparison of regional myocardial motion in mice, rabbits and humans using in-vivo phase contrast CMR. *J. Cardiovasc. Magn. Reson.* **14,** 87 (2012).

108. Pogwizd, S. M. & Bers, D. M. Rabbit models of heart disease. *Drug Discov. Today Dis. Model.* **5,** 185–193 (2008).

109. Kaese, S. *et al.* The ECG in cardiovascular-relevant animal models of electrophysiology. *Herzschrittmachertherapie + Elektrophysiologie* **24,** 84–91 (2013).

110. Panfilov, Al. V. Is heart size a factor in ventricular fibrillation? Or how close are rabbit and human hearts? *Hear. Rhythm* **3,** 862–864 (2006).

111. Burton, R. A. B. *et al.* Microscopic magnetic resonance imaging reveals high prevalence of third coronary artery in human and rabbit heart. *EP Eur.* **14,** v73–v81 (2012).

112. Johnson, M. A. & Beatty, M. F. The mullins effect in uniaxial extension and its influence on the transverse vibration of a rubber string. *Contin. Mech. Thermodyn.* **5,** 83–115 (1993).

113. Cooper, P. J. *et al.* Soft tissue impact characterisation kit (STICK) for ex situ investigation of heart rhythm responses to acute mechanical stimulation. *Prog. Biophys. Mol. Biol.* **90,** 444–68 (2006).

114. Axel, D. I. *et al.* Paclitaxel inhibits arterial smooth muscle cell proliferation and migration in vitro and in vivo using local drug delivery. *Circulation* **96,** 636–45 (1997).

115. Melgari, D. *et al.* hERG Potassium Channel Blockade by the HCN Channel Inhibitor Bradycardic Agent Ivabradine. *J. Am. Heart Assoc.* **4,** e001813–e001813 (2015).

116. Calaghan, S. C. & White, E. The role of calcium in the response of cardiac muscle to stretch. *Prog. Biophys. Mol. Biol.* **71,** 59–90 (1999).

117. Honoré, E., Patel, A. J., Chemin, J., Suchyna, T. & Sachs, F. Desensitization of mechano-gated K2P channels. *Proc. Natl. Acad. Sci. U. S. A.* **103,** 6859–64 (2006).

118. Calabrese, B., Tabarean, I. V, Juranka, P. & Morris, C. E. Mechanosensitivity of N-type calcium channel currents. *Biophys. J.* **83,** 2560–74 (2002).

119. Lewis, A. H., Cui, A. F., McDonald, M. F. & Grandl, J. Transduction of Repetitive Mechanical Stimuli by Piezo1 and Piezo2 Ion Channels. *Cell Rep.* **19,** 2572–2585 (2017).

120. Towe, B. C. & Rho, R. Ultrasonic cardiac pacing in the porcine model. *IEEE Trans. Biomed. Eng.* **53,** 1446–8 (2006).